

**APPLICATIONS OF SUPERCONDUCTING MAGNETIC ENERGY STORAGE
SYSTEMS IN POWER SYSTEMS.**

by

Prem Kumar

Thesis submitted to the Faculty of the
Virginia Polytechnic Institute and State University
in partial fulfillment of the requirements for the degree of
Master Of Science
in
Electrical Engineering

APPROVED:

K.S.Tam Ph.D., Chairman

A.G.Phadke Ph.D.

S.Rahman Ph.D.

Aug 1989

Blacksburg, Virginia

APPLICATIONS OF SUPERCONDUCTING MAGNETIC ENERGY STORAGE SYSTEMS IN POWER SYSTEMS.

by

Prem Kumar

K.S.Tam Ph.D., Chairman

Electrical Engineering

(ABSTRACT)

A Superconducting Magnetic Energy Storage (SMES) system is a very efficient storage device capable of storing large amounts of energy. The primary applications it has been considered till now are load-levelling and system stabilization. This thesis explores new applications/ benefits of SMES in power systems. Three areas have been identified.

- Using SMES in conjunction with PV systems. SMES because of their excellent dynamic response and PV being an intermittent source complement one another. A scheme for this hybrid system is developed and simulation done accordingly.
- Using SMES in an Asynchronous link between Power Systems. SMES when used in a series configuration between two or more systems combines the benefits of asynchronous connection, interconnection and energy storage. A model of such a scheme has been developed and the control of such a scheme is demonstrated using the EMTP. The economic benefits of this scheme over pure power interchange, SMES operation alone and a battery/dc link is shown.
- Improvement of transmission through the use of SMES. SMES when used for diurnal load levelling provides additional benefits like reduced transmission losses, reduced peak loading and more effective utilization of transmission facility, the im-

pact of size and location on these benefits were studied, and if used as an asynchronous link provides power flow control.

Acknowledgements

I would like to express my deep gratitude to Dr K.S.Tam for his constant encouragement and assistance over the course of my thesis. Dr Tam has been a source of great inspiration and drive for which I will be ever grateful. I wish to thank Dr A.G.Phadke and Dr S.Rahman for serving on my advisory committee, their knowledge and instruction as teachers is appreciated. I would like to thank the Dept of Electrical Engineering for offering me a teaching assistantship, the Virginia Center for Coal & Energy and E.I. du Pont de Nemours and Company for supporting me as a research assistant.

Table of Contents

1.0	Introduction	1
1.1	Background	1
1.11	Working principle of the SMES	1
1.12	Status of Research Work On SMES	2
1.13	Applications of SMES in Power Systems	4
1.2	Objectives	4
1.3	Thesis Outline	5
1.3.1	Chapter 2 Enhancing the utilization of PV systems with SMES	5
1.3.2	Chapter 3 Application of SMES in a asynchronous link between power systems	6
1.3.2	Chapter 4 SMES Impact on Transmission Systems.	6
2.0	Enhancing the utilization of PV with SMES	8
2.1	Hybrid PV-SMES control	10
2.2	Operating Scheme For the PV/SMES operation	11
2.2.1	Plain SMES operation	12
2.2.2	SMES/PV operation	13
2.3	Simulation study on the combined PV/SMES operation.	17

2.4	Possible locations for PV arrays	19
3.0	Application of SMES in an asynchronous link between Power Systems.	28
3.1	Basic Principle	29
3.1.1	Multiterminal system.	37
3.2	Modelling of the system to demonstrate the modes	38
3.2.1	The basis for selection of model parameters.	38
3.2.2	Mathematical modelling of the system.	39
3.2.3	Description of the operating schemes.	42
3.2.4	Discussion of results.	44
3.3	EMTP simulation.	45
3.3.1	Basis for the model parameters.	45
3.3.2	The Control Scheme.	46
3.4	Economic savings in operating system with SMES used as an asynchronous link.	52
3.4.1	Economic Dispatch equations	53
3.4.2	Cost of SMES power.	56
3.4.3	Case Studies.	58
3.5	Battery storage in an asynchronous link	60
4.0	SMES Impact on Transmission System.	92
4.1	Basic Concept	93
4.1.1	Without SMES	93
4.1.2	With SMES.	94
4.2	Simulation Study.	97
4.2.1	Modelling the SMES for the load flows.	97
4.2.2	Sizing the SMES.	100
4.3	Case Studies.	101
4.3.1	Case 1(system without SMES) Base case .	101

4.3.2 Case 2 with SMES	102
4.3.3 Methodology of estimating total savings in transmission loss energy.	103
4.4 Savings due to producing cheaper energy.	106
4.5 Impact of SMES on planning.	109
4.6 Power Flow Control	111
4.6.1 Case studies.	113
4.6.2 Multiterminal link	119
5.0 Conclusions	127
5.1 Further Work	128
Bibliography	130
Appendix A. Model Results on BPA SMES system	134
Vita	136

List of Illustrations

Figure 1. Schematic diagram for the SMES system	7
Figure 2. PV output from a 4 KW test facility	20
Figure 3. Load curve with and without PV generation.	21
Figure 4. PV/SMES alternate schemes	22
Figure 5. Schematic for combined PV/SMES system.	23
Figure 6. Schematic diagram to demonstrate the operation scheme.	24
Figure 7. Load curve with/without coordinated PV/SMES operation on a sunny day.	25
Figure 8. Load curve with/without coordinated PV/SMES operation on a cloudy day.	26
Figure 9. Load curve with/without coordinated PV/SMES operation on a rainy day.	27
Figure 10. SMES connected to a power system in a conventional arrangement ...	64
Figure 11. SMES/DC link connecting two power systems.	65
Figure 12. SMES/DC link connecting n power systems.	66
Figure 13. Model results for scheme C	67
Figure 14. Model results for scheme C	68
Figure 15. Model results for scheme D	69
Figure 16. Model results for scheme D	70
Figure 17. Model results for scheme E	71
Figure 18. Model results for scheme E	72

Figure 19. EMTP Model diagram	73
Figure 20. alpha calculator schematic	74
Figure 21. EMTP Model results scheme A	75
Figure 22. EMTP Model results scheme A	76
Figure 23. EMTP Model results scheme A	77
Figure 24. EMTP Model results scheme A	78
Figure 25. EMTP Model results scheme A	79
Figure 26. EMTP Model results scheme C	80
Figure 27. EMTP Model results scheme C	81
Figure 28. EMTP Model results scheme C	82
Figure 29. EMTP Model results scheme C	83
Figure 30. EMTP Model results scheme C	84
Figure 31. EMTP Model results scheme C	85
Figure 32. EMTP Model results scheme C	86
Figure 33. EMTP Model results scheme D	87
Figure 34. EMTP Model results scheme D	88
Figure 35. EMTP Model results scheme D	89
Figure 36. EMTP Model results scheme D	90
Figure 37. EMTP Model results scheme D	91
Figure 38. A simple Power system	121
Figure 39. AEP 14 BUS system with SMES locations.	122
Figure 40. Load curve with/without SMES	123
Figure 41. Transmission losses curve	124
Figure 42. Test system	125
Figure 43. Multi-terminal link	126
Figure 44. Model Results for BPA system	135

List of Tables

Table 1. Operating Conditions for SMES Charging Modes	32
Table 2. Operating Conditions for SMES Discharging Modes	33
Table 3. Operating Conditions for SMES Standby Modes	34
Table 4. Operating Conditions for simultaneously SMES Charging Modes and power interchange modes.	35
Table 5. Operating Conditions for simultaneously SMES Discharging Modes and power interchange modes.	36
Table 6. Mode / Power signal correspondence.	47
Table 7. Test System Data	54
Table 8. Operating Cost comparison for interconnected operation with / without SMES	61
Table 9. Operating Cost comparison for interconnected operation with / without Battery	63
Table 10. Bus data for test system	98
Table 11. Line data for test system	99
Table 12. A comparison of the transmission line loadings between the original system and system equipped with SMES of different ratio	107
Table 13. A comparison of the reduction in transmission losses and the reduction in fuel cost	108
Table 14. The swing generator output for 24 hour period.	110
Table 15. A comparison of the maximum transmission line loading for system with/without SMES	112
Table 16. Test Data	114

Table 17. Line Loadings. 116
Table 18. Line Losses. 117
Table 19. Voltages. 118

1.0 Introduction

The introduction is divided into three sections. Section 1.1 briefly gives the background of SMES systems. Section 1.2 gives the objectives of this thesis. Section 1.3 deals with the thesis outline.

1.1 Background

1.11 Working principle of the SMES

A Superconductive magnetic energy storage is capable of storing a large amount of energy in the magnetic field of a superconducting magnet at high efficiencies ($> 90\%$). This form of energy storage device is more efficient than pumped storage and batteries. It has very fast dynamic response which makes it attractive for system applications. Figure

1 shows the schematic diagram of a SMES system. The main components are the superconducting magnet, which functions like an inductor in the form of a solenoid, toroid or variations of these shapes as discussed in section 1.12. The magnet is kept in the superconducting state by the cryogenic system. Energy exchange between the SMES and the three phase AC system is through the AC/DC converters. These AC/DC converters for most of the conventional designs is the three phase Graetz bridge. Artificially commuted thyristors and gate turn off thyristors can also be used. Control of firing angle of thyristors gives various modes of real and reactive power operation.

1.12 Status of Research Work On SMES

In the U.S most of the work had been done in the University of Wisconsin and Los Alamos labs. A 30 MJ (8.4 Kwh) SMES was installed and commissioned at Bonneville Power Administration (BPA) substation in Tacoma Washington, [1] it was designed primarily to damp the dominant power swing mode of the Pacific AC intertie. In 1984 Bechtel under contract from EPRI came out with a detailed design of a 1000 MW (5500 Mwh) set [2]. There have since been conceptual design improvements. The Japanese have been doing work on it and have come out with a conceptual design for a 1000 Mw set [3]. Work has begun for a 20 Mwh SMES unit for Madison Gas & Electric Company. Most of the research effort has been concentrated in optimizing the magnet design. The two important shapes for SMES applications are solenoid and the toroid from which there have been a lot of variations, like in solenoids there is the single tunnel [4], multitunnel [5], low aspect ratio [6], single layer, multilayer [2] and in toroids the variations are force balanced schemes [7] and quasi force free [8] structures.

There are three important parameters considered in magnet design

1.0 Energy/Mass-This is the energy stored per unit mass of conductor (this will vary with the geometry of coil shape) as the conductor cost forms the main cost of the system this is a very important parameter.

2.0 Forces in the coil- Lorentz forces generated by the coil are enormous. Forces developed on the current carrying conductors is given by the cross product of current density vector and the flux density vector, as in a superconductor the current density is very high extreme forces are developed which cause limitation in magnet design.

3.0 Stray Magnetic field-As the operating field strength for SMES applications is around 6T, and most SMES designs favour solenoid design which have high stray magnetic field. The different solenoid designs have different stray field patterns.

Summary of SMES system design For the magnet the solenoid is the best in terms of energy/mass (almost twice that of a toroid), but it has a lot of stray magnetic field. For load levelling applications this configuration is preferred. The toroid has half the energy density of the solenoid but it has no stray magnetic field. For the power conversion equipment in most cases the conventional graetz bridge is preferred. As the converter consumes reactive power both in rectifier and inverter mode it could be considerable in certain operating modes of the SMES. The reactive power consumption is due to the fact that the firing angle can only be delayed. In artificially commuted thyristors the firing angle can be advanced thus it can introduce reactive power to the system, but this is more in the research stage. The superconducting material used / considered for the design so far has been Niobium-Titanium which exhibits superconducting properties at around 4 degrees Kelvin. The material cost forms a significant portion of the system cost. There have been recent discoveries of higher temperature superconductors (ceramics at 125 degrees k) work is in progress to make them useful for engineering applications

and also a lot of research is in the material science to discover higher temperature superconductors. As forces are enormous, SMES for large storage applications are proposed to be buried, and to make use of the bedrock to counterbalance the forces.

1.13 Applications of SMES in Power Systems

SMES have very high efficiencies and fast dynamic responses, they have been primarily considered for diurnal load levelling. At night, when the load demand is low, electric power produced by relatively low cost generators is used to charge up the SMES systems. During day time, when the load demand is high the energy stored in the SMES system is discharged to supply the load, thus minimizing the use of more costly generators. SMES have also been considered for stabilizations. The only built SMES by BPA at Tacoma, Washington has been used for this application.

1.2 Objectives

The research work till now has been concentrated on the actual magnet design for applications as outlined in the previous section. The thrust of this thesis is to explore new applications/benefits of SMES in power systems. There have been three areas that have been identified. Enhancing the utilization of PV systems with SMES, application of SMES in a asynchronous link between power systems, Impact of SMES on transmission

systems. Each topic is the theme of a chapter in this thesis. Section 1.3 provides the outline of this thesis and presents a summary of the major results and contributions.

1.3 Thesis Outline

1.3.1 Chapter 2 Enhancing the utilization of PV systems with SMES

As the needs of Photovoltaic (PV) systems and SMES are complementary a hybrid scheme could result in an effective system. PV power has the limitation of rapid fluctuation due to transient clouds and therefore is considered as an unreliable source, an SMES has very fast dynamic response, it has a 50m-sec power reverse capability. Further SMES designs are for burying the magnet underground to support the forces and due to the stray field there is a lot of vacant land available above ground on which PV could be installed. A scheme of operation for a 24 hr operating period is proposed. A simulation study has been performed showing the SMES output/ PV output for a 24 hr period for different weather conditions. Most of the results of this chapter have been published [9,10].

1.3.2 Chapter 3 Application of SMES in a asynchronous link between power systems

It introduces the concept that SMES can be incorporated into a back to back DC link. With a SMES/DC link a SMES can be shared between several neighboring power systems, furthermore it can be used as an asynchronous link and can be operated such that significant economic benefits can be obtained over pure interchange or SMES operation alone. The basic operating modes of a two system link is explained. A computer model has been simulated showing the various parameters over a 24 hour period. The model was validated by the BPA test model. The control of such a scheme has been developed and an EMTP simulation has been done showing the feasibility of the control scheme. The economic benefit for a two system operation over a conventional tie has been done to show the savings in cost due to such a scheme. Some of the contributions of this chapter has been published [11].

1.3.2 Chapter 4 SMES Impact on Transmission Systems.

Additional benefits like transmission line loss cost, reduction of transmission line loading and better utilization of existing transmission facility were identified for SMES performing load levelling applications. Simulation studies were performed for studying the impact of the size and location of SMES on the benefits obtained. A SMES when used as an asynchronous link is shown to provide power flow control.

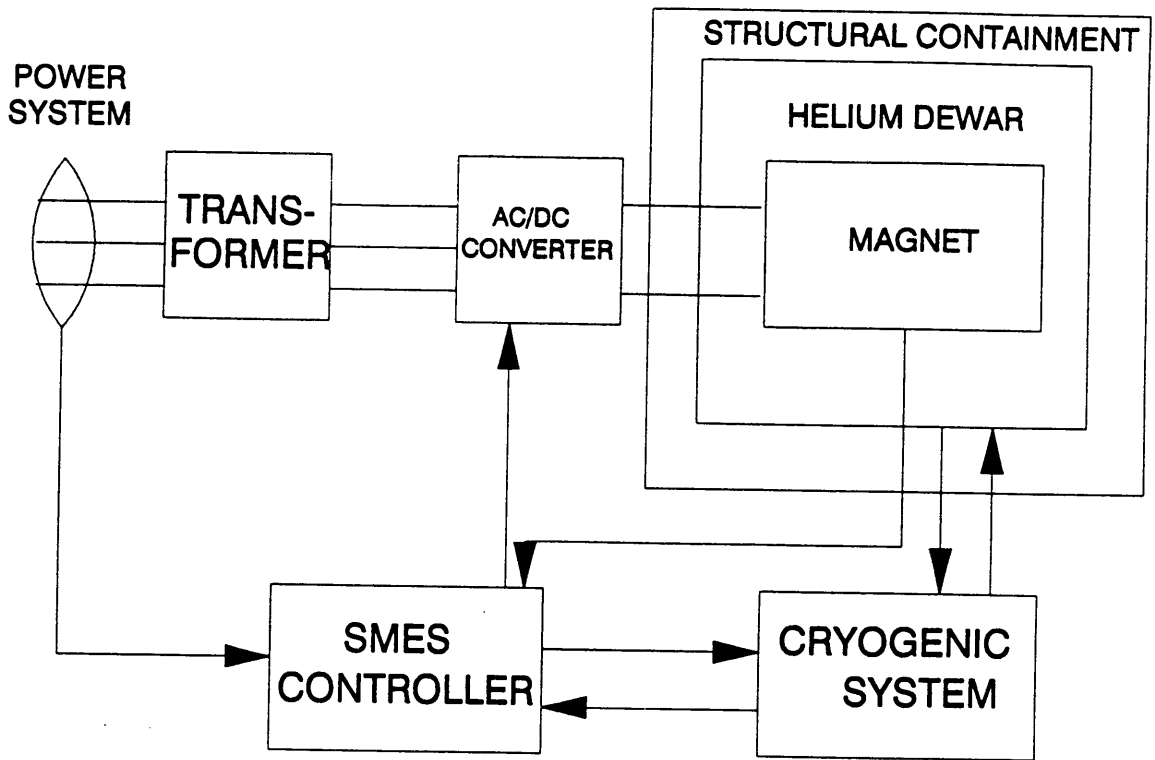


Figure 1. Schematic diagram for the SMES system

2.0 Enhancing the utilization of PV with SMES

This chapter demonstrates the concept of a hybrid PV-SMES system. Solar photovoltaic energy is an important source of energy because of the unlimited resources, maintenance free equipments and the absence of environment problems. One drawback of PV systems has been the low efficiency of the solar cells (around 10%), but recently Sandia National lab [12] have reported cells with over 30% efficiency, this is comparable to coal or oil fired generation. Another major drawback is the fluctuation of PV power. This is because the power produced by the solar cells is dependent on the amount of sunlight they receive and therefore variations in atmospheric conditions like clouds are reflected in the electric power produced. Figure 2 shows the PV output of a 4KV test facility on a three minute interval in the southeastern U.S. If the capacity of the PV system relative to the size of the power system is small (<5%) the fluctuations in PV power are relatively insignificant compared with the power systems load curve and therefore does not present much problem to the operation or control of the power system [13,14]. Traditionally PV systems have therefore been considered for small scale applications.

If the PV power forms a significant portion of the power system, there are a lot of technical problems associated with it. To consider such a case, using the 4KV system as the building block for a central PV system so that it supplies 15% of the power system's peak demand. A typical summer load curve[16] for S.E U.S with a peak rating of 259 MW is considered PV generation is treated as negative load, the original load curve and the modified load curve seen by the rest of the system are shown in figure 3. The modified load curve contains many sharp spikes and as can be observed has very high ramp rates and would impose an increase in spinning reserve requirement, load following requirement and control difficulty [13,14,15]. The response rates of thermal units need to be considered before they are committed which would lead to operations other than economic dispatch. Existing approaches for such a problem is reducing the PV power output, changing the generation mix of the system, forcing the economic reserve to always provide the higher spinning reserve.

The objective of this chapter is to show the feasibility of using SMES to support large scale PV generation. A coordinated PV/SMES scheme is proposed, an operating scheme is developed over a 24 hour period, simulation studies based on the developed scheme are conducted and the combined PV/SMES output is shown as smooth and controllable under different weather conditions.

2.1 Hybrid PV-SMES control

The primary goal of the SMES would be diurnal load levelling. As there are large Lorentz forces encountered the present SMES designs favor burying the magnet so that the bedrock could provide mechanical support. There is a lot of vacant space because of the stray magnetic field and would not be accessible due to environmental reasons. This hybrid PV/SMES proposes the utilization of the already available space to store the PV arrays and to extend the use of SMES, because of its very fast response rates, with the ability to absorb/release large amount of power make it an excellent choice to regulate power fluctuation caused by an intermittent source such as PV. The PV and SMES can be connected as a system in many configurations. Figure 4 indicates three possible configurations. For this study the PV and the SMES are connected in parallel across the same bus. Figure 5 shows the schematic diagram for the combined PV/SMES operation. Each system may operate independent of each other or may operate in a coordinate fashion and in that case it is controlled by the PV/SMES coordinated control system. The input are the measured PV power output (P_{pv}) the measured SMES power output (P_s) the power demand signal issued from the power system control (P_d) the measured power from the AC system. The difference between P_d and P_{pv} is the power command signal for the SMES system. This is compared with the measured P_s to generate an error signal for the integral controller which then joins the power command to form the composite input to the firing angle calculator which computes the firing angle for the converter based on the SMES current level.

$$\cos \alpha = \frac{\left(\frac{P_c}{IDC} + IDC \times R_c \right)}{V_{DC}} \quad [2.1]$$

where

α = Firing angle

P_c = Composite Power signal

I_{DC} = DC current

R_c = Commutation resistance

V_{DC} = DC Voltage

The firing pulse generator then issues a sequence of firing pulses according to the firing angle and with reference to the AC bus voltage to the converter in the SMES system.

2.2 Operating Scheme For the PV/SMES operation

A typical summer day daily load curve [16] is represented by curve A-B-C-D-E-F-G-H-I-J-K in figure 6. When a SMES system installed to perform diurnal load levelling electric power generated from low cost base units is used to charge up the SMES between t_0 t_2 The base load units would be at setting SP1

Define the following parameters

t_0 = Time when SMES begins charging

t_1 = Time when PV begins generating power

t_2 = Time when Original Load curve ends charging

t_3 = Time when Modified Load curve ends charging

t_4 = Time when Original Load curve begins discharging

t_5 = Time when Modified Load curve begins discharging

t_6 = Time when PV generation ends

t_7 = Time when Original Load curve ends discharging

t_8 = Time when Modified Load curve ends discharging

PV_g = Total PV generation

PV_s = PV power feeding SMES

PV_l = PV power feeding Load

S_c = SMES charging power

S_d = SMES discharging power

L = Original load curve

ML = Modified load curve

$SP1$ = Load setting during charge

$SP2$ = Load setting during discharge for original load curve

$SP2M$ = Load setting during discharge for modified load curve

The modified load curve has been shown as smooth, this is just to illustrate the concept of the scheme.

2.2.1 Plain SMES operation

$$t_0 \leq t \leq t_2$$

$$SP1 = L + S_c \quad [2.2]$$

The stored energy is then released during heavy load hours during interval t_4 t_7 to replace the power generated from higher cost peak/intermediate units.

$$t_4 \leq t \leq t_7$$

$$SP2 = L - S_d \quad [2.3]$$

2.2.2 SMES/PV operation

With diurnal load levelling the load curve is modified to A-D-E-F-I-J-K. With a significant level of PV power generation the load curve would be changed to A-B-C-L-M-N-H-I-J-K. This curve does not have spikes as they have been smoothed out by controlling the SMES power output and the PV/SMES combined power is dispatchable. With PV power shouldering some of the peak load the new setpoint will be SP2M. Discharge would begin at t_5 and continue until t_6 when the stored energy is reduced to the designated level.

When sunrise begins at t_1 there is enough generation (consisting of mainly base units) to supply load as well as charge up the SMES. Between t_1 t_2 the PV power can be used to provide extra charging power for the SMES. Any temporary change in the PV power would only cause a temporary change in the charging power for the SMES.

$$t_1 \leq t \leq t_2$$

$$S_s = SP1 - L + PV_s \quad [2.4]$$

$$PV_g = PV_s \quad [2.5]$$

$$PV_l = 0 \quad [2.6]$$

Starting at t_2 the base power unit is no longer enough to supply the system load. The base unit power output can be maintained at the same setting SP1 until t_3 but between t_2 and t_3 PV/SMES power would be employed for dispatch. When PV power is available during this period part of it would be used to supply part of the load enclosed by D-M-E-D and the rest (enclosed by D-L-M-D) would be used to charge up the SMES. If the PV power fluctuates the SMES would switch rapidly from charging mode to discharging mode or do whatever necessary so that the combined PV/SMES output is dispatchable and the fluctuations would not effect the power system.

$$t_2 \leq t \leq t_3$$

$$PV_l = L - SP1 \quad [2.7]$$

$$PV_s = PV_g - PV_l \quad [2.8]$$

$$S_c = PV_s \quad [2.9]$$

When there is reduction in PV Power due to fluctuations the discharge by SMES (to maintain the fixed load setting) would be given by

$$S_d = L - SP1 - PV_g \quad [2.10]$$

Beyond t_3 all of the available PV power is used to supply the system load. The load curve would follow the curve M-N until t_5 at which the SMES discharge begins. From t_3 to t_5 the SMES output would still be used to smooth out the PV fluctuations.

$$t_3 \leq t \leq t_5$$

$$PV_s = 0 \quad [2.11]$$

$$PV_g = PV_l \quad [2.12]$$

$$S_d = SOS \quad [2.13]$$

where .

SOS = Smoothing out spikes

From t_5 to t_6 the SMES is discharging so that the composite PV-SMES power flattens the load curve. All the PV power is used to supply the load.

$$t_5 \leq t \leq t_6$$

$$PV_g = PV_l \quad [2.14]$$

$$S_d = L - PV_g - SP2M \quad [2.15]$$

If PV power goes to zero SMES discharging power increases.

From t_6 to t_7 the load curve is flattened by SMES discharging.

$$t_6 \leq t \leq t_7$$

$$S_d = L - SP2M \quad [2.16]$$

With the PV/SMES combined operation, the system load curve is modified to A-D-M-N-J-K. This is better than the load curve modified by PV or SMES alone. The SMES is being charged from t_0 to t_2 by the base units with total energy indicated by the area enclosed by A-B-C-D-A, and by PV generation from t_1 to t_2 with total energy indicated by the area enclosed by C-L-M-D-C. The latter is relatively small when compared to the former. Thus, the SMES charging would not be affected significantly by the weather dependent PV power. On cloudy days the PV power output is reduced. However the pattern shown in figure still remains the same except the curve C-L-M-N-H would be shifted closer to the curve C-D-E-F-G-H. On rainy days, the PV output is very small and the curves C-L-M-N-H and C-D-E-F-G-H almost coincide (point N coincides with point F, point M coincides with point D). In this case, the SMES operates alone to perform its primary function, diurnal load levelling. In any event, the combined PV/SMES output power is dispatchable and is free of fluctuation.

2.3 Simulation study on the combined PV/SMES

operation.

The daily load curve used is a typical daily load curve in the southeastern region of U.S.A with a peak load of 259 MW. The PV system assumed to deliver power upto 40 MW (about 15% of the power systems maximum load). The observed PV data is from a 4 Kw test facility and has been scaled up to model the 40 MW PV generator. The SMES system has a power rating of 40 MW a storage capacity of 200 Mwh and roundtrip of 97%.

The simulation study was done using the equations for SMES charge/ discharge described in equations in section 2.2.2 for the time frame t_0 to t_7 . The input to the program was the the two set points SP1 and SP2M these two points are on the load curve and are computed as follows. Let the area of ABCLMD be A_1 the energy rating of the SMES. (i.e 200 Mwh in this case). Let the area of NHIJN be A_2 . Let PC , be the power rating of the converter, 40 MW in this case.

$$A_1 = \int_{t_0}^{t_3} (ML - SP1) dt \quad [2.17]$$

SP1 is the only unknown above

$$A_2 = A_1 \times \eta \quad [2.18]$$

where

η = efficiency

$$A_2 = \int_{t_5}^{t_8} (ML - SP2M) dt \quad [2.19]$$

SP2M is thus obtained.

SP1 and SP2M are limited by the following constraint

$$\begin{aligned} SP1 - L_{\min} &\leq PC_r \\ L_{\max} - SP2M &\leq PC_r \end{aligned} \quad [2.20]$$

Figure 7 show the complete operation. Figure 7a is PV output Figure 7b is the SMES charge/discharge curve. Figure 7c is the coordinated PV/SMES operation. The PV output is shown in figure 7a peaks at 40MW (with fluctuations) for atleast five hours. With SMES support all the PV power is fully utilized to supply the load. As shown in figure the SMES output releases or absorbs energy to smooth out the PV fluctuations. Because of PV generation, the SMES discharge begins at around 3-15 P.M and shaves of the peak load in the late afternoon and early evening hours. The peak load is reduced from 259 MW to 217 MW. The daily load curve modified by PV/SMES shows the coordinated operation.

If PV generation is employed without SMES support not only would the PV fluctuation adversely affect the operation of the power system the system peak load would still remain at around 259 MW because the PV power peaks between noon and early afternoon while the system load peaks at around 6 P.M. If the SMES operates alone its discharge would begin at around 11 A.M and the system peak load would be reduced to 227 MW. Therefore the combined use of PV/SMES also enhances the primary purpose of the SMES system-diurnal load levelling.

The same operation scheme is applicable for other weather conditions, although PV contribution would vary. Figure 8 shows the PV/SMES operation on a cloudy day (PV power here is reduced by 50%). Since there is less PV power its impact on the combined operation is reduced. The SMES discharge starts at around 1-45 P.M and the system peak is reduced to 219MW. Figure 9 show the PV/SMES operation on a rainy day (the maximum PV power is 5% rated power). Since the PV contribution is small the PV/SMES combined operation is the same as the SMES operation alone. In both cases the PV/SMES is still dispatchable and free of fluctuations.

2.4 Possible locations for PV arrays

The SMES in all the conventional designs is to be buried underground to support the high magnetic forces. As the magnets are operated at very high magnetic fields around 7 Tesla (70000 gauss) and solenoids are used in all the conventional designs there is enormous stray magnetic field and the area upto the point where the field falls to 10 gauss is considered the boundary limit of the SMES. For limited maintenance levels the 100 gauss limit is considered feasible, the EPRI/Bechtel in their design have proposed the switchyard to be located in that field strength. There is enormous area between the 10 gauss line and the 100 gauss line which can be utilized for the installation of the PV arrays. If the 30% PV cells are used it could be used to generate a considerable amount of power. That is though a central PV station and SMES individually require a lot of land the combined PV/SMES system is not the sum of the two individual requirements.

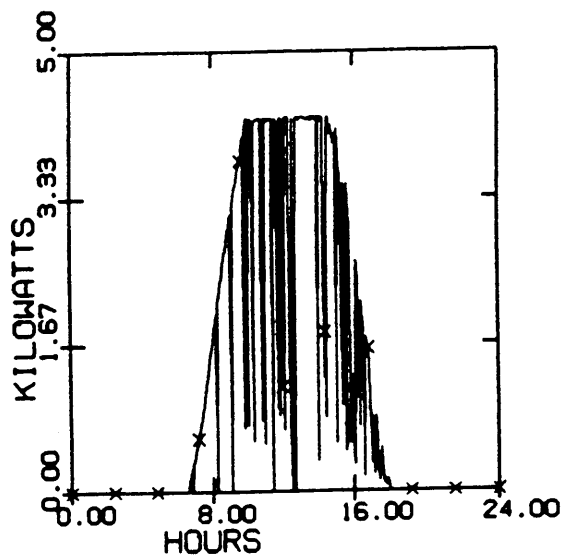


Figure 2. PV output from a 4 KW test facility

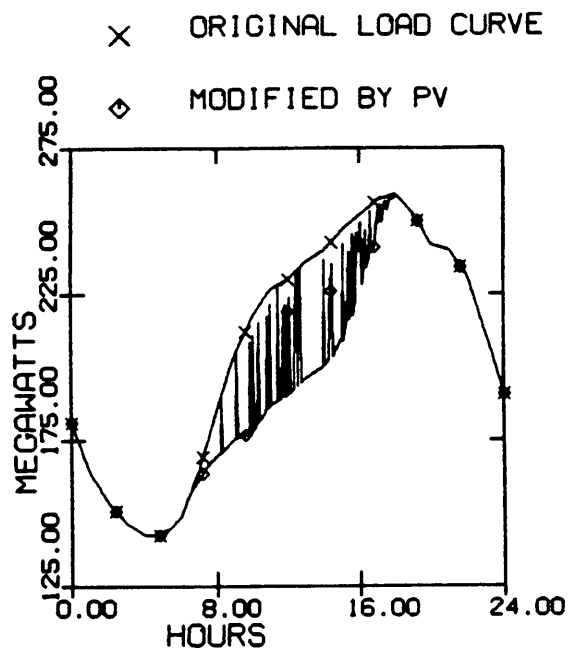


Figure 3. Load curve with and without PV generation.

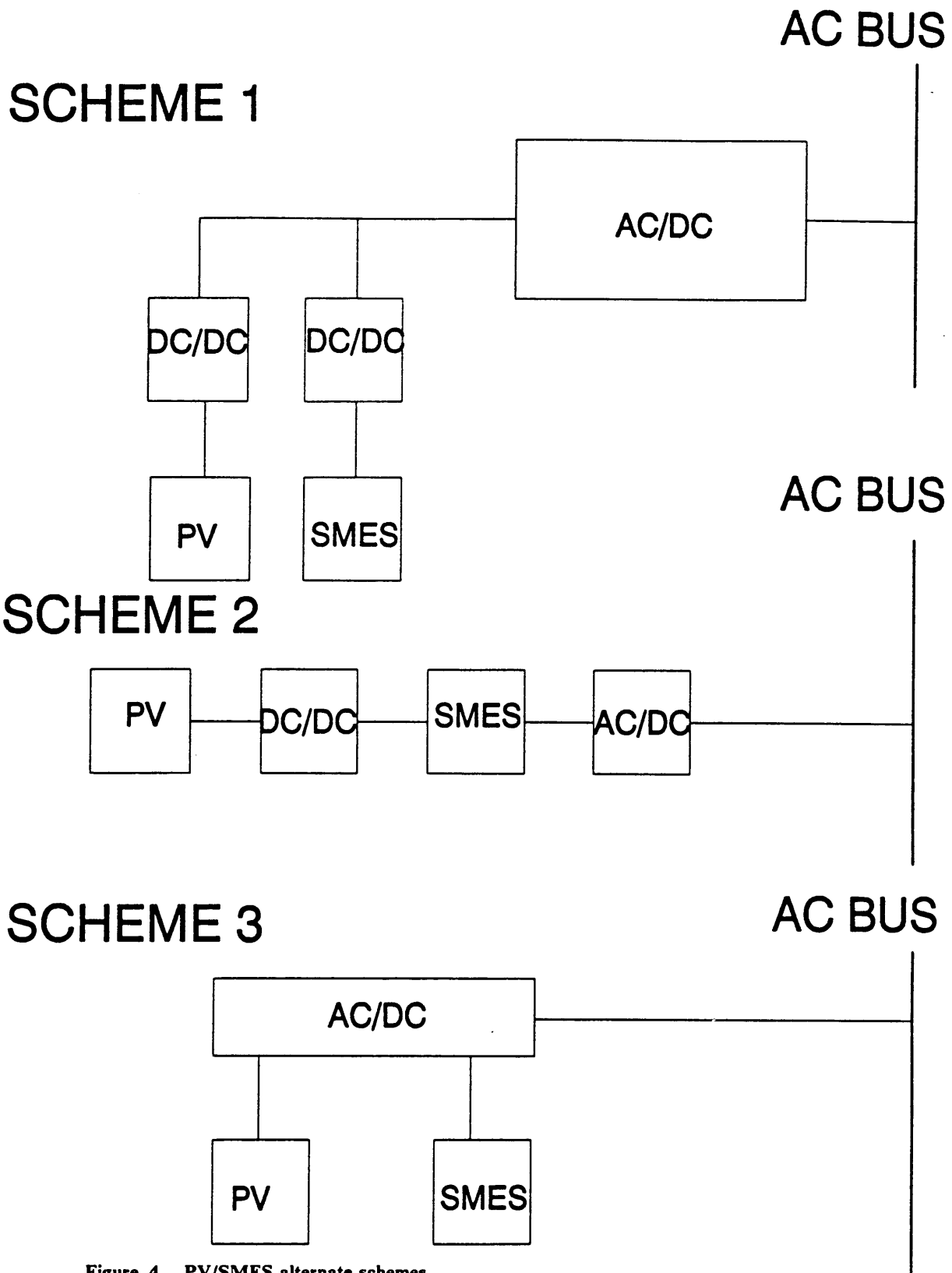


Figure 4. PV/SMES alternate schemes

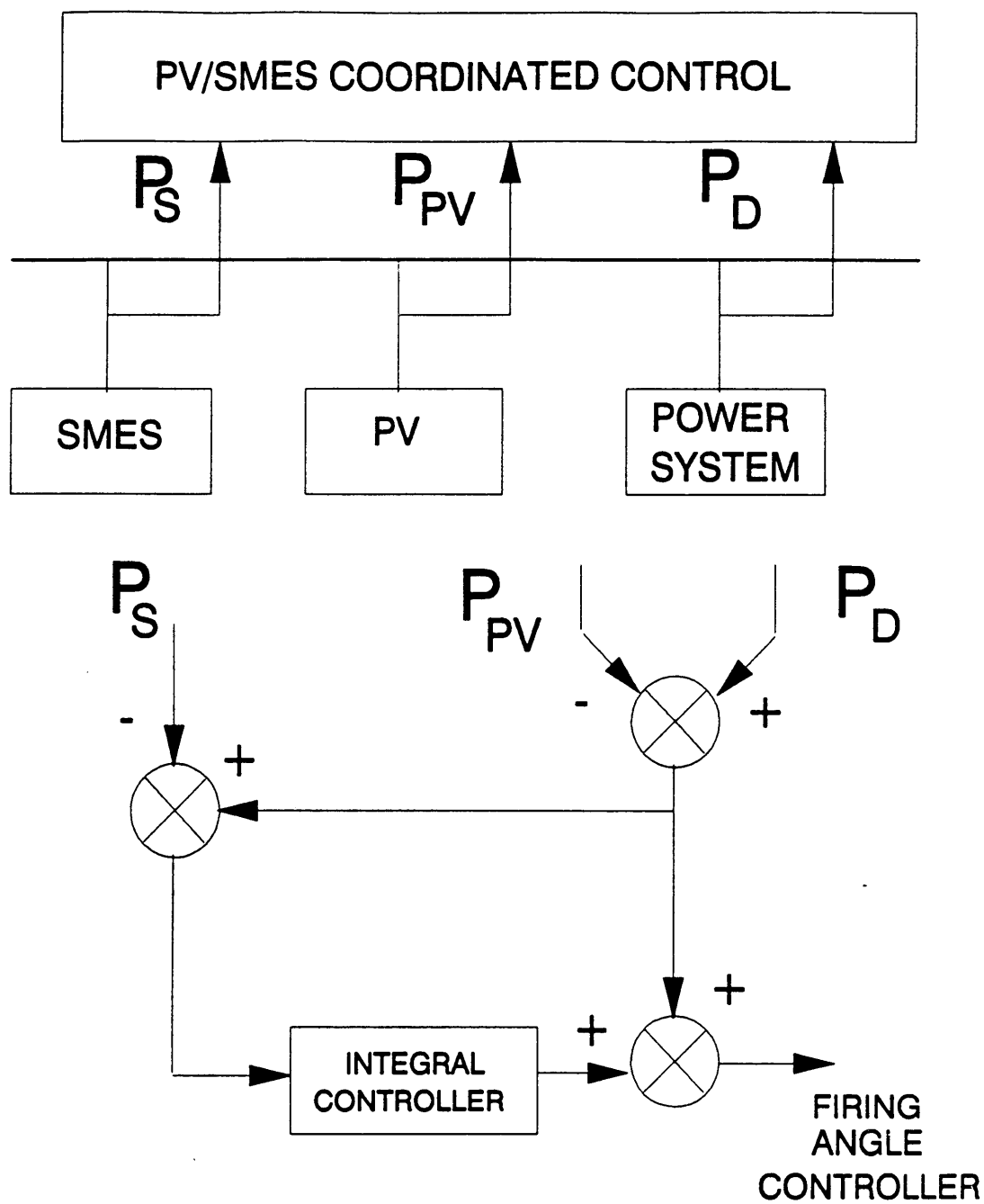


Figure 5. Schematic for combined PV/SMES system.

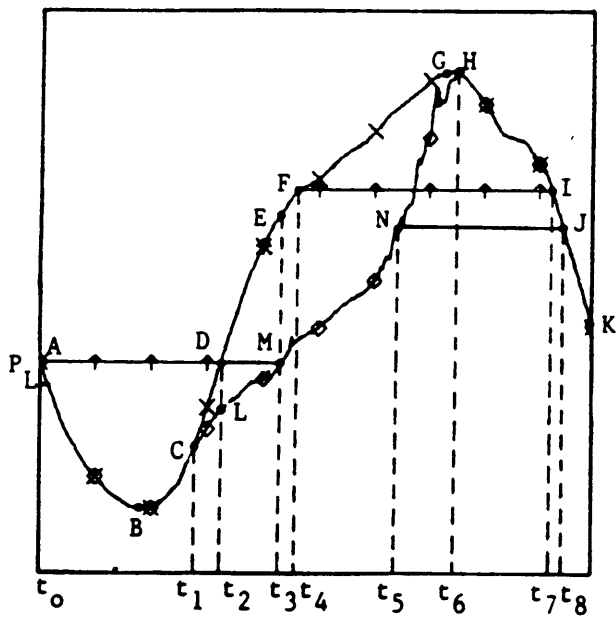
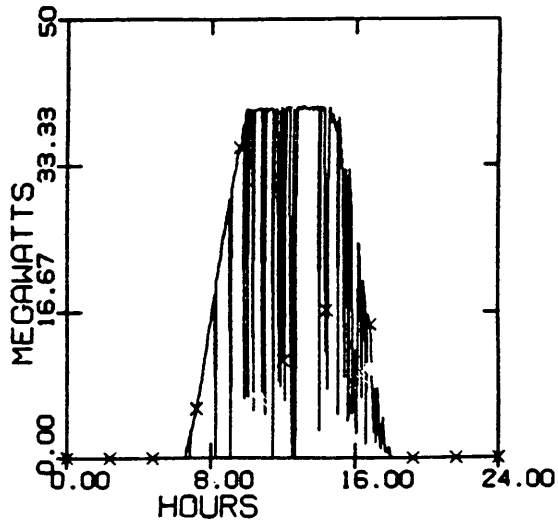


Figure 6. Schematic diagram to demonstrate the operation scheme.

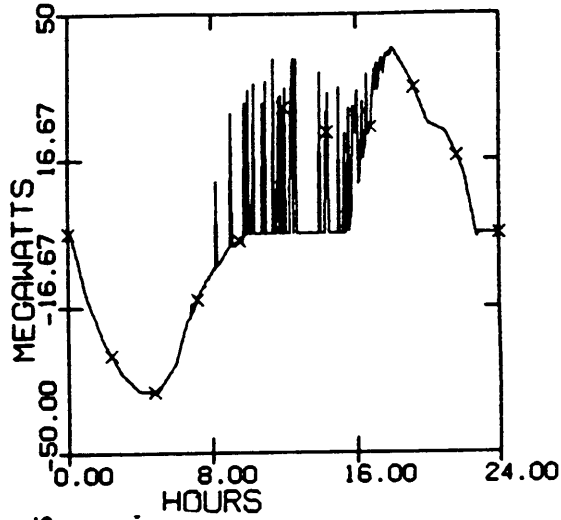
PV output on a sunny day

7a



SMES output on a sunny day

7b



x ORIGINAL LOAD CURVE

◇ MODIFIED BY PV-SMES

7c

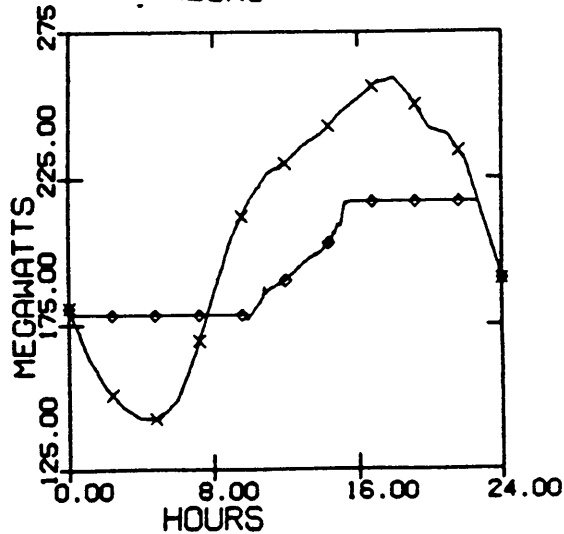


Figure 7. Load curve with/without coordinated PV/SMES operation on a sunny day.

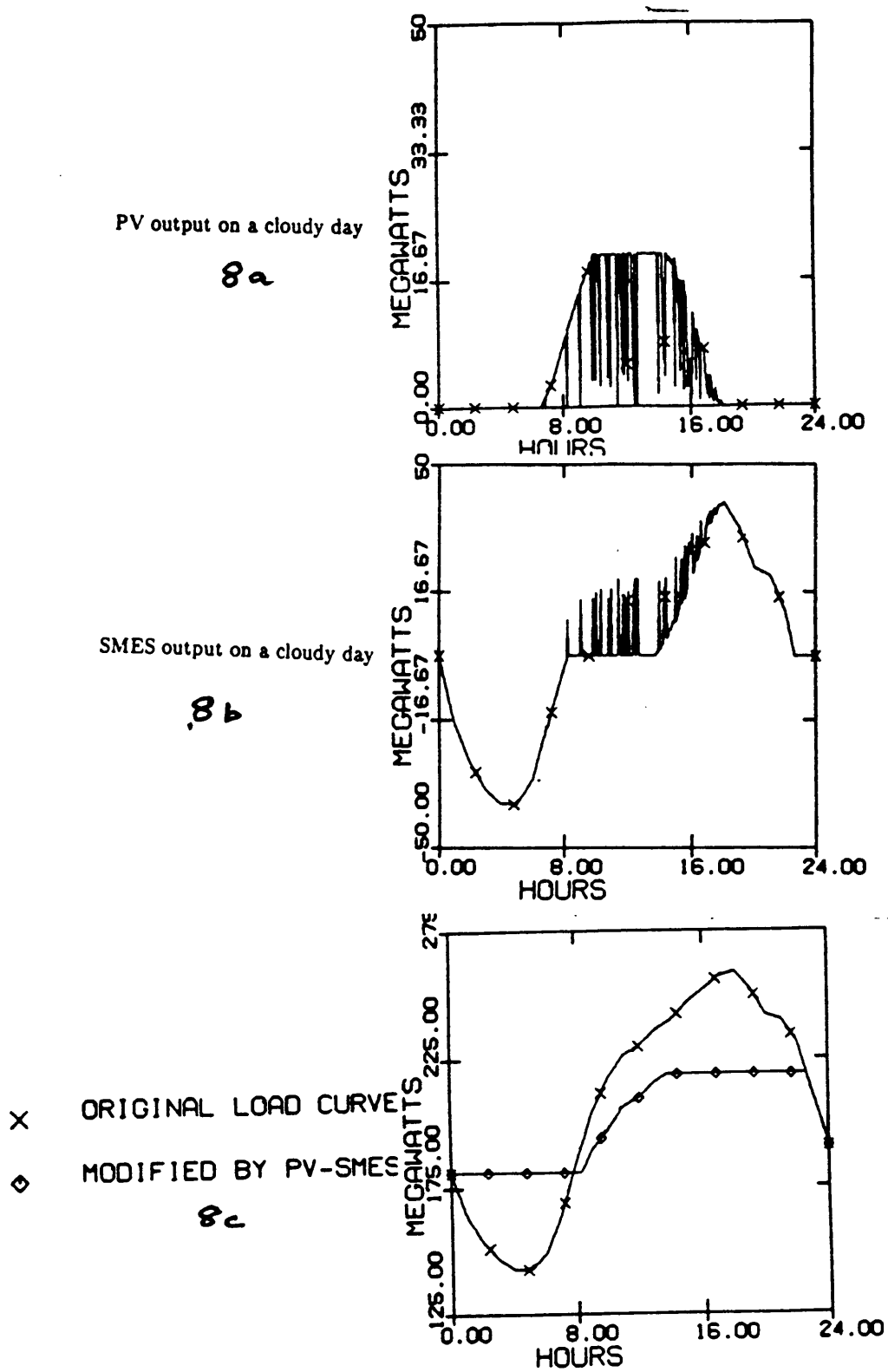
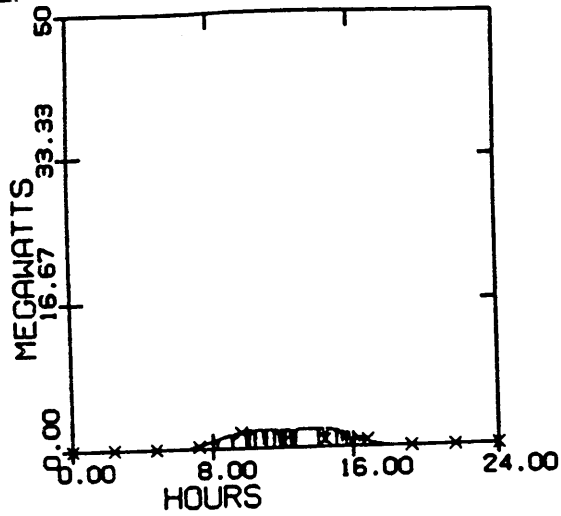


Figure 8. Load curve with/without coordinated PV/SMES operation on a cloudy day.

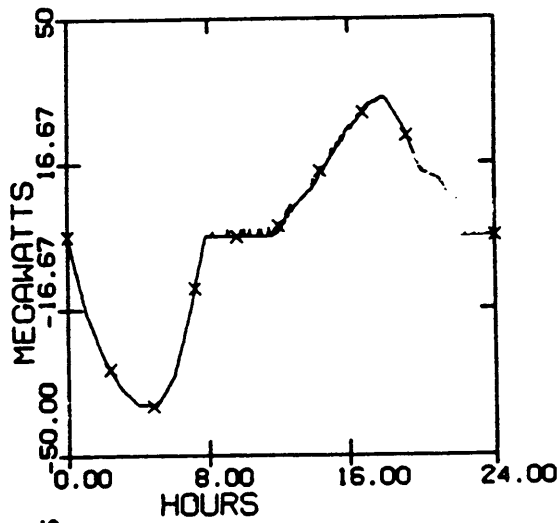
PV output on a rainy day

9a



SMES output on a rainy day

9b



X ORIGINAL LOAD CURVE
◇ MODIFIED BY PV-SMES

9c

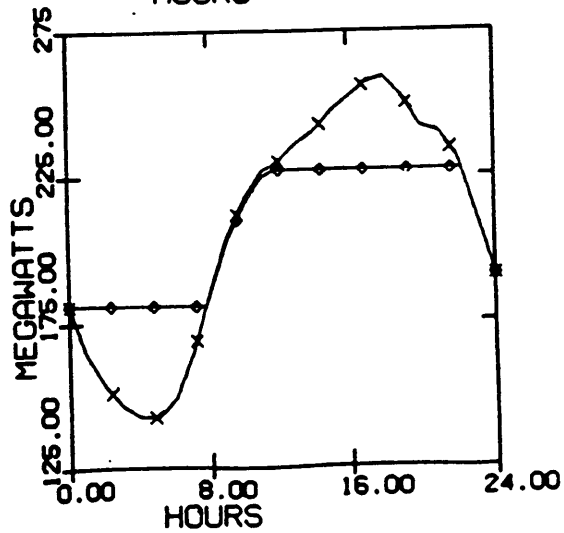


Figure 9. Load curve with/without coordinated PV/SMES operation on a rainy day.

3.0 Application of SMES in an asynchronous link between Power Systems.

The objective of this chapter is to introduce the concept that SMES can be incorporated into a back-to-back DC link and to show that a SMES/DC link provides some unique benefits for interconnected operation. With a SMES/DC link a SMES can be shared between two or more neighbouring power systems. The SMES/DC link enables energy storage, asynchronous connection and interchange of power between neighbouring utilities. The various operating modes for a two link system is shown. A model of such a system has been developed, and all the operating modes have been demonstrated. The control of such a system is also demonstrated using EMTP simulation. This chapter also demonstrates significant economic benefits for a SMES/DC link that can be obtained over pure interchange or SMES operation alone.

3.1 Basic Principle

In the conventional SMES storage applications the SMES is connected parallel across the system as shown in figure 10. When the SMES is connected in series across two systems, it combines the benefits of DC transmission and storage. The SMES functions simultaneously as a storage device and a smoothing reactor needed for smoothing out the ripples in the dc current, and limiting the rate of rise of dc current during faulty and transient conditions.

Figure 11 shows the configuration of a SMES in a series connection. The converters generate a lot of harmonics. The ac/dc converters on both sides are 12 pulse converters are fed from wye-wye and wye-delta transformers to reduce the current harmonics on the ac side. The DC voltage at the terminal of the converter is related to the delay firing angle α_1 by

$$VD_1 = 3 \times \frac{\sqrt{2}}{\pi} \times V_1 \left[\frac{\cos \alpha_1 + \cos(\alpha_1 + \mu_1)}{2.0} \right] \quad [3.1]$$

Where V_1 is the ac line-line voltage at the secondary winding of the transformer, and μ_1 is the commutation overlap angle for converter 1.

The DC voltage at the terminal of converter 2 is related to the delay firing angle α_2 by

$$VD_2 = 3 \times \frac{\sqrt{2}}{\pi} \times V_2 \left[\frac{\cos \pi - \alpha_2 + \cos(\pi - \alpha_2 - \mu_2)}{2.0} \right] \quad [3.2]$$

Where V_2 is the ac line-line voltage at the secondary winding of the transformer, and μ_2 is the commutation overlap angle for converter 2.

When α_1 is in the range of 5 degrees to about 90 degrees converter 1 is operated in the rectifier mode-power is injected from the ac side to the dc side. When α_1 is in the range of 90 degrees to about 165 degrees converter 1 is operated in the inverter mode - power is injected from the dc side to the ac side. These operation modes can also be performed by converter 2 by controlling α_2 . Since converter 1 and converter 2 can be operated in either mode bidirectional power flow is possible.

Because of the inductive nature of the superconducting magnet, its operation is governed by

$$V_m = V_{d1} - V_{d2} = L_m \times \frac{dI_d}{dt} \quad [3.3]$$

where V_m is the voltage across the magnet, L_m is the inductance of the magnet, and I_d is the current flowing in the magnet. The energy stored by the magnet, E_s is given by

$$E_s = \frac{1}{2} \times L_m \times I_d^2 \quad [3.4]$$

Since V_m is the difference between V_{d1} and V_{d2} , V_m is also be controlled by manipulating α_1 and α_2 . When V_m is positive, I_d and E_s would increase and the SMES system is in the charging mode. When V_m is negative I_d and E_s would decrease and the SMES system is in the discharging mode. When V_m is close to zero I_d and E_s would remain unchanged and the SMES system is in the standby mode.

A SMES/DC link interconnecting two power systems provides 13 basic modes of operation. Tables 1 to 5 show the various operating modes for the two systems.

Table 1 shows the operating conditions for three SMES charging modes. The superconducting magnet can be charged from area 1 alone, from area 2 alone, or simultaneously from area 1 and from area 2.

Table 2 shows the operating conditions for three SMES discharging modes. The energy stored in the SMES system can be discharged to area 1 alone, to area 2 alone, or simultaneously to both area 1 and area 2.

Table 3 shows the operating conditions for three SMES standby modes. Although the SMES system undergoes no charging or discharging (I_d remains unchanged), power interchange can still take place between area 1 and area 2 through the control of V_{d1} and V_{d2} .

Table 4 shows the operating conditions for the simultaneous SMES charging and power interchange modes. Using these operating modes, power injected from one area can be used partially to charge up the SMES system and partially supply the need of the other area.

Table 5 shows the operating conditions for the simultaneous SMES discharging and power interchange modes. With these modes, the need of one area can be met partially by the power supplied by the other area and partially by the discharging of the SMES system.

Table 1. Operating Conditions for SMES Charging Modes

	MODE 1 Charging SMES from area 1	MODE 2 Charging SMES from area 2	MODE 3 Charging SMES from area 1 and area 2 simultaneously
Converter 1	Rectifier Mode	Standby Mode	Rectifier Mode
α_1	5° to 90°	$\approx 90^\circ$	5° to 90°
V_{d1}	> 0	≈ 0	> 0
Converter 2	Standby Mode	Rectifier Mode	Rectifier Mode
α_2	$\approx 90^\circ$	5° to 90°	5° to 90°
V_{d2}	≈ 0	< 0	< 0
SMES	Charging Mode	Charging Mode	Charging Mode
I_d	increasing	increasing	increasing
V_m	> 0	> 0	> 0
E_s	increasing	increasing	increasing

Table 2. Operating Conditions for SMES Discharging Modes

	MODE 4 Discharging SMES to area 1	MODE 5 Discharging SMES to area 2	MODE 6 Discharging SMES to area 1 and area 2 simultaneously
Converter 1	Inverter Mode	Standby Mode	Inverter Mode
α_1	90° to 165°	$\simeq 90^\circ$	90° to 165°
V_{d1}	< 0	$\simeq 0$	< 0
Converter 2	Standby Mode	Inverter Mode	Inverter Mode
α_2	$\simeq 90^\circ$	90° to 165°	90° to 165°
V_{d2}	$\simeq 0$	> 0	> 0
SMES	Discharging Mode	Discharging Mode	Discharging Mode
I_d	decreasing	decreasing	decreasing
V_m	< 0	< 0	< 0
E_s	decreasing	decreasing	decreasing

Table 3. Operating Conditions for SMES Standby Modes

	MODE 7 Standby	MODE 8 Power Transfer from area 1 to area 2	MODE 9 Power Transfer from area 2 to area 1
Converter 1	Standby Mode	Rectifier Mode	Inverter Mode
α_1	$\simeq 90^\circ$	5° to 90°	90° to 165°
V_{d1}	$\simeq 0$	> 0	< 0
Converter 2	Standby Mode	Inverter Mode	Rectifier Mode
α_2	$\simeq 90^\circ$	90° to 165°	5° to 90°
V_{d2}	$\simeq 0$	> 0	< 0
SMES	Standby Mode	Standby Mode	Standby Mode
I_d	unchanged	unchanged	unchanged
V_m	$\simeq 0$	$\simeq 0$	$\simeq 0$
E_s	unchanged	unchanged	unchanged

Table 4. Operating Conditions for simultaneously SMES Charging Modes and power interchange modes.

	MODE 10 Power Transfer from area 1 to area 2 SMES charging from area 1	MODE 11 Power Transfer from area 2 to area 1, SMES charging from area 2
Converter 1	Rectifier Mode	Inverter Mode
α_1	5 to 90°	90° to 165
V_{d1}	> 0	< 0
Converter 2	Inverter Mode	Rectifier Mode
α_2	90° to 165°	5° to 90°
V_{d2}	> 0	< 0
SMES	Charging Mode	Charging Mode
I_d	increasing	increasing
V_m	> 0	> 0
E_s	increasing	increasing

Table 5. Operating Conditions for simultaneously SMES Discharging Modes and power interchange modes.

	MODE 12 Power Transfer from area 1 to area 2 SMES discharging from area 1	MODE 13 Power Transfer from area 2 to area 1, SMES discharging from area 2
Converter 1	Rectifier Mode	Inverter Mode
α_1	5 to 90°	90° to 165
V_{d1}	> 0	< 0
Converter 2	Inverter Mode	Rectifier Mode
α_2	90° to 165°	5° to 90°
V_{d2}	> 0	< 0
SMES	Discharging Mode	Discharging Mode
I_d	decreasing	decreasing
V_m	< 0	< 0
E_s	decreasing	decreasing

3.1.1 Multiterminal system.

The basic principle of SMES/DC link can be extended to asynchronous interconnection between n (n is any positive integer greater than 2) Figure 12 shows the schematic diagram of a SMES/DC link for n interconnected areas. Each area is connected to the link through an ac/dc converter which can be operated in the rectifier, inverter or standby mode. The DC voltage at the terminal of converter is related to the firing angle α_i by

$$VD_i = 3 \times \frac{\sqrt{2}}{\pi} \times V_i \left[\frac{\cos \alpha_i + \cos(\alpha_i + \mu_i)}{2.0} \right] \quad [3.5]$$

The ac/dc converters are connected in series to form a multiterminal DC link which allows power interchange between any two or more of the n areas. The SMES system is connected in series with the converter so that the SMES system can be charged from or discharged to any of the n areas. The operation of the SMES system is governed by

$$V_m = V_{d1} + \sum_2^n V_{di} = L_m \times \frac{dI_d}{dt} \quad [3.6]$$

Depending on whether V_m is positive, negative or zero the SMES system can be operated in charging, discharging or standby modes. The number of modes would increase. Each area can operate individually, interchange power with any one or more of the areas.

3.2 *Modelling of the system to demonstrate the modes*

3.2.1 The basis for selection of model parameters.

As there was only one detailed conceptual design of a large scale SMES by Bechtel/EPRI, the parameters chosen by them were used as a guide for deciding the model parameters.

Ratings for the model parameters

Size	11000Mwh
Current Rating	750KA
Voltage across magnet	4Kv
Inductor	140.8H
Tap Range	+/- 25% ..

Basis for Model ParametersThe EPRI/Bechtel design was for 5500 Mwh with a current rating of 750 KA.A typical summer load curve for SE and SC was chosen from [16] as the load profiles of the two systems.The size was chosen as 11000 Mwh as two systems would be using the SMES. The peak rating was chosen as 9000 MW and 8400 MW to ensure that the selected size was around 8% of the system capacity.(10% is recommended).The current rating was retained as it was already high, the voltage across the inductor was therefore doubled.The inductor was therefore 140.8 H. The tap were given a range of +-25%.The commutating resistance was chosen as a very low value so as to prevent commutation failure.This can be achieved in practical systems by paralleling several converter transformers.

3.2.2 Mathematical modelling of the system.

Let the load curves be $P_1(t)$ and $P_2(t)$ for the two systems 1 & 2 Let the charging times be t_{c1} and t_{c2} for system 1 & 2 to charge up the SMES to its share.

$$E_1 = \int_0^{t_{c1}} P_1 dt$$

$$\simeq \Delta t \times \sum P_{1i}$$
[3.7]

$$E_2 = \int_0^{t_{c2}} P_2 dt$$

$$\simeq \Delta t \times \sum P_{2i}$$
[3.8]

Δt for this case is a 10 minute interval. i varies in 10 minute intervals.

$$E_t = E_0 \pm E_{1i} \pm E_{2i}$$
[3.9]

Where E_t is the energy at the end of current interval i and E_0 is the stored energy at interval $(i - 1)^{th}$ E_{1i} and E_{2i} can either be positive negative or zero depending on whether the respective system is charging/discharging or not using the SMES.

The coil stores energy in the magnetic field. The current level is a function of the amount of charge and is given by

$$I_d = \sqrt{\frac{2 \times E_t}{L}}$$
[3.10]

Let VDO_1 and VDO_2 represents the ideal no load DC voltages it is related to the ac line to line voltages V_{LL1} and V_{LL2} by

$$VDO_1 = 3 \times \frac{\sqrt{2}}{\pi} \times V_{LL1} \quad [3.11]$$

$$VDO_2 = 3 \times \frac{\sqrt{2}}{\pi} \times V_{LL2} \quad [3.12]$$

Assuming the ac power = dc power (i.e neglecting losses)

$$P_{ac1} \simeq P_{dc1} \quad [3.13]$$

$$P_{ac2} \simeq P_{dc2} \quad [3.14]$$

This would enable to determine the dc voltage required to meet the power demand as the current has been determined from equation 3.10.

$$P_{dc1} = VD_1 \times I_d \quad [3.15]$$

$$P_{dc2} = VD_2 \times I_d \quad [3.16]$$

Once VD_1 and VD_2 are determined the respective alphas can be computed from the following equations. The effect of firing angle is to reduce the average direct voltage by $\cos \alpha$, there is a further drop due to commutation overlap. As α can range from almost 0 to 180 degrees VDO can range from VDO to -VDO as the current cannot reverse because of the unidirectional property of the valves negative voltage in conjunction with positive current represents reversed power.

$$VD_1 = VDO_1 \cos \alpha_1 - I_d \times R_{c1} \quad [3.17]$$

$$VD_2 = VDO_2 \cos \beta_2 + I_d \times R_{c2} \quad [3.18]$$

$$\alpha_2 = \pi - \beta_2 \quad [3.19]$$

$$V_m = VD_1 - VD_2 \quad [3.20]$$

R_c is called equivalent commutating resistance and although it is the ratio of drop of direct voltage to direct current it consumes no power.

$$R_{c1} = \frac{3}{\pi} \times X_{c1} \quad [3.21]$$

$$R_{c2} = \frac{3}{\pi} \times X_{c2} \quad [3.22]$$

where

X_{c1} = commutating reactance for converter transformer 1

X_{c2} = commutating reactance for converter transformer 2

The converter bridges present associated complex load S_1 S_2 ac load. For each S_i the powerfactor $\cos \phi_1$ can be adjusted via bridge firing angle α_i . The ac power can be equated to the dc power if the converter is considered ideal.

$$P_{ac} \simeq P_d \quad [3.23]$$

$$Q \simeq P_d \tan \phi \quad [3.24]$$

The computer model calculates the parameters α V_d , I_d , V_m , E_s and Q for the entire day using a 10 minute interval. The inputs are the two load curves. It was tested for specific operating schemes mentioned below. The model was validated using the BPA data which is shown in the appendix.

3.2.3 Description of the operating schemes.

These define possible mode of operation for each hour of the day. There are 5 schemes considered for this study which together make use of all the thirteen modes of operation. The list below shows the operating scheme over a 24 hour period. Let the SMES be charged for a period of t_c hours, let the period when it is charged and standby be denoted t_{s1} , let the discharge period be t_d , let the period when it is discharged and standby be t_{s2} .

Scheme A This scheme has system 1 alone using SMES and system 2 having no interaction with SMES. The SMES is charged by system 1 for a period t_c , then it is in standby for a period of t_{s1} , it then discharges to system 1 for a period t_d , it then is again in a standby mode for the period t_{s2} . Modes used in this scheme are 1, 7 and 4.

Scheme B This is similar to scheme A but the charging/ discharging is done by system 2. Modes used in this scheme are 2, 7 and 5.

Scheme C This has both the systems going through the cycle of charging, standby, discharging and standby again. Modes used are 3, 7 and 6.

Scheme D This scheme makes use of power transfer and SMES functions. For the full period (i.e. $t_c + t_{s1} + t_d + t_{s2}$) there is a power transfer from system 1 to system 2. Simultaneously system 1 is using the SMES to charge up the SMES for the period t_c , it is standby for the period t_{s1} , it then discharges to system 2 for the period t_d . The modes used are 10, 8 and 12.

Scheme E This scheme again makes use of power transfer and SMES functions. For the full period (i.e. $t_c + t_{d1} + t_d + t_{s2}$) there is a power transfer from system 2 to system 1. Simultaneously system 2 is charging the SMES for period t_c , it is in standby for the period t_{s1} and it discharges to system 1 for the period t_d . The modes used are 11, 9 and 13.

10 plots describe each scheme of operation. The input charge/discharge curves of the 2 converters, the corresponding voltages, SMES current and energy are in one page. The converter alphas and their reactive power consumption in the following page (as the reactive power is a strong function of the alphas as brought out in the following discussion). Schemes C, D, E are described in figures 13 to 18.

Scheme	0-7 Hrs	8-9 Hrs	10-19 Hrs	20-24 Hrs
A	1	7	4	7
B	2	7	5	7
C	3	7	6	7
D	10	8	12	8
E	11	9	13	9

3.2.4 Discussion of results.

The variation of α is fundamental in understanding the extreme reactive power consumption. The α curve shows the high value for low power levels and comes down to a minimum say α_{\min} then goes up again. This is different for a conventional HVDC scheme where they are always low(5-15).The initial high α is due to initial circulating current which is determined so that the entire charge cycle can be met, for this case α_{\min} is 15 degrees if a lower circulating current was chosen there would be a possibility that all the charging power available could be used for charging.The α is also high in the standby mode where it is almost 90 degrees.The power factor angle ϕ is strongly dependent on α and is related by the following equation, μ is generally very small.

$$\cos \phi = \frac{\cos \alpha + \cos \mu}{2} \quad [3.25]$$

The reactive power consumption by the converters is given by $VI \times \sin \phi$ and is high for the period of high α This is a drawback the reactive power consumption can be reduced by increasing the tap range of the converter transformer.Other alternatives is to limit the value of α which means all the charging power available is not utilized and therefore there would not be a flattening of the load curve.Another way to reduce reactive power consumption is to use a bypass switch during standby mode this would therefore disconnect SMES from the system during that period of time.

3.3 *EMTP simulation.*

The objective of this simulation is to demonstrate a feasible control scheme to ensure, the operation of all the thirteen modes discussed previously and to show a smooth transition between them. Figure 19 shows the model circuit diagram used for the simulation.

3.3.1 Basis for the model parameters.

The 24 hour load curve was scaled down to 2.4 seconds, as the EMTP is a transient analysis program this would ensure the transition of modes which takes place during the period of the day. The parameters defined were the maximum rated current of 750 KA and a maximum voltage of 4 Kv across the SMES. For the scaled load curves and for the maximum rated current, results in an inductor of 2.3 mh. This ensures the model being tested for rated current and voltage values. The AC system voltage value was chosen as 110 KV as it is a rated H.V line transmission value. The converter generates a lot of harmonics predominantly the 5th, 7th, 11th and 13th antiresonant-filters are added in the circuit which offer low impedance to these frequencies and high impedance to for the fundamental component.

3.3.2 The Control Scheme.

The control scheme for the SMES/DC link is different from that of a conventional DC asynchronous link. For a HVDC link, usually one converter is operated in rectifier mode and performs constant current control(C.C), while the other converter is operated in the inverter mode and performs constant extinction angle (C.E.A) control. In a SMES/DC link the current is either increasing/decreasing or constant(during pure transfer mode) the control of the link is obtained by controlling the voltage across the inductor. The Voltage V_m across the inductor is given by

$$V_m = V_{d1} - V_{d2} = L_m \frac{dI_d}{dt} \quad [3.26]$$

Also the energy stored is given by

$$E_s = \frac{1}{2} \times L_m \times I_d^2 \quad [3.27]$$

V_m for the SMES scheme is controlled by the converter alphas. Using the convention +VE P charges the SMES and -VE P discharges the SMES. P_{d1} and P_{d2} are the the command signals from the respective power systems. The sign and type of variation of the power command signal of the two systems with time gives the 13 modes of operation as described earlier. This is shown in table 6.

The block diagram for the alpha calculation is shown in figure 20. The Power signal for the alpha calculator is actually a composite signal consisting of the power demand signal

Table 6. Mode / Power signal correspondence.

PD1	V/K	PD2	V/K	MODE
POSITIVE	VARYING	0	-	1
0	-	POSITIVE	VARYING	2
POSITIVE	VARYING	POSITIVE	VARYING	3
NEGATIVE	VARYING	0	-	4
0	-	NEGATIVE	VARYING	5
NEGATIVE	VARYING	NEGATIVE	VARYING	6
0	-	0	-	7
POSITIVE	CONSTANT	NEGATIVE	CONSTANT	8
NEGATIVE	CONSTANT	POSITIVE	CONSTANT	9
POSITIVE	VARYING	NEGATIVE	CONSTANT	10
NEGATIVE	CONSTANT	POSITIVE	VARYING	11
POSITIVE	CONSTANT	NEGATIVE	VARYING	12
NEGATIVE	VARYING	POSITIVE	CONSTANT	13

and the error signal (which is difference between the measured and delivered power) which is limited to some absolute value PLIMIT. Once the EMTP model has been set up, this value is obtained iteratively (by setting different values and looking at the response).For the set up considered it was found to be 20MW. The measurement of the SMES power can be either in the ac or dc side.The ac side has current harmonics the dc side has voltage harmonics.The ac side measurements are chosen for this study. The gain parameter is adjusted to get the best possible response. A low value gives a slow response, a very high value makes the system unstable.The optimum value is found by varying this parameter and studying the response.For the given system a value of 200 was found to be the best. The initial estimate for α for both the converters (n in case of a multiterminal system) for any mode of operation can be computed from the independant signals(P_{d1} , the current level I_d in the SMES which can be measured, and the no-load DC voltage which can be calculated) by using the basic converter equations shown below. The maximum value of $\cos \alpha$ is subject to a maximum of ± 1 which defines the theoretical limit for charging/discharging the SMES.

This model has two six pulse bridges in series.

Converter 1

$$P_{d1} = 2 \times V_{D1} \times I_d \quad [3.28]$$

As stated before the DC voltage is related to the no-load DC voltage.

$$V_{d1} = V_{D01} \times \cos \alpha - I_d \times R_{c1} \quad [3.29]$$

From which α is computed as

$$\alpha_1 = \arccos \frac{\left[\frac{P_{C1}}{2 \times I_d} + I_d R_c \right]}{VDO_1} \quad [3.30]$$

Converter 2

$$P_{d2} = -2 \times V_{D2} \times I_d \quad [3.31]$$

As stated before the DC voltage is related to the no-load DC voltage.

$$V_{d2} = VDO_2 \times \cos \beta_2 + I_d \times R_{c2} \quad [3.32]$$

From which α is computed as

$$\beta_2 = \arccos \frac{\left[\frac{P_{C2}}{2 \times I_d} + I_d R_c \right]}{VDO_2} \quad [3.33]$$

$$\alpha_2 = \pi - \beta_2 \quad [3.34]$$

where

P_{c1} = Composite power signal for area 1

P_{c2} = Composite power signal for area 2

Imposing limits on alpha α minimum is chosen as 5 degrees. The maximum is $180 - \gamma - \mu$ where γ is the extinction angle and μ is the overlap angle. The γ is obtained by running a particular operation sequence and ensuring there is no commutation failure. The discharge phase is more critical as the converter is in inverter mode and the chance of commutation failure are higher (i.e the voltage across the valve reverses before the cur-

rent goes to zero).As the magnitude of current is very high the extinction angle is very high.For the case set up 25 degrees was required.

Computation of μ As the transformer secondary has inductance there is a finite time for current to commute from one bridge to another during that interval there are 3 switches on (instead of the normal 2).The logic used to estimate the commutation overlap is by monitoring the switch status for one set of bridges.As time step of one degree is used, at every time step the number of switches on is monitored.When more than two switches is on it represents commutation.The number of time steps (degrees) for which more than two switches is on is integrated for one cycle (360 degrees).There would be six switches going through overlap at some part of the cycle.Therefore the number obtained would have to be divided by 6 to give the overlap angle.

Therefore with γ and μ the upper limit of α is set.To prevent the system from responding to random variations, individual bridge alphas are allowed to change a max/min of ± 30 degrees over the α computed for the previous bridge.

Testing of the model

The EMTP model was tested for all the thirteen modes of operation. Schemes discussed in section 3.2.3 was used on the scaled load curves to demonstrate the different modes. Figures 21 to 37 show the results of the simulation of schemes A, C and D Figure 21, 26 & 33 show the demand and response of converter 1 for schemes A, C and D. Similarly Figure 22, 27 & 34 shows the demand and response of converter 2.Figures.23, 24, 28, 29 & 35, 36 shows the variation of α and μ for converter 1 and converter 2. and figures 25, 30, 37 indicate the variation of current. There is slight reduction in current when there is no SMES operation, this is due to the resistances in the circuit. There are

two additional figures shown for scheme C Figure 31 shows the DC voltage across the two converters, Figure 32 shows the voltage across the superconducting inductor.

Scheme A results Figure 18a and 18b indicates the tracking of the SMES is fine until the time when α hits the limit of 5 degrees, therefore the charging power limit has been reached. This response can be improved by increasing the circulating current. The simulation was done for a starting current of 239KA.

Scheme B results As this case is similar to the previous the results are identical except that the converters have been interchanged the figures for this scheme have not been included.

Scheme C results Figures 19a to 19e indicate the operation of this scheme. In this scheme both the systems are charging and discharging. Here the SMES response is much better as the alpha limit is not reached, this is because as both the systems are charging and the current level at any instant is high enough to meet the required power command signals.

Scheme D results Figures 20a to 20e indicate the operation of this scheme. The operation of this scheme is most critical as there is simultaneous charging (from system 1) and discharging to system 2. The tracking of the charge signal is difficult as for higher power levels the current level is very low as the rate of increase of power is greater than the rate of increase of current. (because of simultaneous charging and discharging) This problem is circumvented by starting the operation of the SMES at a higher starting current. This mode of operation was started an initial starting current of 500KA. There is therefore a

limit of the maximum power that can be transferred to ensure both power transfer and to charge at the required rate.

Scheme E results This is similar to scheme D only the converters are flipped. The figures for this scheme have not been included.

From the results the conclusions that can be drawn are the amount of current flowing in the SMES will decide the feasibility of operation of the different modes, a high current level will ensure operation of all the modes, but this would result in a very high reactive power consumption at low power levels. (This was discussed in 3.2.4) Also Scheme D shows there is a limit to the maximum power that can be transferred when a certain charging profile is required.

3.4 Economic savings in operating system with SMES used as an asynchronous link.

This section shows the savings in operational cost by operating an SMES/DC link. Two test systems have been set up for this purpose each consisting of base load, intermediate loads and peak load units. The generator cost data for the two systems are shown in table 7. All systems operate so as to minimize generation cost. Since this section compares the operational cost using economic dispatch for various scenarios the economic dispatch equations are outlined in section 3.4.1. The test system data is obtained from

typical power system data [17].As some of the scenarios considered use SMES power, the methodology for estimating the same is discussed in section 3.4.2.

3.4.1 Economic Dispatch equations

Let c_i be the cost in dollars of producing energy in the generator units at bus i .The overall system production cost therefore will be

$$C = \sum_{i=1}^n c_i \$/hr \quad [3.35]$$

The generated real power PG_i accounts for the major influence on c_i as the individual real generations are raised by increasing the prime- mover torques, and this requires an expenditure of fuel.The reactive power generation QG_i do not have any measurable influence on c_i because they are controlled by varying the field current.The individual production cost c_i of generation i is therefore for all practical purposes only a function of PG_i and therefore it can be written

$$C = \sum_{i=1}^n c_i(PG_i) \quad [3.36]$$

A set of generation variables PG_i must now be selected that will minimize the cost function subject to the equality and inequality constraints.

Table 7. Test System Data

SYSTEM 1				
Number	Type	I/O curve	Pmin/Pmax	Fuel Cost
9	Coalfired	$540 + 7.63 * P_i + .00156 * P_i^{**2}$	200/800	2.35
9	Oil fired	$310 + 7.92 * P_i + .00191 * P_i^{**2}$	75/300	6.15
9	Oil fired	$80 + 8.05 * P_i + .00485 * P_i^{**2}$	30/125	8.15
SYSTEM 2				
Number	Type	I/O curve	Pmin/Pmax	Fuel Cost
9	Coalfired	$500 + 7.00 * P_i + .0012 * P_i^{**2}$	200/800	1.15
9	Oil fired	$310 + 7.30 * P_i + .00171 * P_i^{**2}$	80/310	6.15
9	Oil fired	$78 + 7.8 * P_i + .004 * P_i^{**2}$	30/125	8.15

The equality constraints is neglecting losses the total power generated should be equal to the power demand.

$$\sum_{i=1}^n PG_i = P_d \quad [3.37]$$

The inequality constraints is that each generator is limited in operation to a maximum corresponding its rating and to some minimum value.

$$PG_{i \min} \leq PG_i \leq PG_{i \max} \quad [3.38]$$

Therefore

$$\frac{\partial C}{\partial x} = \lambda \quad N \text{ equations} \quad [3.39]$$

$$PG_{i \min} \leq P_i \leq PG_{i \max} \quad 2N \text{ inequalities} \quad [3.40]$$

$$\sum_{i=1}^n PG_i = P_d \quad [3.41]$$

The necessary conditions may be expanded slightly as shown in the set of equations.

$$PG_{i \min} \leq PG_i \leq PG_{i \max} \quad [3.42]$$

$$\frac{\partial C}{\partial x} = \lambda \quad [3.43]$$

$$PG_i = PG_{i \max} \quad [3.44]$$

$$\frac{\partial C}{\partial x} \leq \lambda \quad [3.45]$$

$$PG_i = PG_{i \min} \quad [3.46]$$

$$\frac{\partial C}{\partial x} \geq \lambda \quad [3.47]$$

The partial derivatives $\frac{\partial c_i}{\partial p_i}$ are referred to as incremental costs IC of generation. They represent the slope of the cost curve. As the unit for c_i is dollars per hour, the incremental cost unit must be in dollars per Megawatthour. For optimum dispatch the individual generators operate at equal incremental production costs. The economics of the SMES/DC link increases significantly when the incremental production cost of the two systems differ considerably.

Four cases have been investigated. For all the cases an economic dispatch is done using equations 3.35 to 3.47 and accordingly the generations have been allocated, subject to the minimum and maximum indicated in the test data. However when the SMES is in the scenario under study the minimum power for peak and intermediate units have been reduced to zero as the SMES is very fast responding and can therefore pick up peak and intermediate loads.

3.4.2 Cost of SMES power.

The load curve for this study has been approximated by step functions of one hour interval an economic dispatch is done every hour and by multiplying by the cost curve the cost of generating power for that hour is obtained. This is done for every hour from t_0 to

t_c the period for which the SMES is charged, the demand values considered for every hour is the original load curve values.

Cost of generating power from t_0 to t_c is C_0 \$.

When the SMES is there the load has a constant value say SP1 for the period t_0 to t_c . An economic dispatch is done for this load value and this multiplied for the period in hours between t_0 and t_c gives the cost when the SMES is also in the system.

Cost of generating power from t_0 to t_c with SMES also in system is C_n \$.

If S_r is the SMES rating the setting SP1 is obtained as follows

$$S_r = \int_{t_0}^{t_c} (L - SP1) dt \quad [3.48]$$

where

L = load curve value which is a function of time.

All the stored energy cannot be discharged. The efficiency of the SMES must be taken into account (around 92%). Define η as the efficiency.

The energy available for discharge is $S_r * \eta$.

The cost of Mwh of SMES energy.

$$\$/Mwh = \frac{(C_n - C_0)}{(S_r \times \eta)} \quad [3.49]$$

3.4.3 Case Studies.

Base case This is the reference case all the costs are compared with this as the standard. In this case system 1 and system 2 operate independently and there is no power interchange between them. Each system minimizes its own operating cost as if there is no connection between the two systems.

Case 1 In this case the SMES/DC link is used only as an asynchronous DC link between the two systems. The two systems are economically dispatched as one system. Power interchange takes place between them. Mode 8 and Mode 9 operation conditions shown in table 3 is applicable in this case.

Case 2 In this case the SMES/DC link functions only as an energy storage unit to each system. The SMES storage capacity of 11000 Mwh is shared equally between system 1 and system 2. Each system uses its own share of SMES to perform load-levelling and to minimize the operating costs. The two systems operate independently and no power interchange takes place between them. Each system charges up the SMES with power from its base load units during the off-peak hours and discharges the stored energy during peak hours to replace power from its peak and intermediate units.

Case 3 In this case the SMES/DC link performs both its asynchronous connection and energy storage functions. The SMES storage capacity is shared equally between system 1 and system 2. During the off-peak hours, each system operates independently and charges up its own share of SMES with its base-load unit. During the hours of peak demand, the two systems are treated as one system.

Case 4 System 1 and System 2 are interconnected by the SMES/DC link as shown in case 3. In this case the two systems are treated as one system during the charging period as well as the discharging period. During the charging period, the SMES is charged with power coming from the cheapest available units regardless of which units the units belong to. During the hours of peak demand the power from SMES discharge is dispatched to each system, according to their contribution to the charging of SMES, to shave of peak of the load curve. The two systems are then economically dispatched as one system. Table 8 shows that pure power interchange between the two systems (Case 1) results in a 3% reduction of the total operating cost for the two systems. Pure SMES operation (Case 2) reduces the total operating cost by 14.8%. Combining SMES operation and power interchange causes a 19.5% reduction of the total operating if SMES charging and discharging are shared equally between the two systems (Case 3) and a 20.9% reduction if SMES is charged from the cheapest units among the two systems and power from SMES discharge is dispatched proportional to the charging contribution from each system.

Converter rating To operate the SMES/DC link in many configurations would mean the converter would have to be sized accordingly. The converter limits the charge/discharge capability of the SMES. Define SPC & SPD as the load setting during charge and discharge, L_{\max} and L_{\min} be the peak demand and the minimum demand.

$$SPC - L_{\min} \leq PC_r$$

$$L_{\max} - SPD \leq PC_r \quad [3.50]$$

The charging time is normally less than the discharge therefore the Power Converter rating is normally defined by the charge inequality. When case 3 or 4 operation is con-

sidered one converter may be needed to charge up much higher power (If that area has a lot of cheap surplus power), therefore the converter would have to be sized accordingly. For the test cases a converter rating of 1250 MW would be sufficient for cases 1&2, but for cases 3 & 4 it would have to be increased to 2000 MW.

3.5 Battery storage in an asynchronous link

Battery storage systems have been considered in recent years for storage applications in power systems, some test facilities have been built and a demonstration plant is underway [18,19,20] SMES and battery systems have very fast responses. There are differences in the efficiency, the battery stores energy in chemical form. The electrochemical process gives an overall roundtrip efficiency of 70% to 75% for battery storage, however an SMES stores energy in magnetic field and the overall roundtrip efficiency is around 92%. Another major difference as the battery functions more like a voltage source the ac/dc converters will be better suited with voltage-source converters, [21] the SMES functions as a current source the ac/dc converters used will be current source converters, as the existing HVDC technology uses current source converters SMES has the advantage of using a tested technology. The capacity of the battery is an important function of temperature and rate of discharge. The batteries are normally designed for a 10 hour discharge rating, that is the full capacity is available over 10 hours but if the discharge is required over a shorter period the available capacity is reduced, thus batteries are generally oversized to meet the various discharge cycles. The SMES is limited in discharge only by the converter rating there is however a minimum charge al-

Table 8. Operating Cost comparison for interconnected operation with / without SMES

SYSTEM 1					
	Base Case	Case 1	Case 2	Case 3	Case 4
P_{A1}	7020	7020	7020	7020	7020
P_{B1}	1716.4	702	1155	0	0
P_{C1}	263.3	0	0	0	0
Interchange	0	1278	0	1235	1719.3
Storage	0	0	825	745	260.8
Operating Cost	285178	209179	254001	177001	163854
\$/h					
SYSTEM 2					
	Base Case	Case 1	Case 2	Case 3	Case 4
P_{A2}	7020	7020	7020	7020	7020
P_{B2}	1116.7	2394.7	715	1870	1870
P_{C2}	263.3	263.3	0	0	0
Interchange	0	-1278	0	-1235	-1719.3
Storage	0	0	665	745	1229.3
Operating Cost	160223	222990	125464	181853	188677
\$/h					
Total Operating Cost	445401	432169	379466	358854	352531
\$/H	100%	97.0%	85.2%	80.5%	79.1%

ways maintained in the SMES. Batteries are also limited by the cycle of operation as they are designed for a finite cycles of operation, but an SMES has no such limitation.

Cases 5, 6 and 7 a battery/DC link is used to interconnect system 1 & 2. These cases correspond to cases 2, 3 and 4 and battery efficiency is considered as 74%.

Table 9 shows the battery storage operation results. Case 5 results in a 11.9% saving in total operating cost. Battery storage operation combined with power interchange causes a 16.6% reduction and using the storage facilities equally between system 1 and system 2 results in a 16.6% reduction in total operating cost (Case 6), and a 18.1% reduction if the battery is charged from the cheapest units and power from battery discharge is dispatched proportional to the charging contribution of each system. Another point to note is that the corresponding savings for a SMES are better this is due to the higher roundtrip efficiency.

Table 9. Operating Cost comparison for interconnected operation with / without Battery

SYSTEM 1					
	Base Case	Case 1	Case 5	Case 6	Case 7
P_{A1}	7020	7020	7020	7020	7020
P_{B1}	1716.4	702	1265	0	0
P_{C1}	263.3	0	0	0	0
Interchange	0	1278	0	1347.5	1758.6
Storage	0	0	715	632.5	221.4
Operating Cost	285178	209179	261188	178051	164164
$\$/h$					
SYSTEM 2					
	Base Case	Case 1	Case 5	Case 6	Case 7
P_{A2}	7020	7020	7020	7020	7020
P_{B2}	1116.7	2394.7	830	2095	2095
P_{C2}	263.3	263.3	0	0	0
Interchange	0	-1278	0	-1347.5	-1758.6
Storage	0	0	550	632.5	1043.6
Operating Cost	160223	222990	131259	193565	200764
$\$/h$					
Total Operating Cost	445401	432169	392447	371616	364928
$\$/H$					
	100%	97.0%	88.1%	83.4%	81.9%

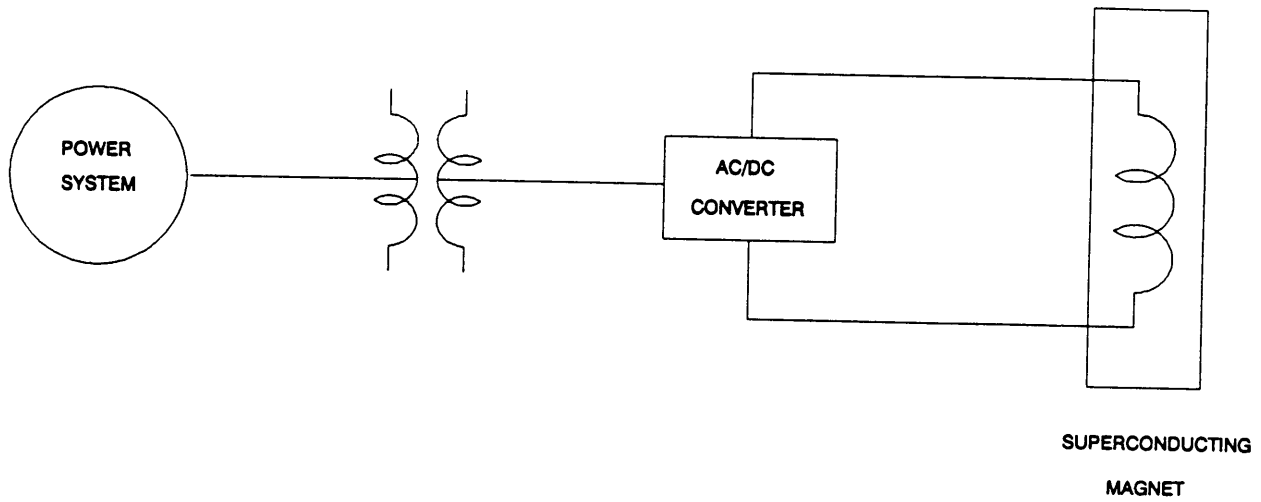


Figure 10. SMES connected to a power system in a conventional arrangement

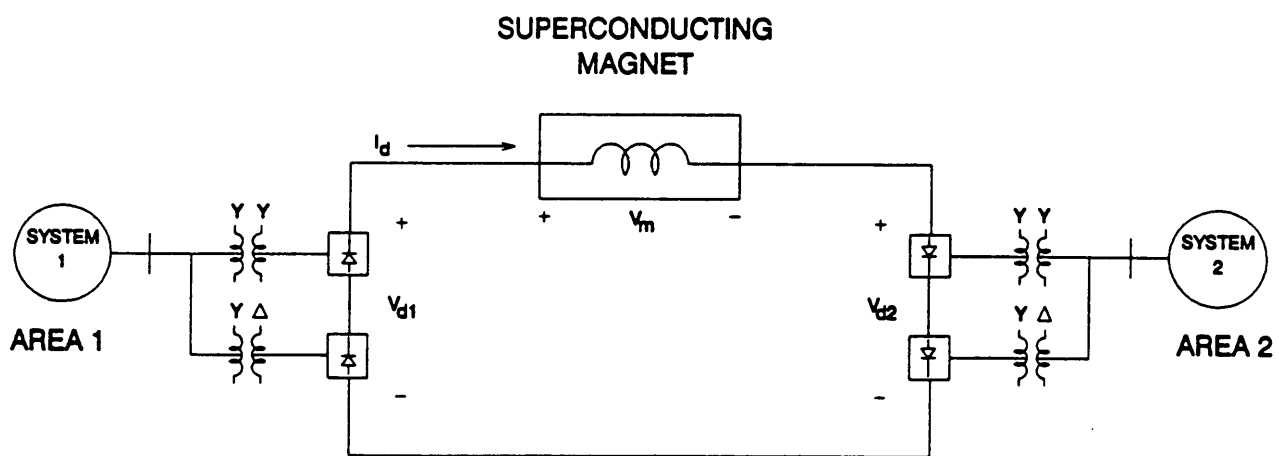


Figure 11. SMES/DC link connecting two power systems.

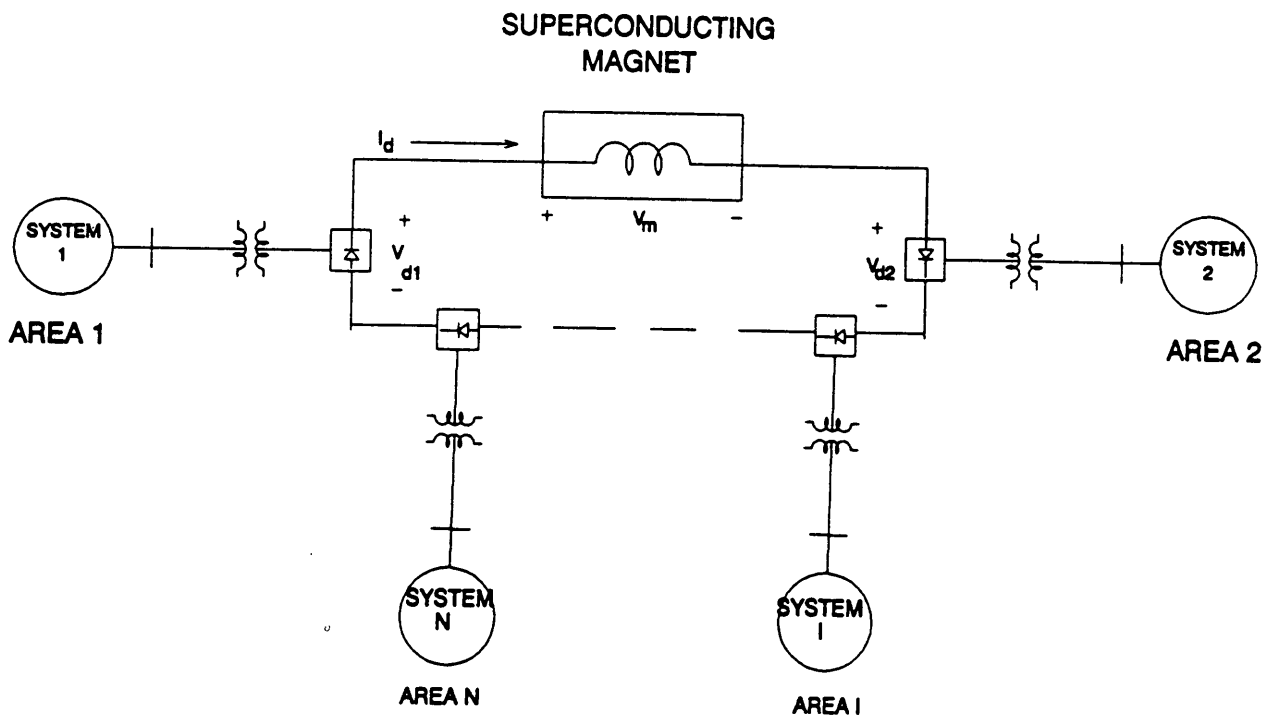


Figure 12. SMES/DC link connecting n power systems.

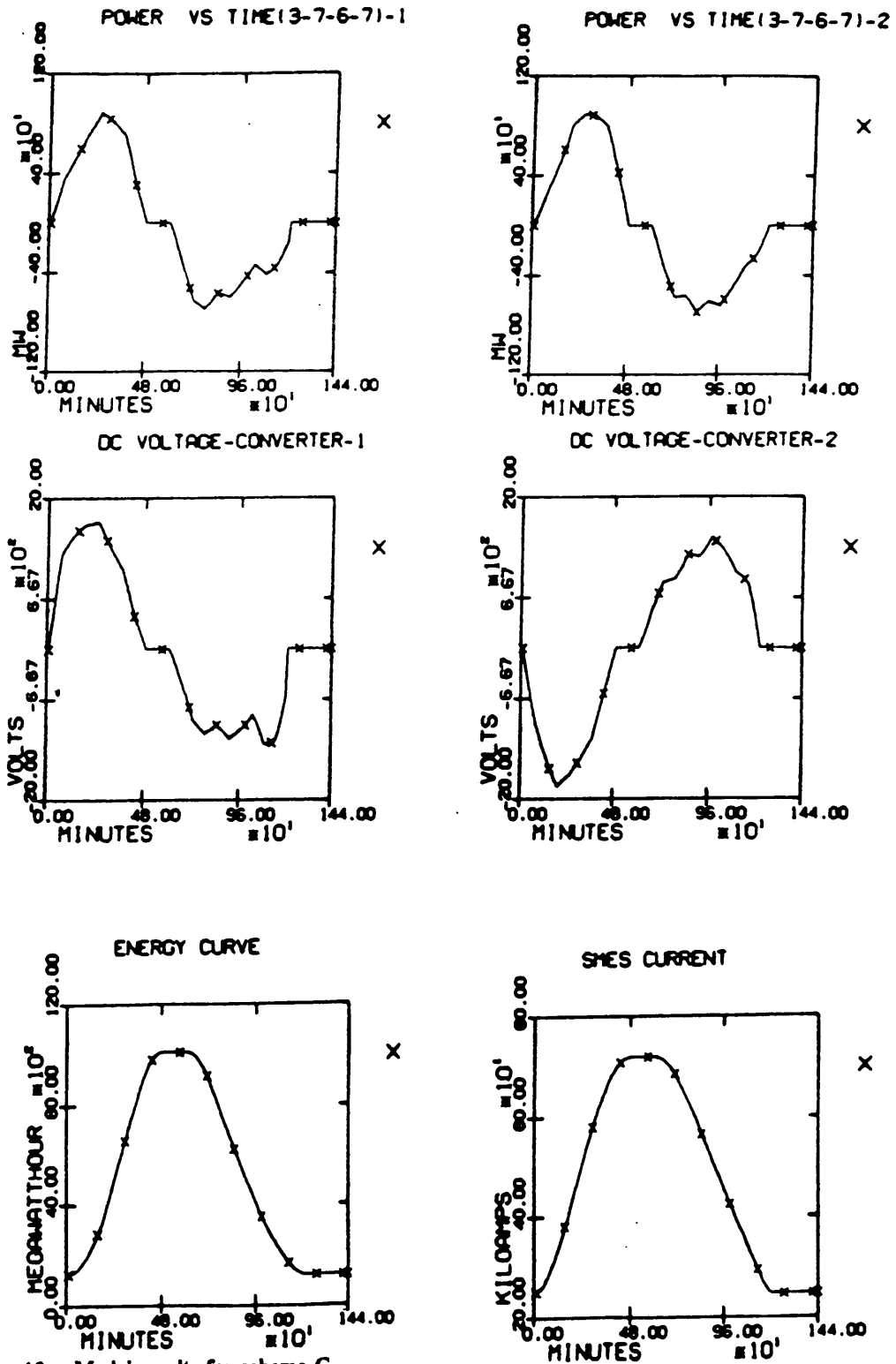


Figure 13. Model results for scheme C

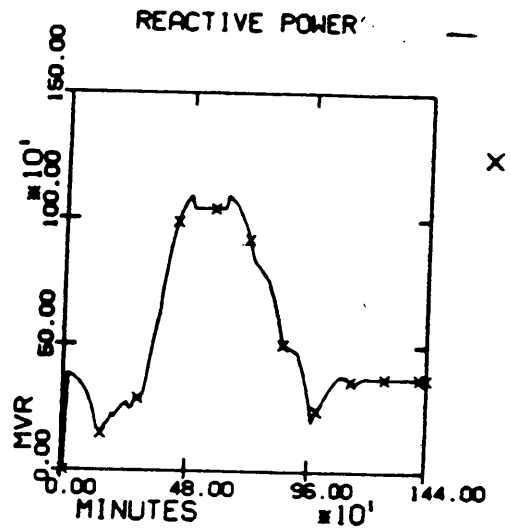
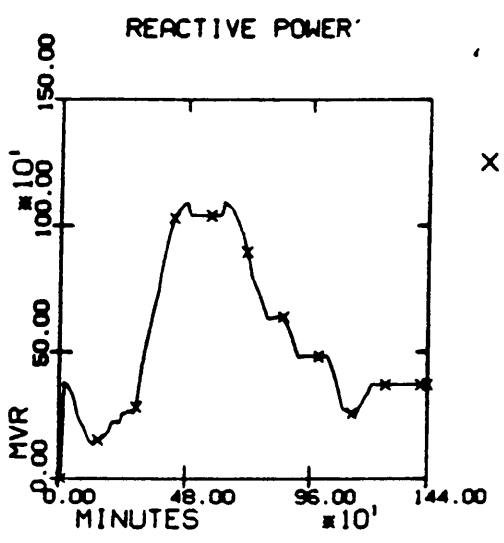
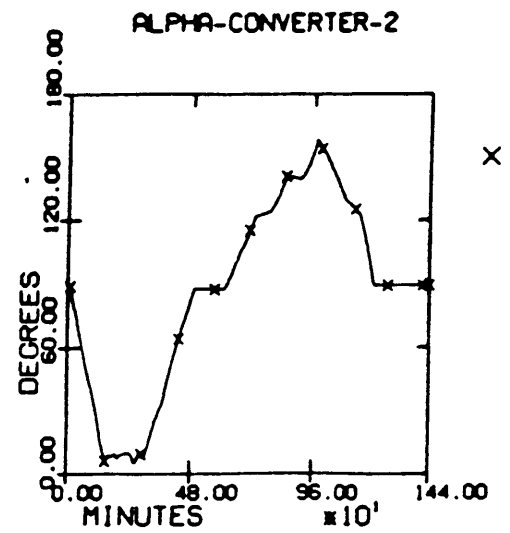
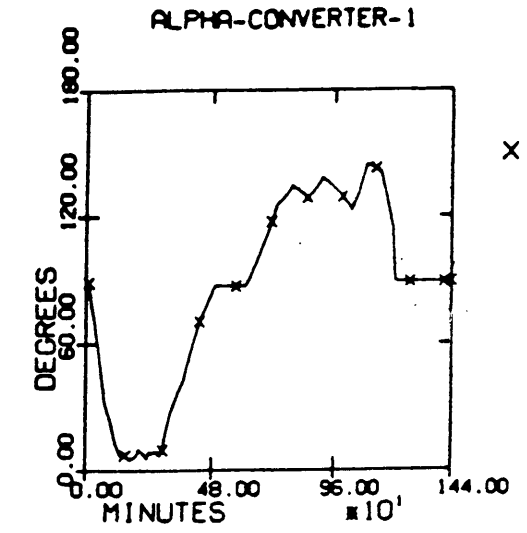


Figure 14. Model results for scheme C

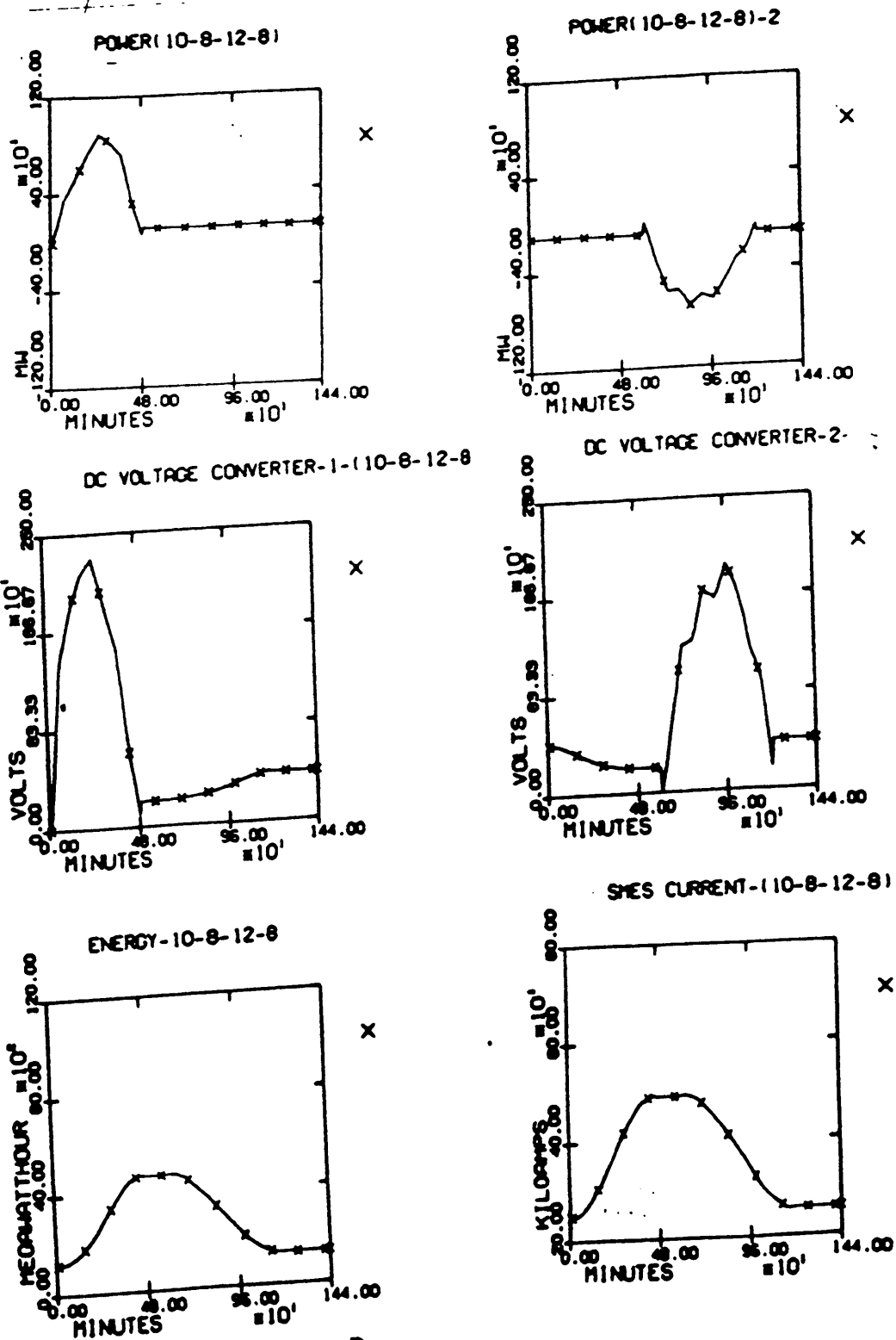


Figure 15. Model results for scheme D

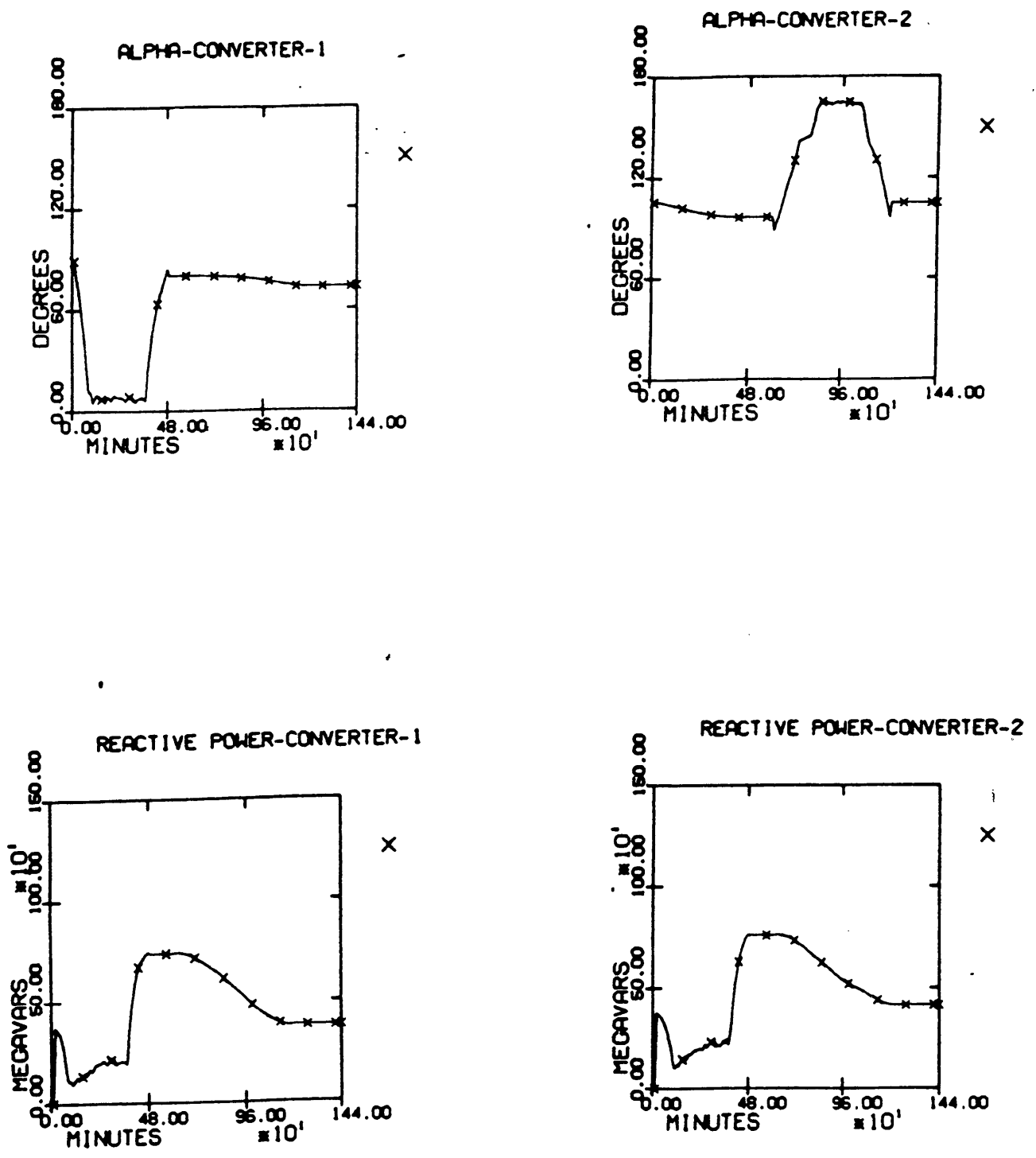


Figure 16. Model results for scheme D

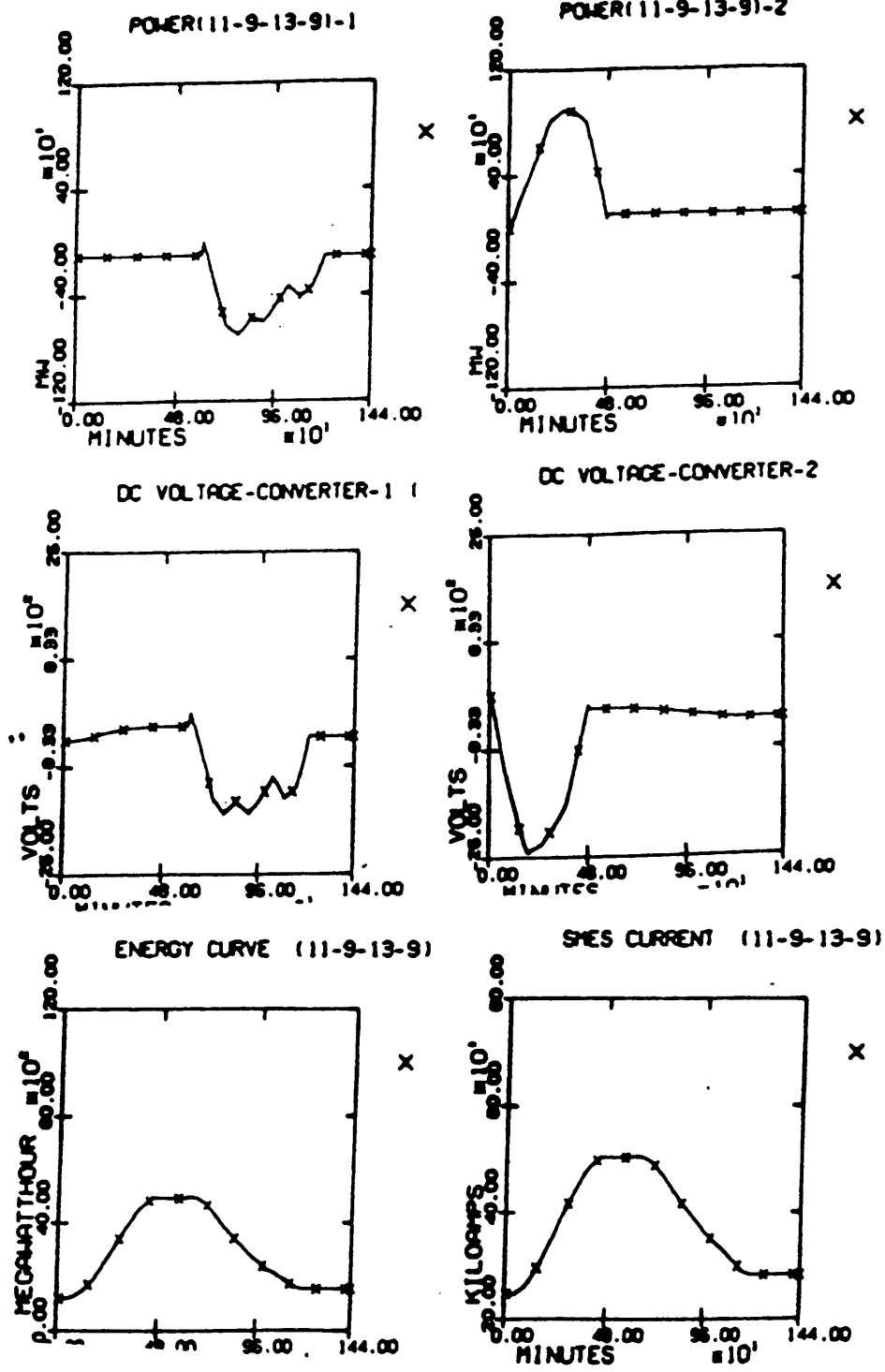


Figure 17. Model results for scheme E

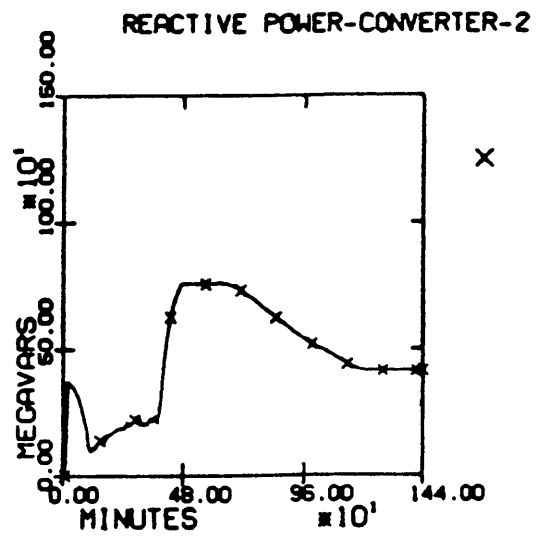
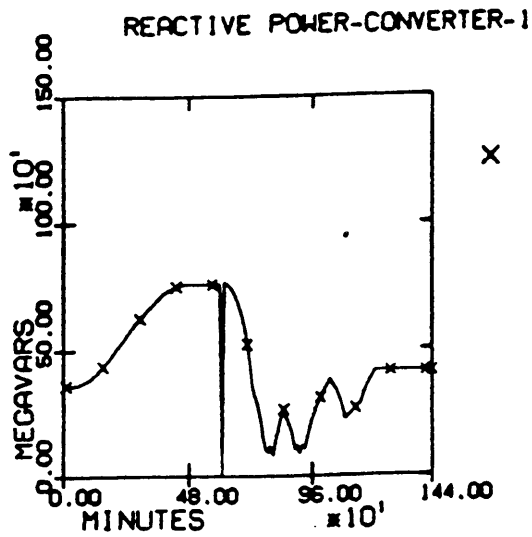
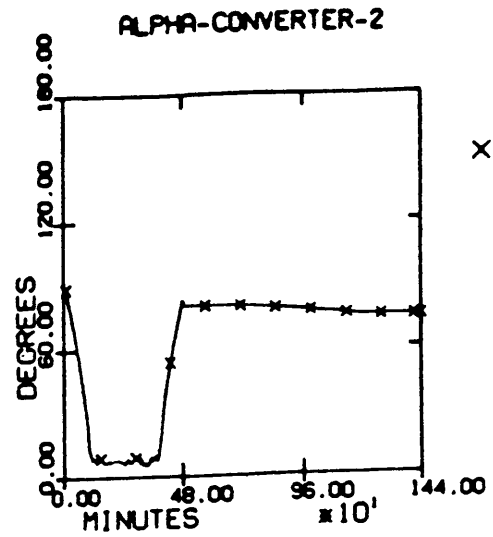
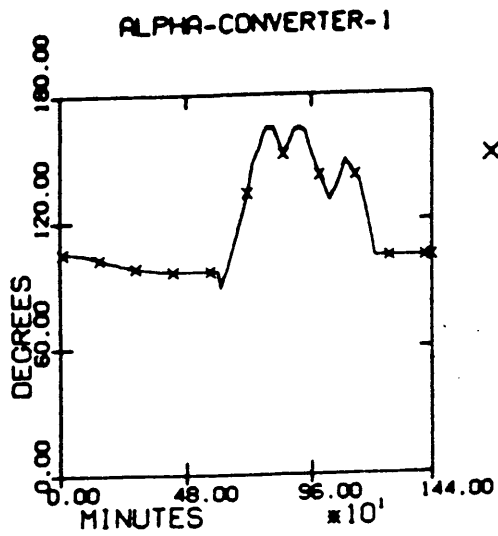


Figure 18. Model results for scheme E

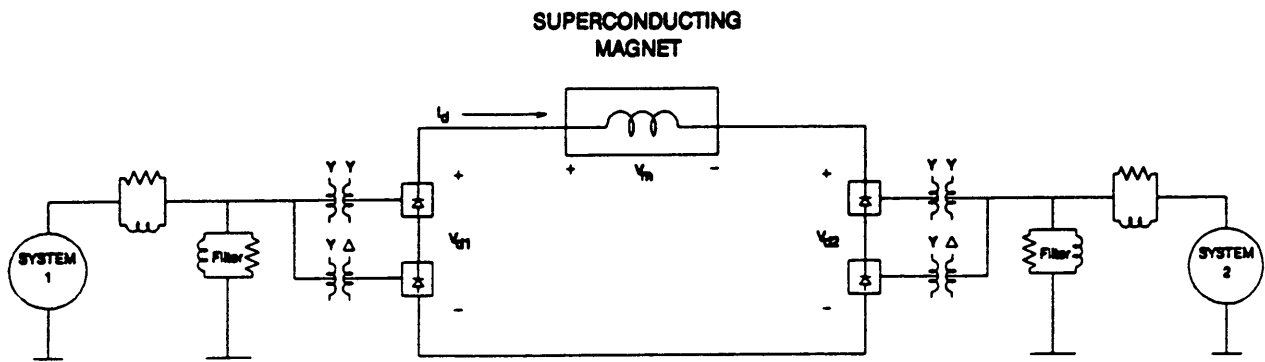


Figure 19. EMTP Model diagram

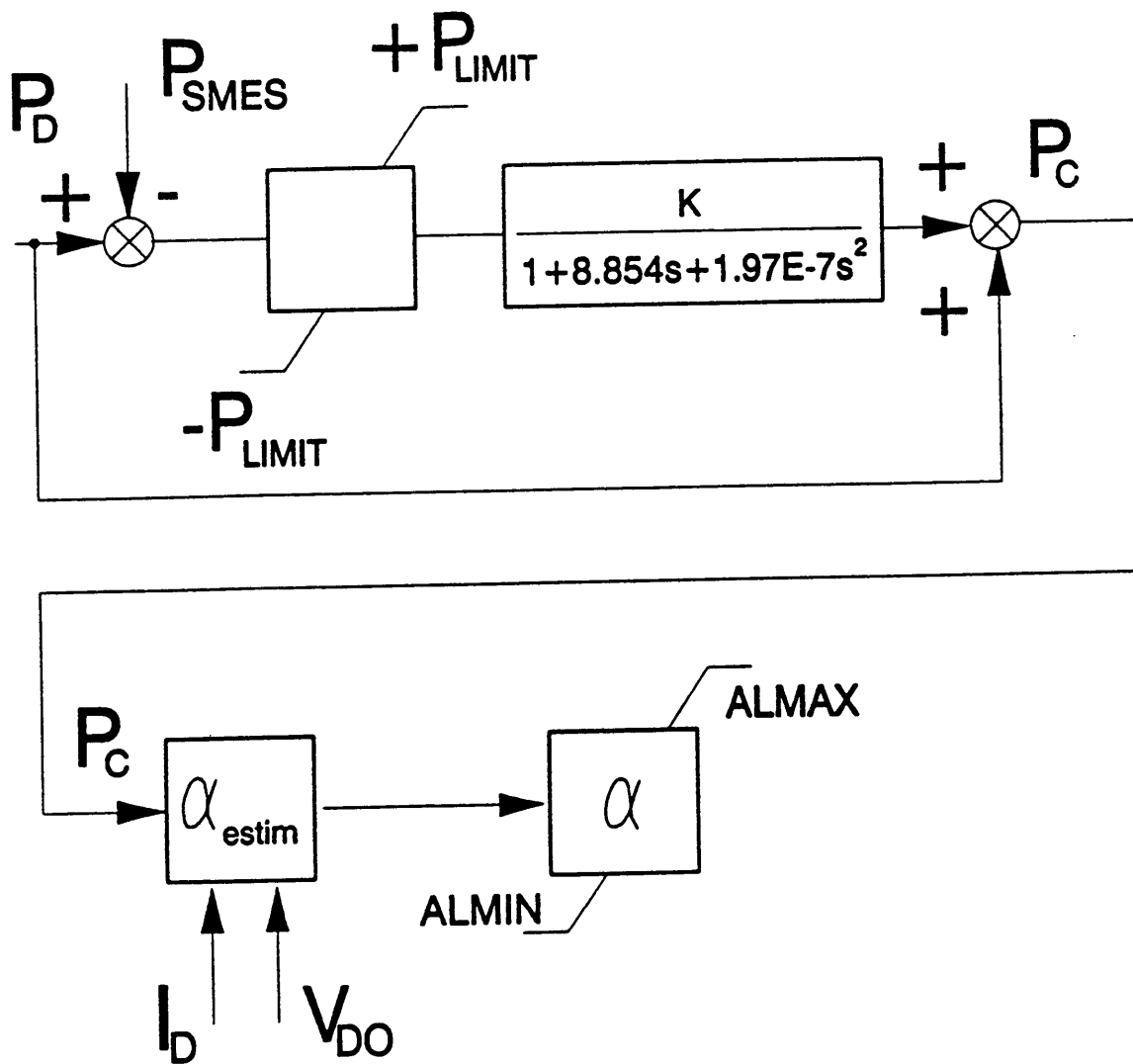


Figure 20. alpha calculator schematic

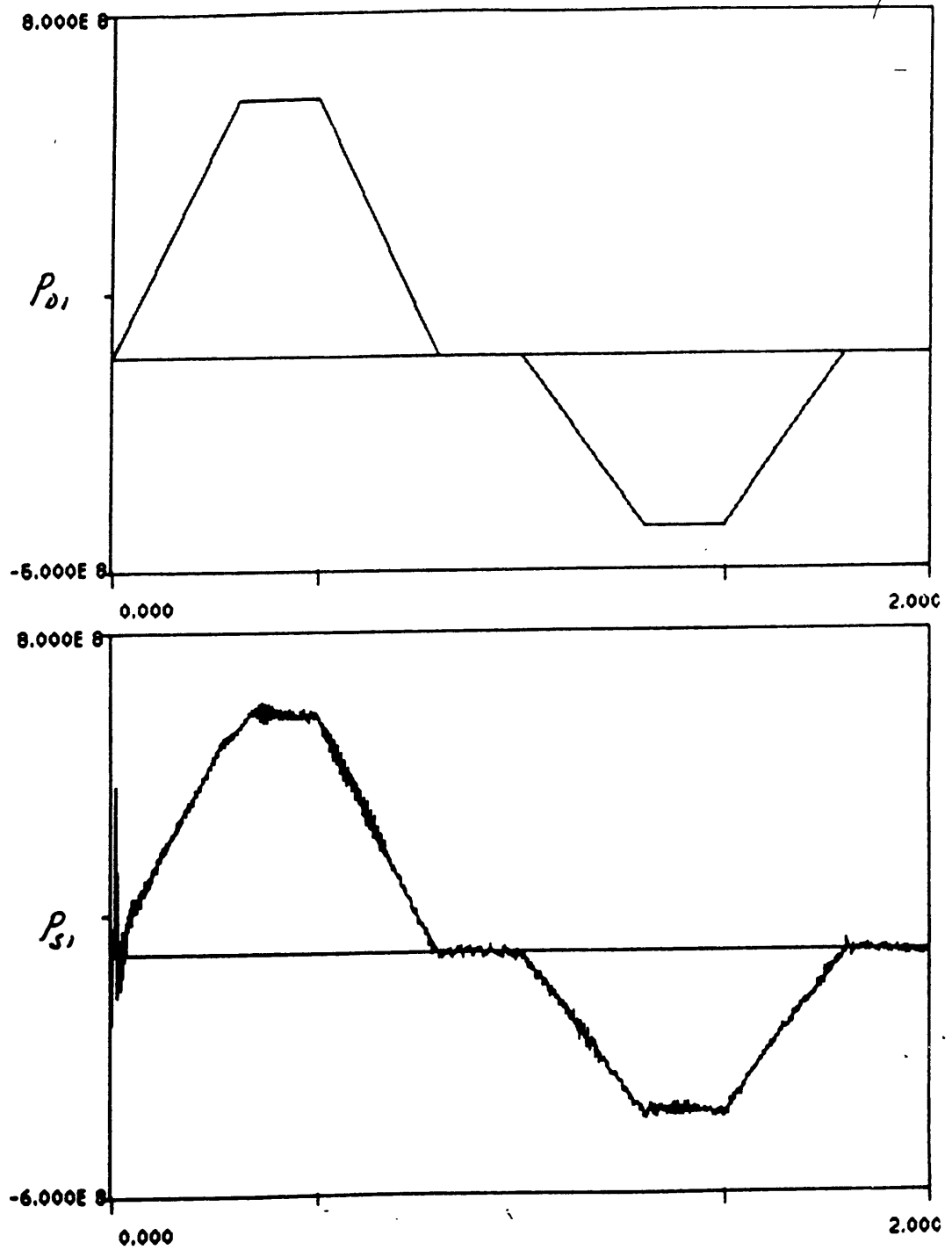


Figure 21. EMTP Model results scheme A

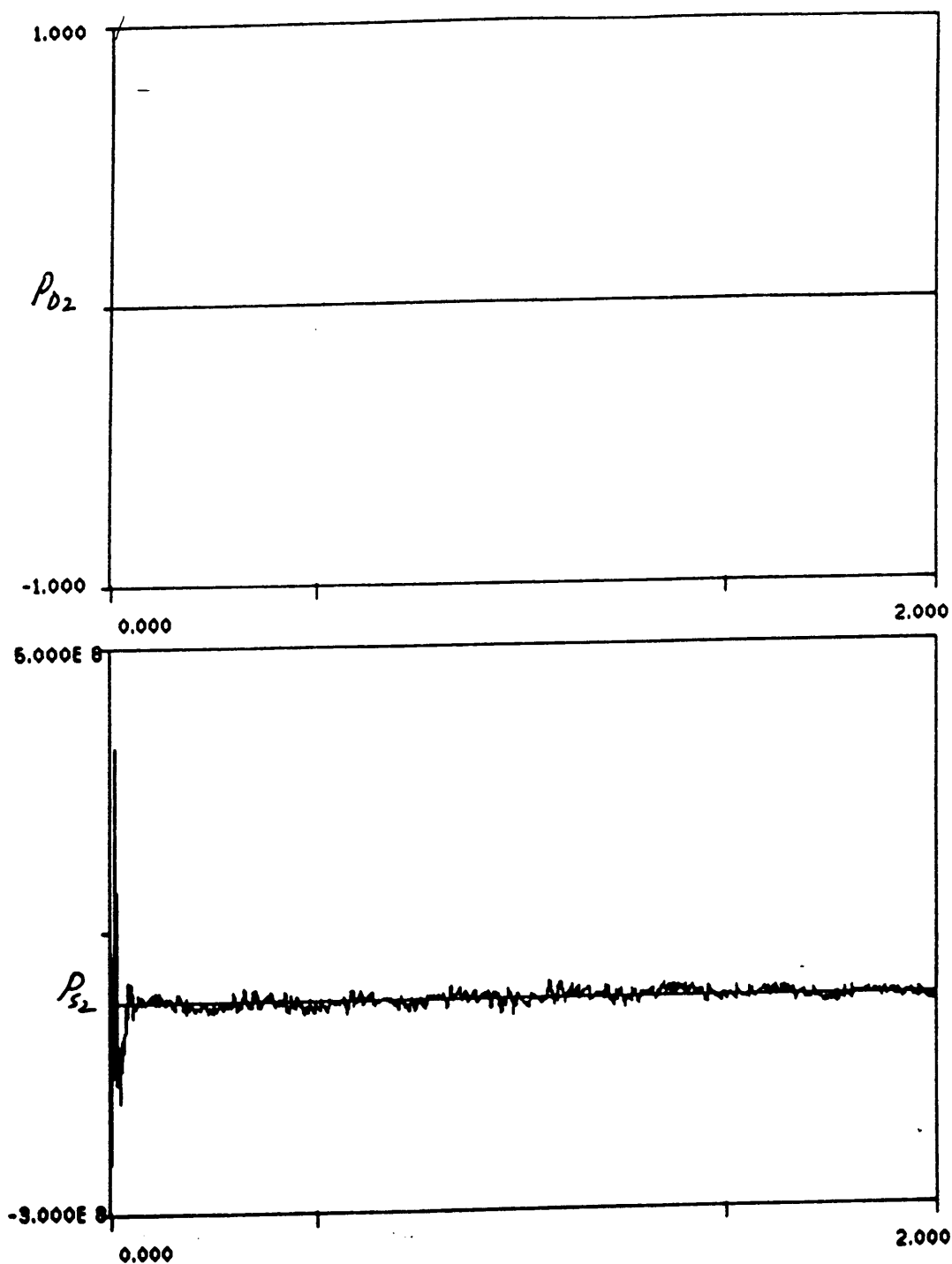


Figure 22. EMTP Model results scheme A

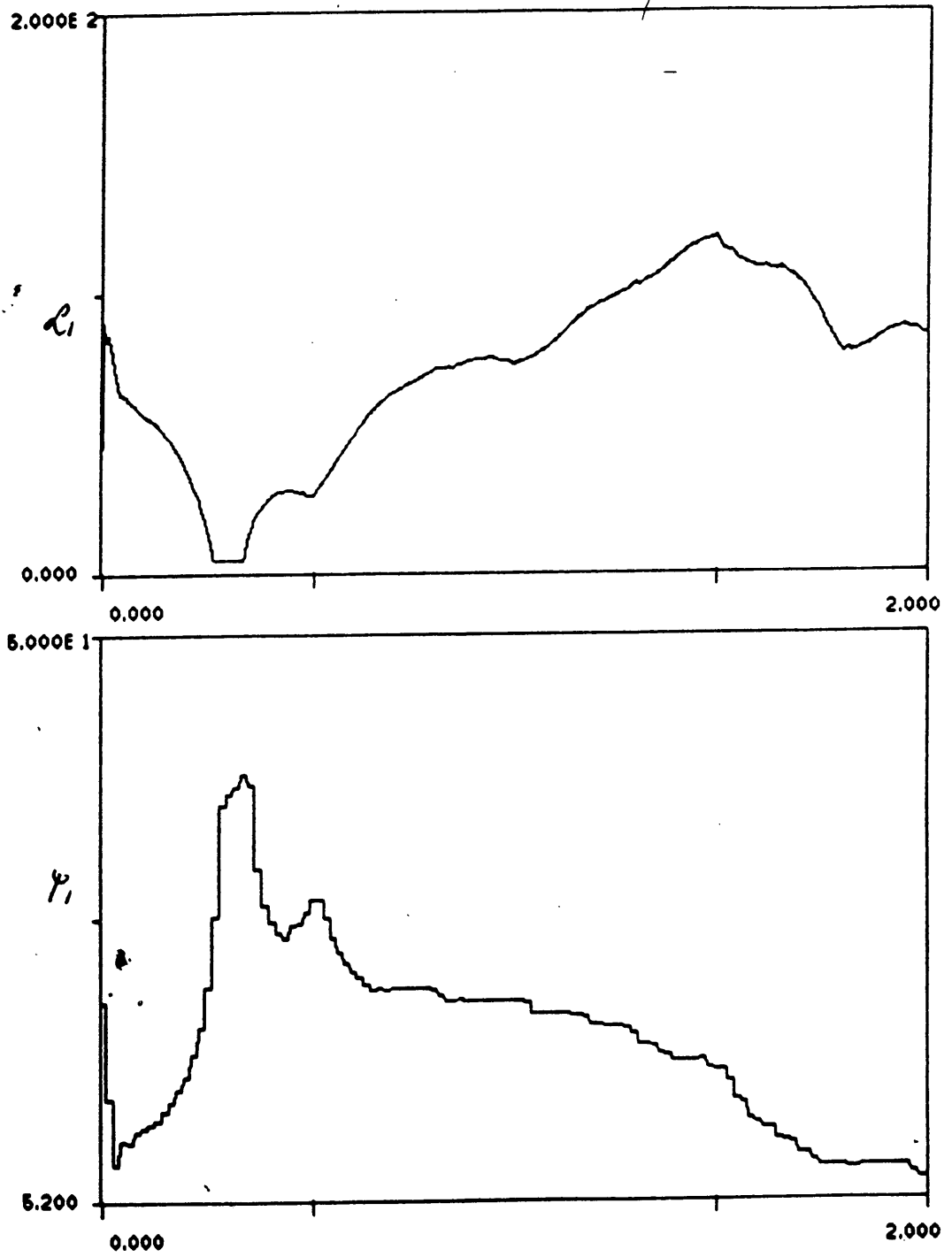


Figure 23. EMTP Model results scheme A

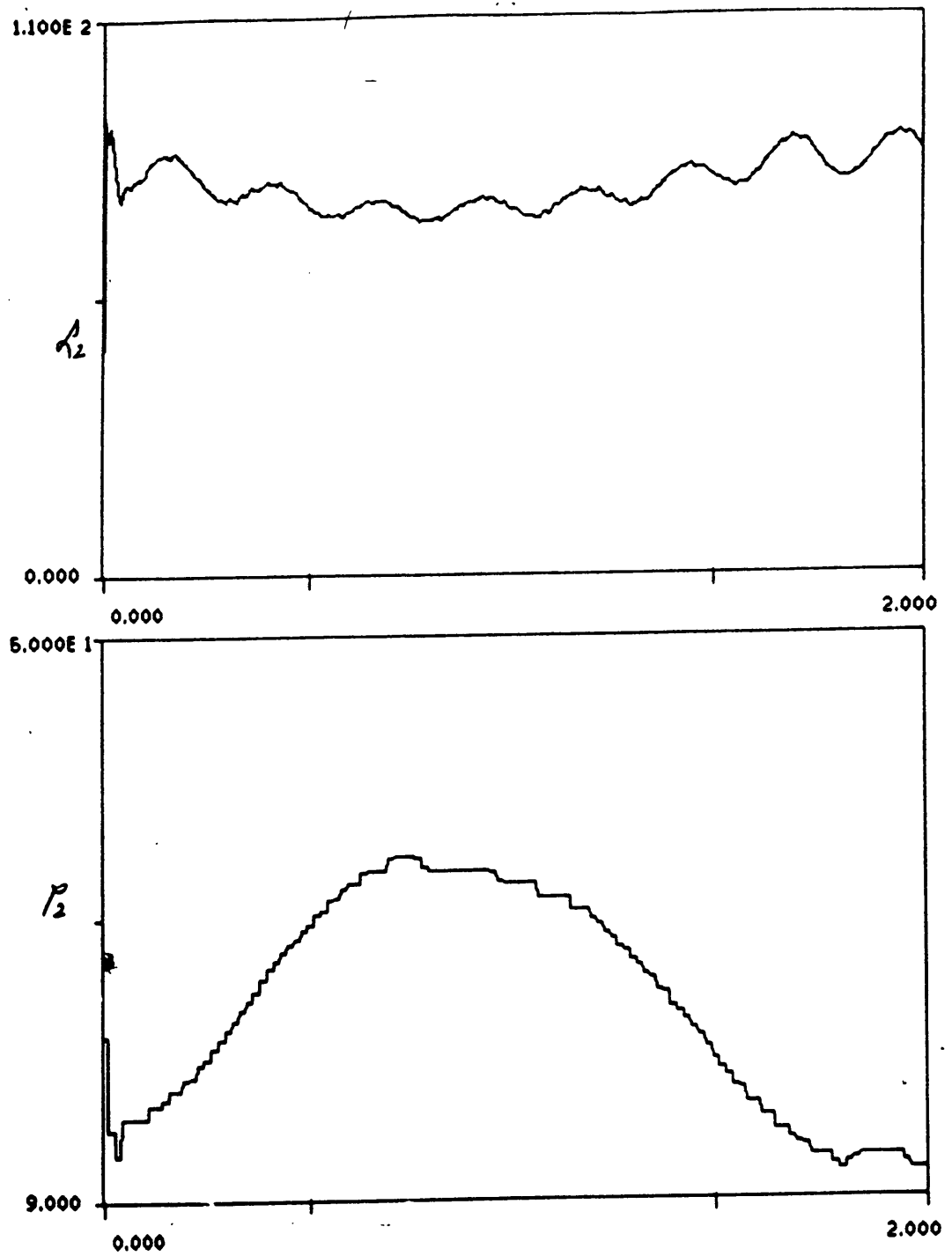


Figure 24. EMTP Model results scheme A

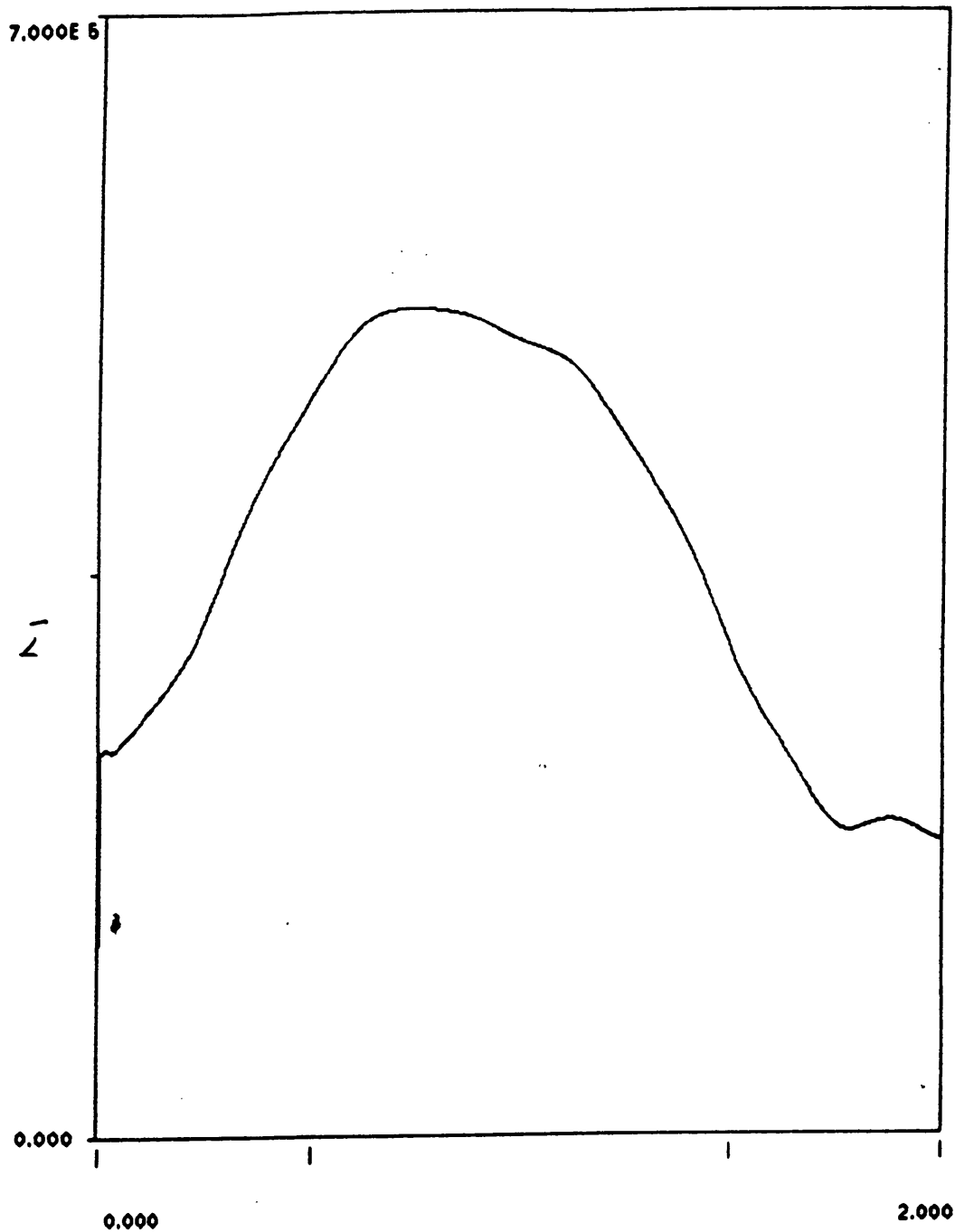


Figure 25. EMTP Model results scheme A

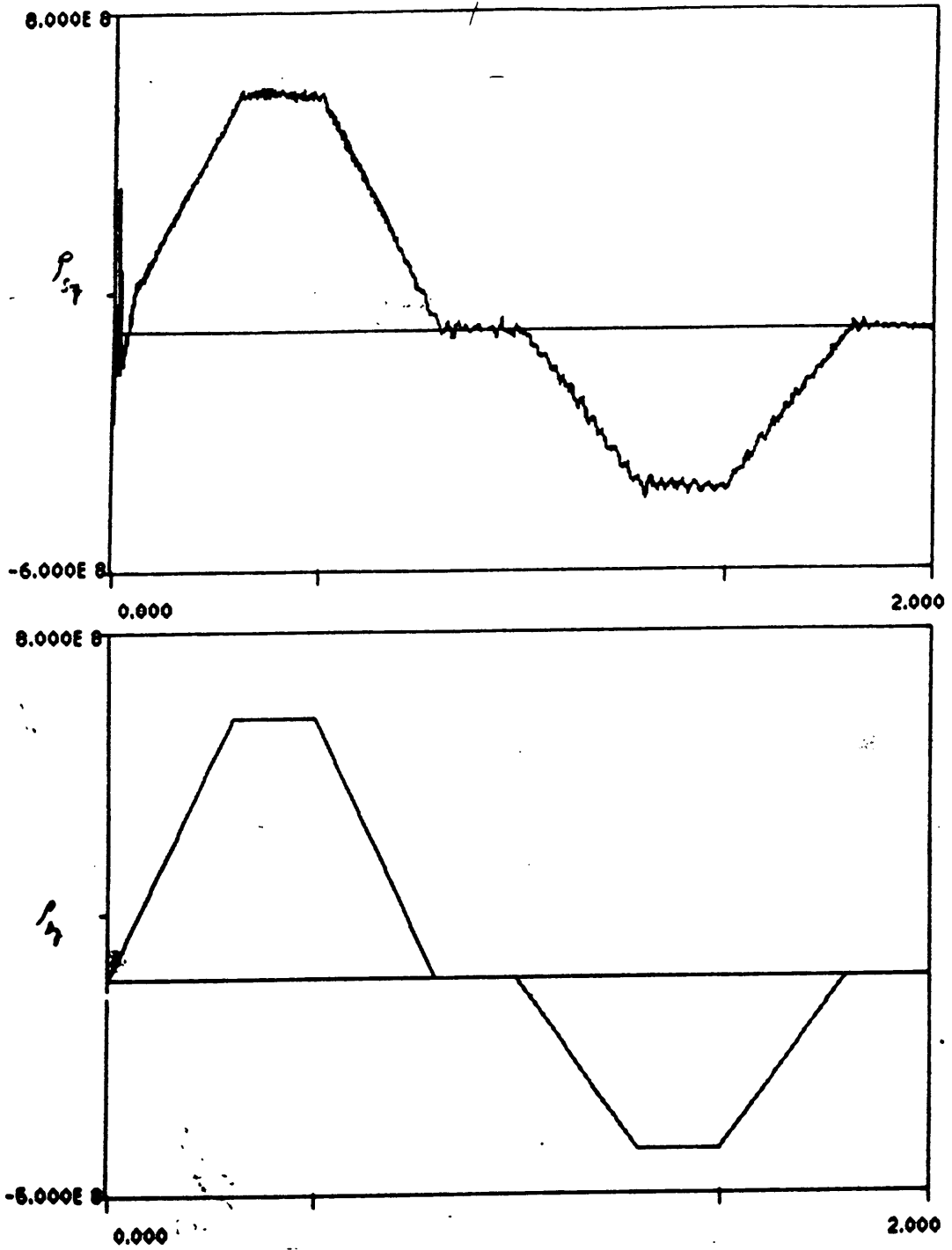


Figure 26. EMTP Model results scheme C

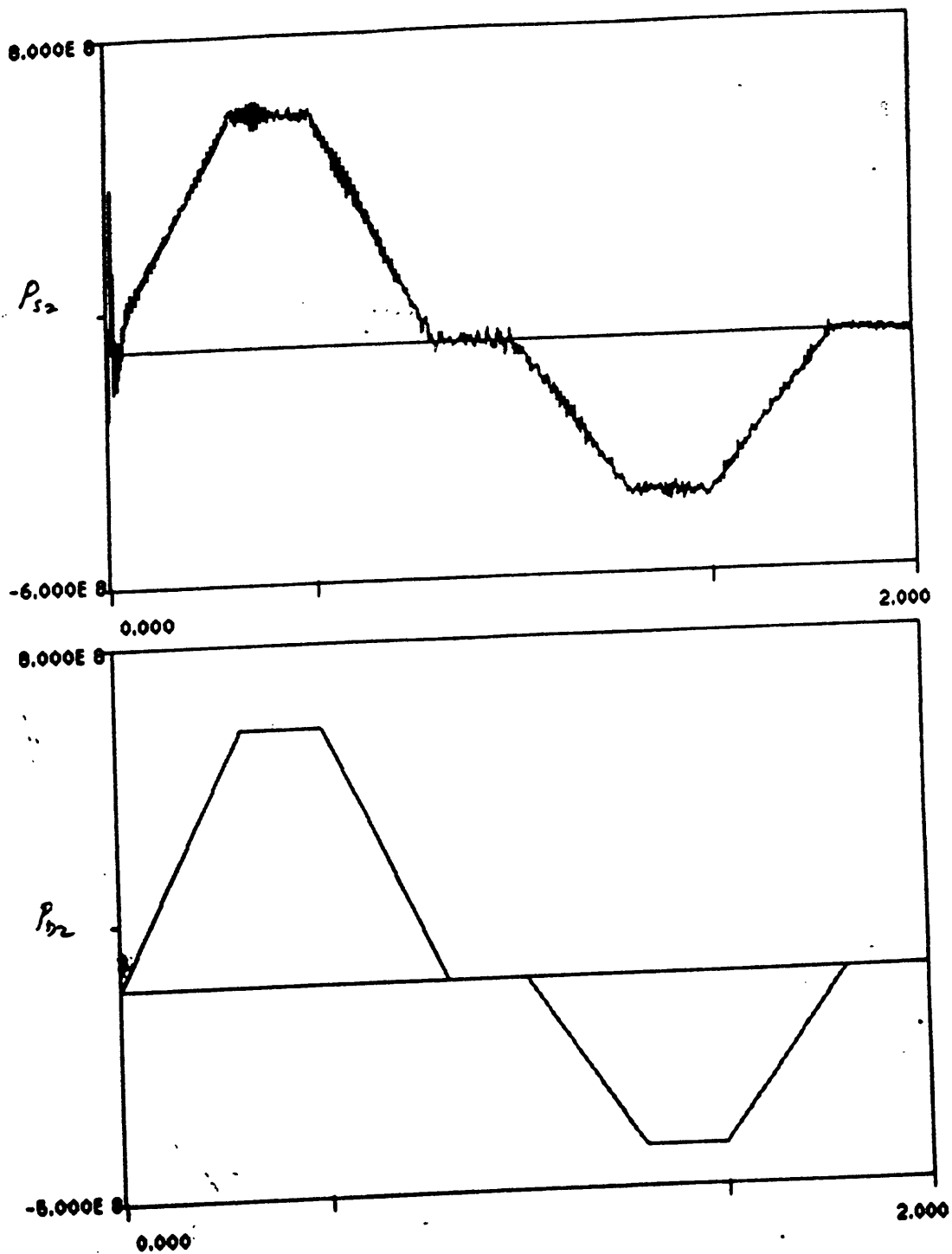


Figure 27. EMTP Model results scheme C

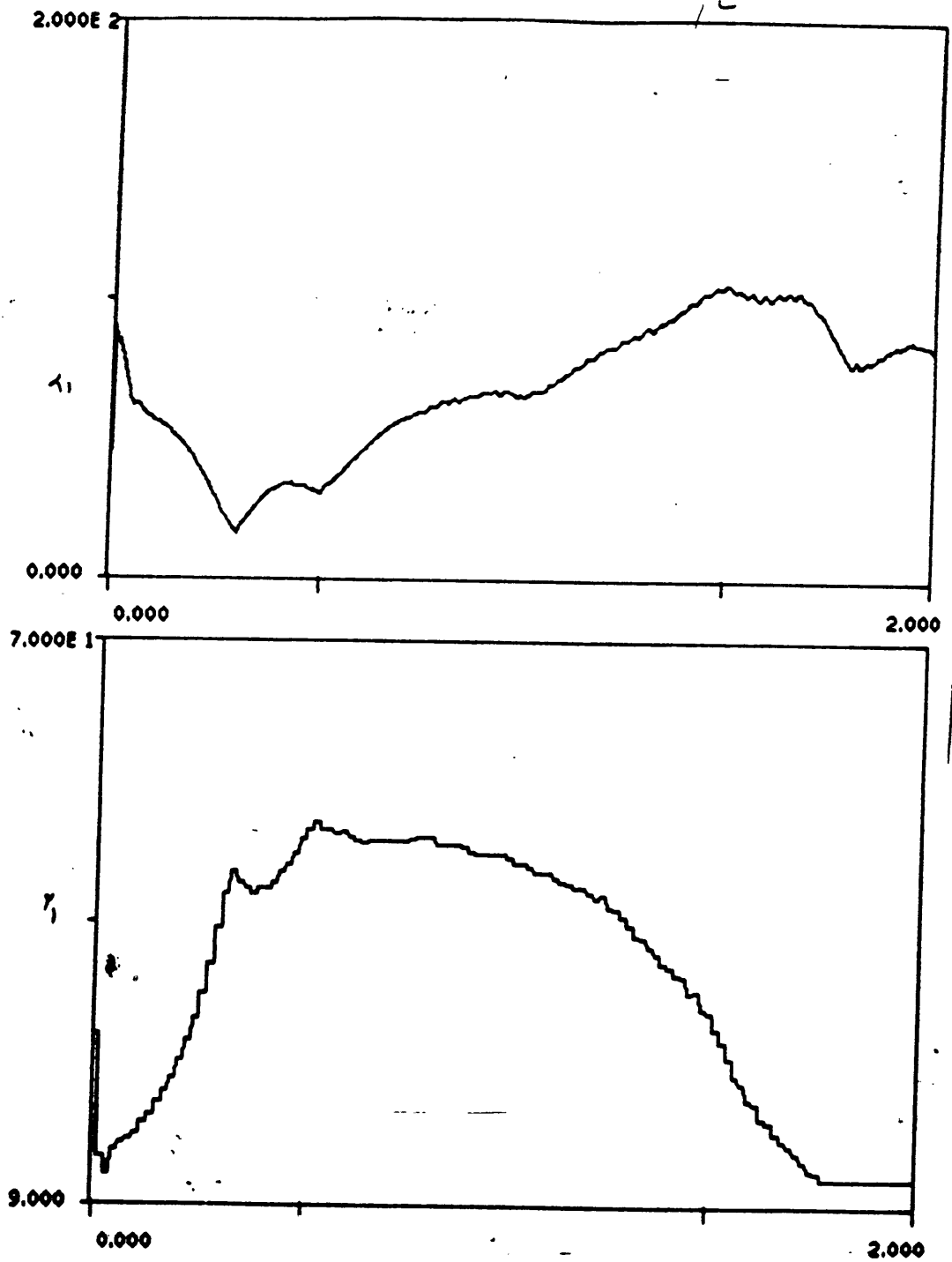


Figure 28. EMTP Model results scheme C

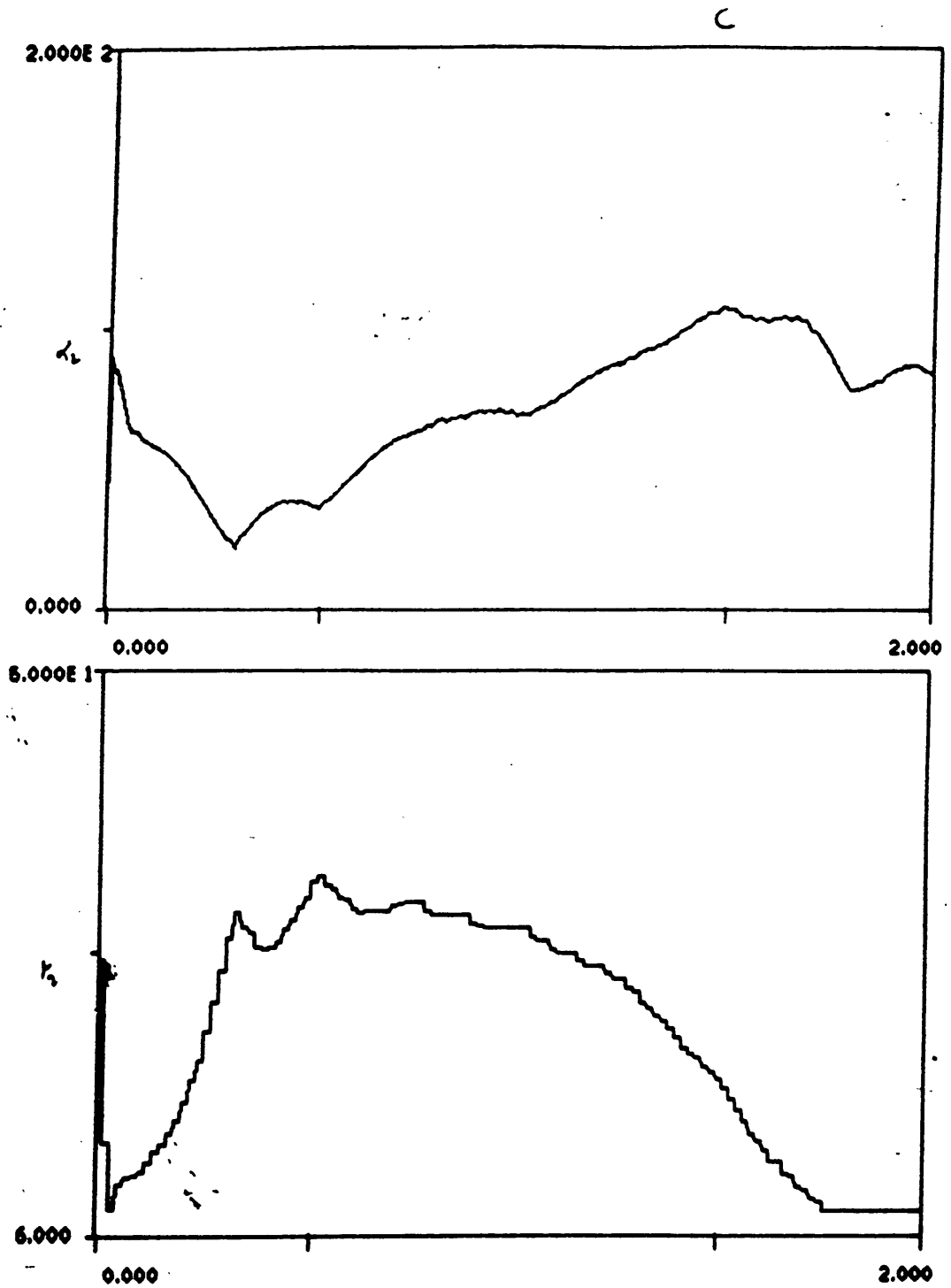


Figure 29. EMTP Model results scheme C

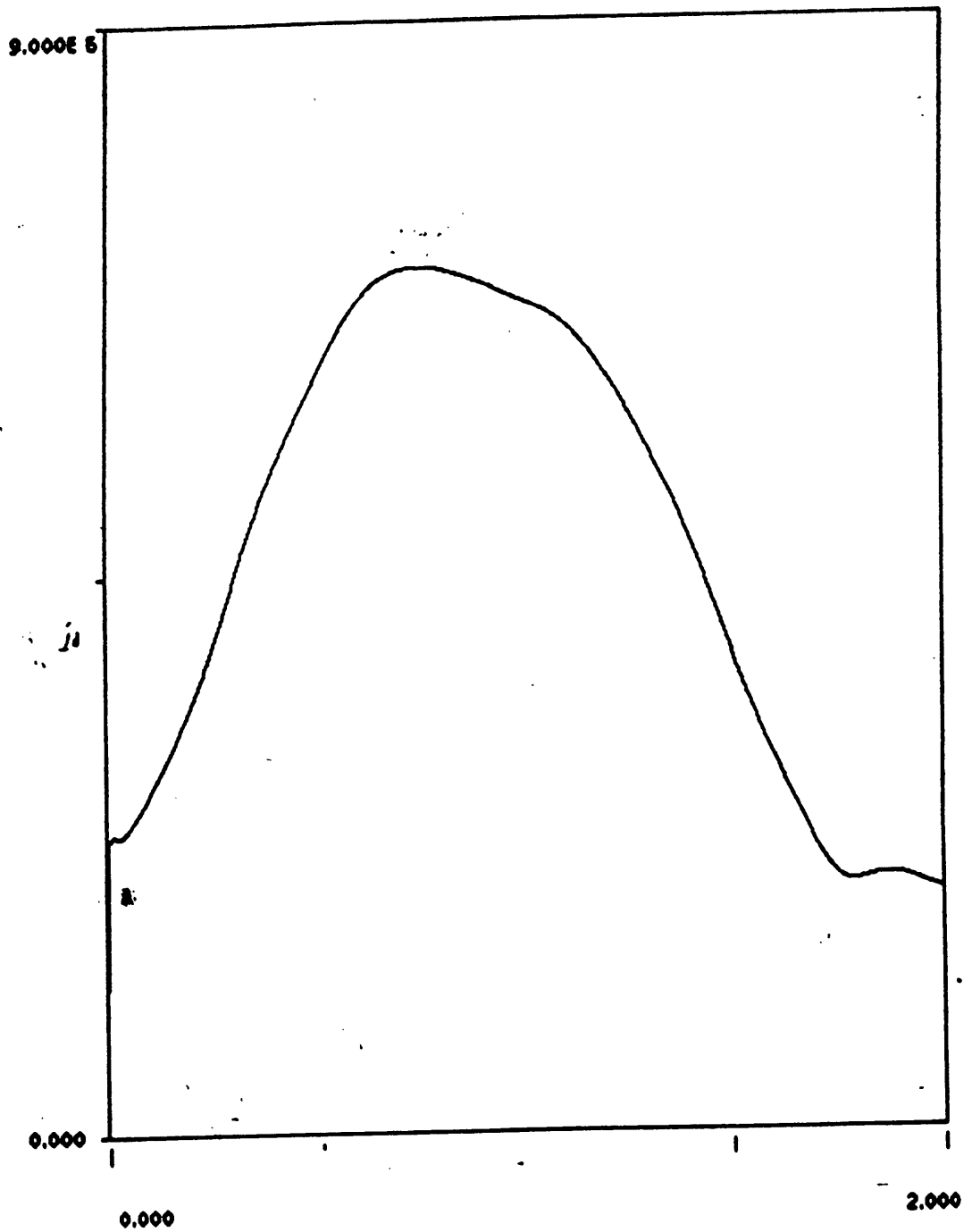


Figure 30. EMTP Model results scheme C

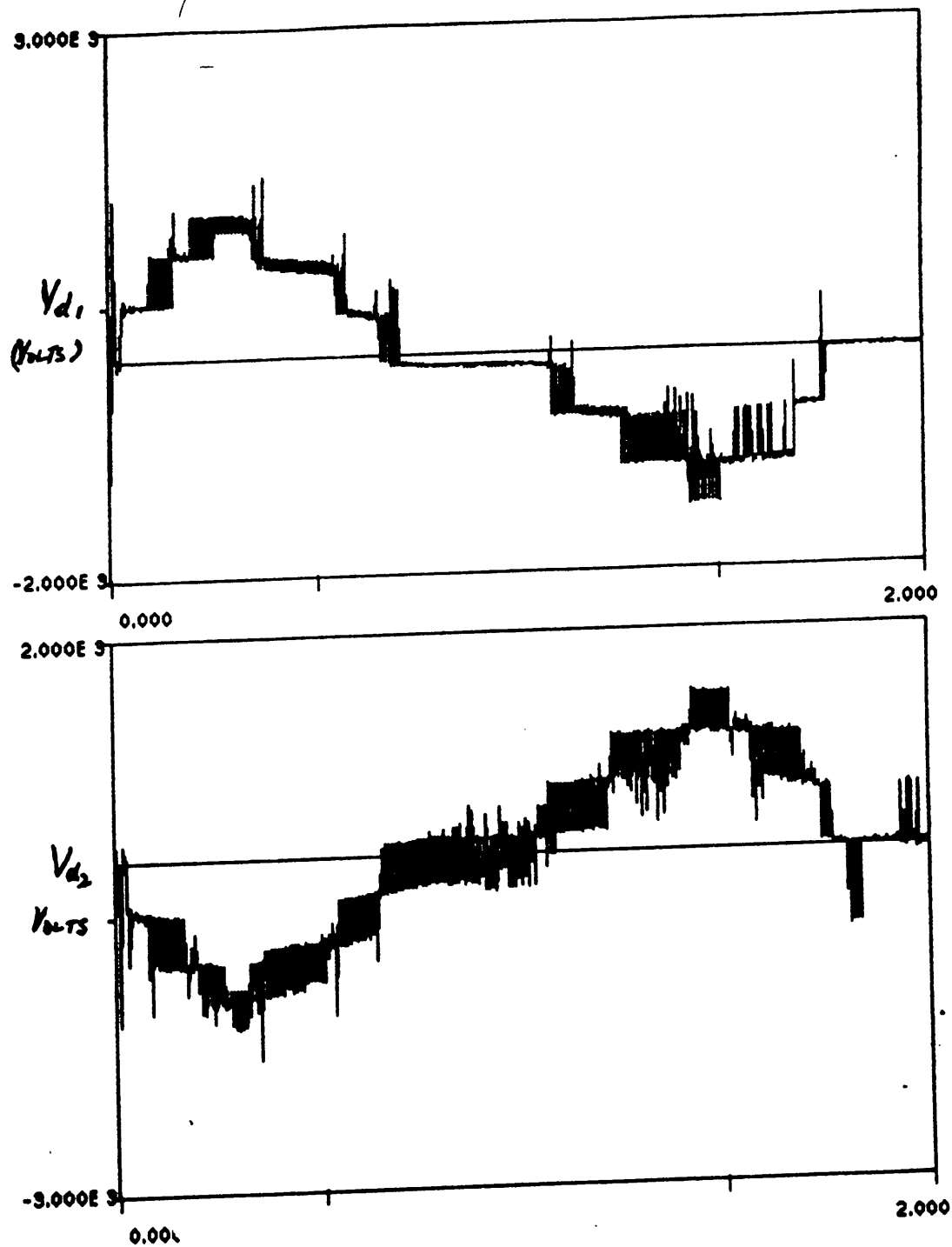


Figure 31. EMTF Model results scheme C

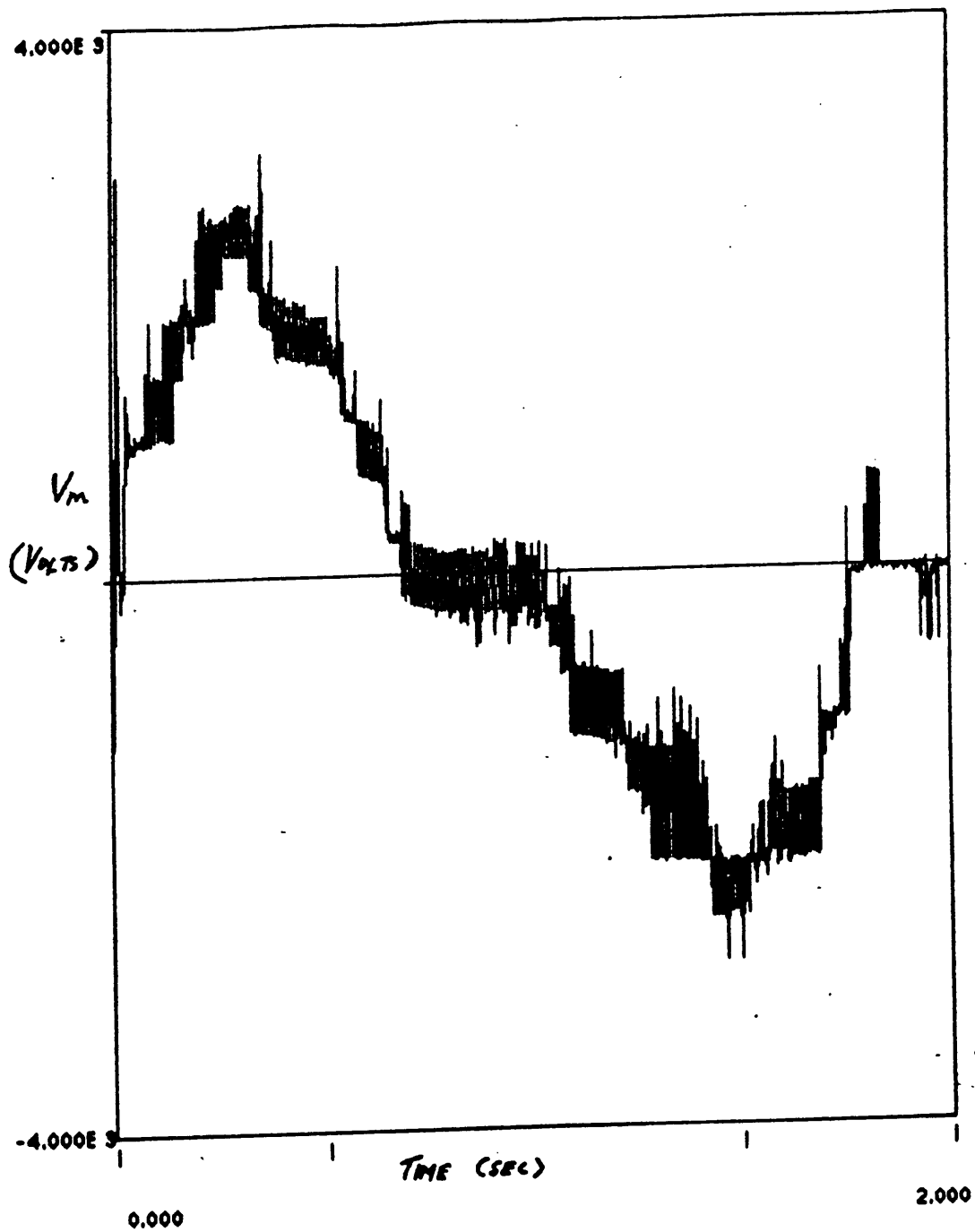


Figure 32. EMTP Model results scheme C

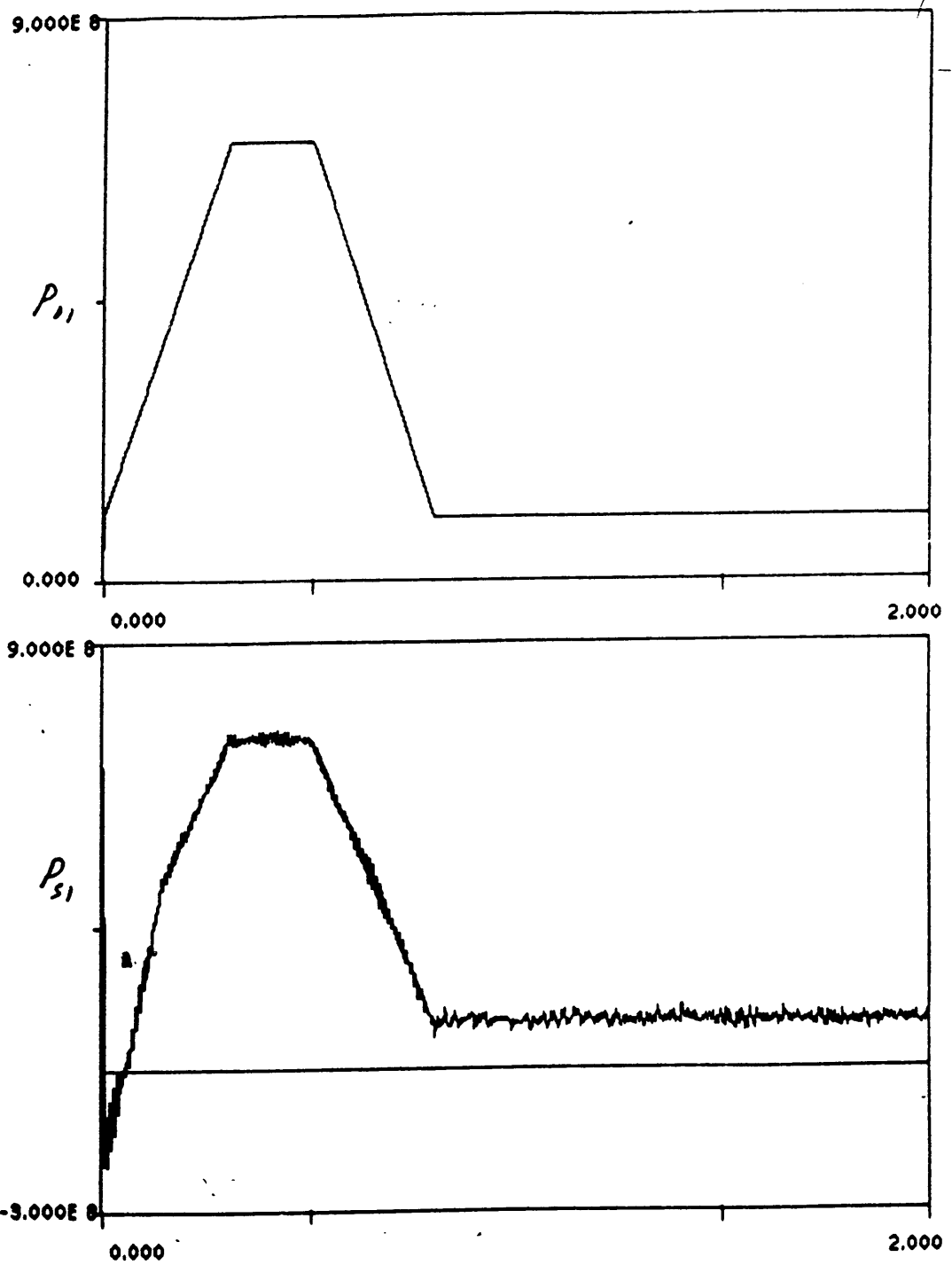


Figure 33. EMTF Model results scheme D

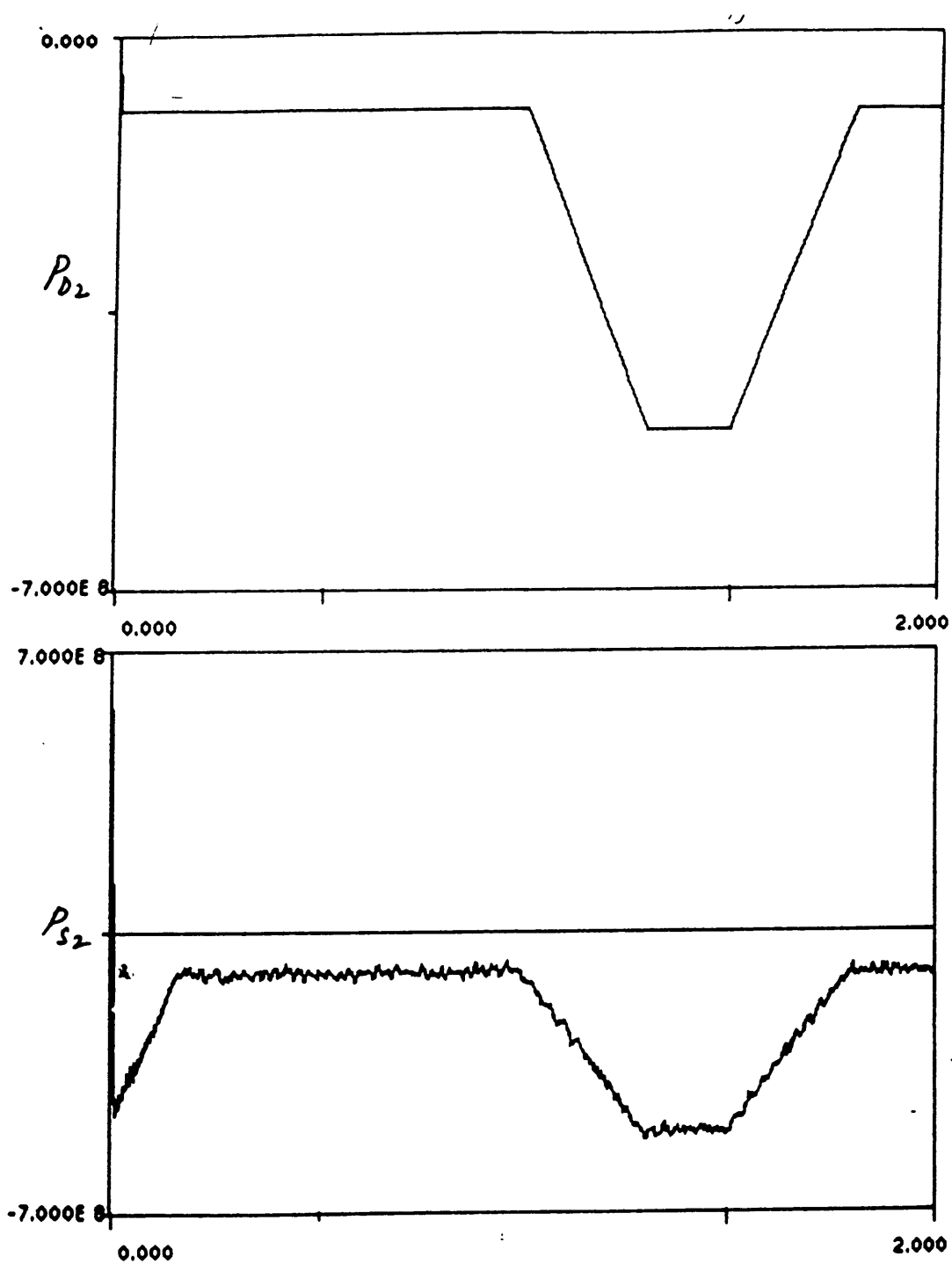


Figure 34. EMTP Model results scheme D

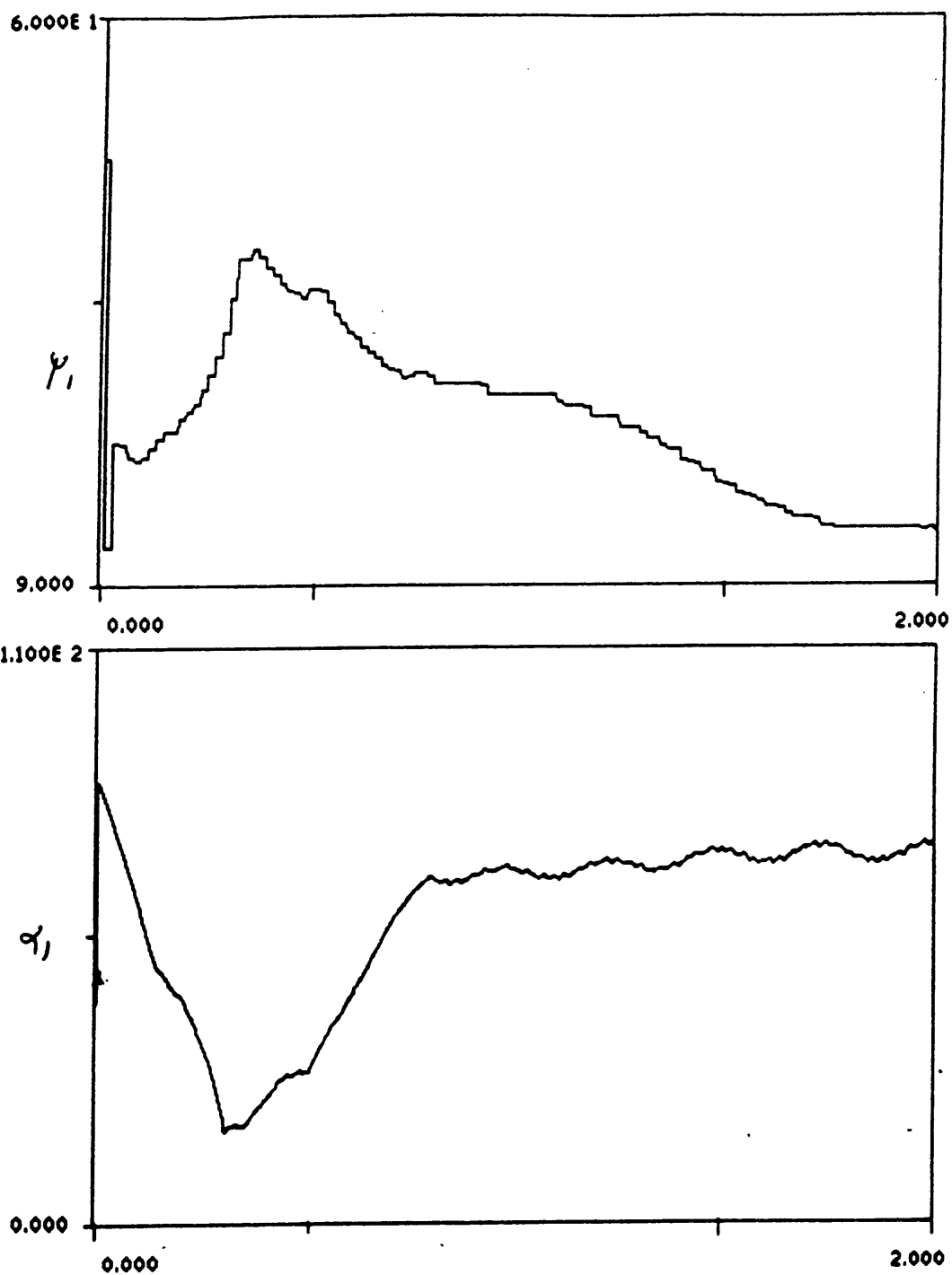


Figure 35. EMTF Model results scheme D

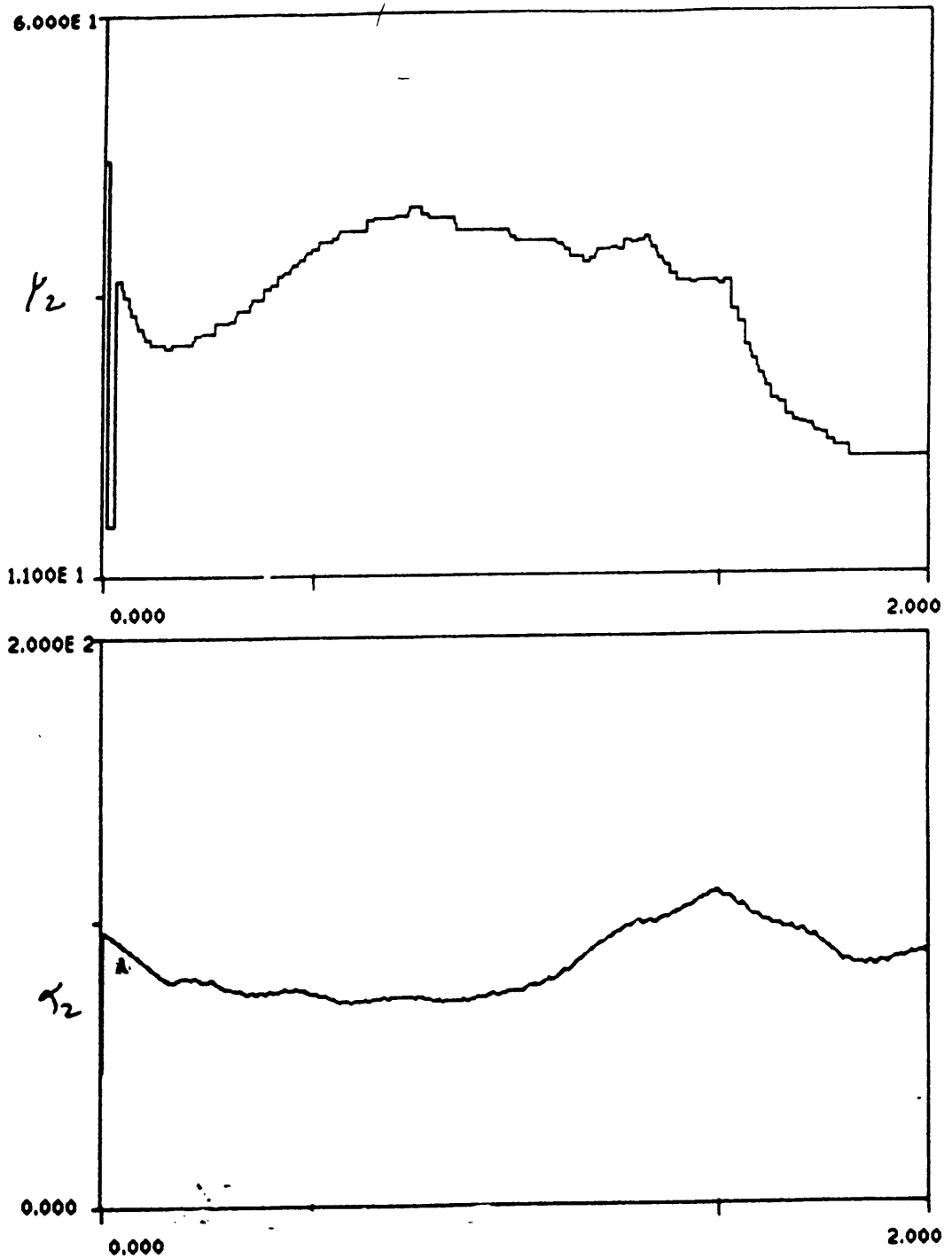


Figure 36. EMTP Model results scheme D

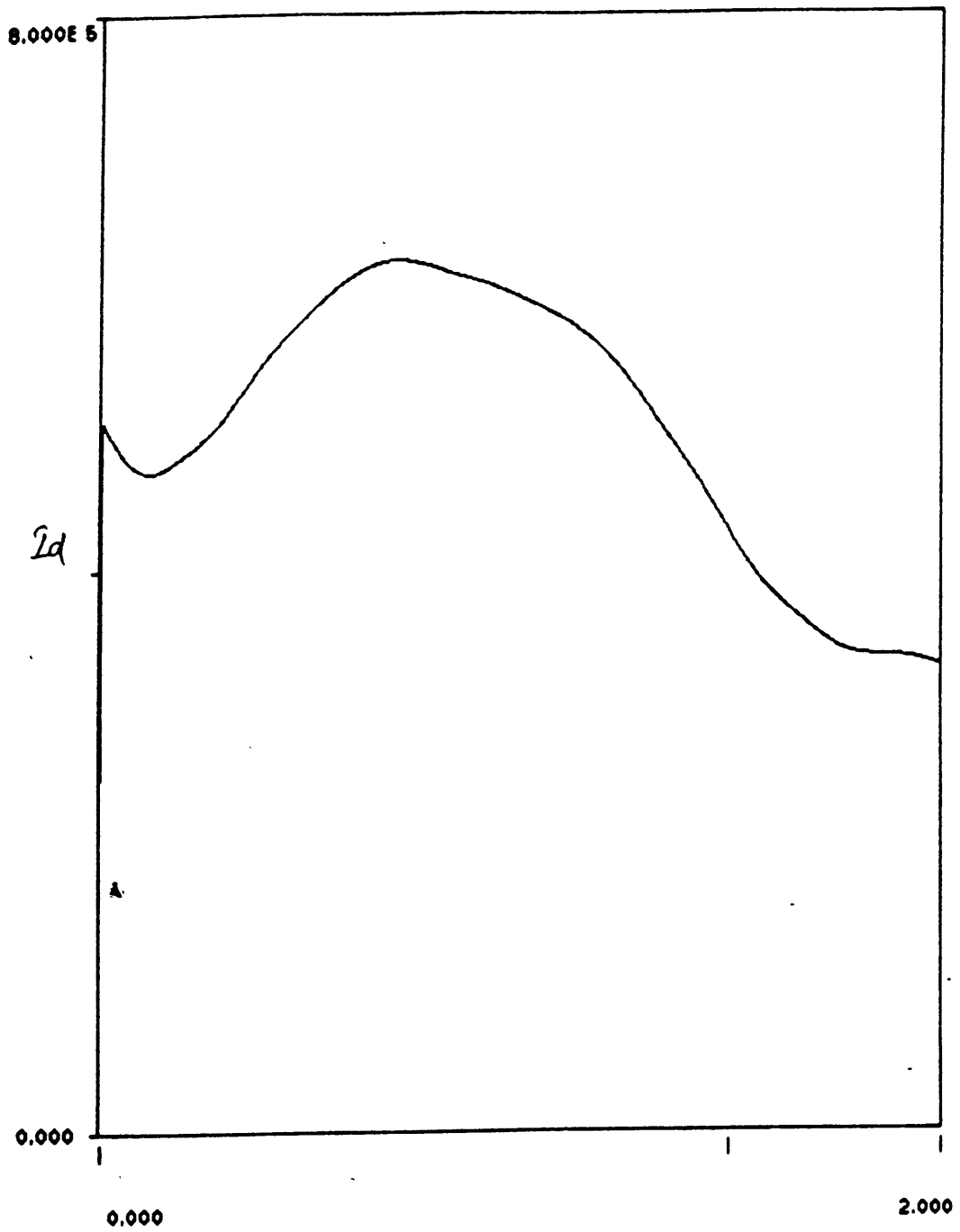


Figure 37. EMTP Model results scheme D

4.0 SMES Impact on Transmission System.

The objective of this chapter is to show that the use of SMES for diurnal load levelling provides improvement in the transmission of electric power. The benefits are reduction in transmission losses, which results in fuel cost saving, reduction of transmission line loading during peak load hours which enhances stability and operation flexibility and offers economic benefits as the need for new transmission facility could be delayed. The impact of size and location of the SMES on these benefits is studied. SMES when operated in series configuration [11] can offer group control of parallel lines, and other possible benefits.

4.1 Basic Concept

This is to introduce the idea of savings in transmission line costs by the proper location of the SMES. Consider figure 38 A group of generators supplies electric power to a load center through a transmission line.

4.11 Without SMES

During the day, the load requires a peak power of P_d for a duration of t_d hours. To supply the load, the transmission line must carry an electric current I_d given by

$$I_d = \frac{P_d}{V \times PF} \quad [4.1]$$

where

V = voltage at the load bus
 PF = power factor of load
The maximum transmission line loading is proportional to I_d . The transmission line loss is given by

$$P_{LLd} = I_d^2 \times R \quad [4.2]$$

R is the transmission line resistance at the operating frequency. The transmission losses during t_d is

$$E_{Ld} = P_{LLd} \times t_d \quad [4.3]$$

At night, the load demand decreases to kP_d $k < 1.0$, for a duration of t_n hours. To supply the load, the transmission line must carry I_n given by

$$I_n = \frac{k \times P_d}{V \times PF} = k \times I_d \quad [4.4]$$

The transmission line loading at night is proportional to I_n . Since the load demand is low at night (k ranges from .5 to .65) the transmission line loading at night is

$$P_{LLn} = I_n^2 \times R = k^2 \times P_{LLd} \quad [4.5]$$

The transmission loss during t_n is

$$E_{ln} = P_{LLn} \times t_n = k^2 \times \frac{t_n}{t_d} \times E_{Ld} \quad [4.6]$$

4.12 With SMES.

A SMES system is connected to the load bus and is designed such that it can be charged at P_{sn} for t_n at night and discharged at P_{sd} for t_d hours during the day. For t_d hours during the day, the current supplied by the SMES system to the load is

$$I_{sd} = \frac{P_{sd}}{V \times DF_d} \quad [4.7]$$

with DF_d as the displacement factor of the SMES converter for charging. The total transmission line current is then

$$\vec{I}_{td} = \vec{I}_d - \vec{I}_{sd} \quad [4.8]$$

The reference for these vectors is the load bus voltage. While the phase angle of \vec{I}_d depends on the power factor of the load, the phase angle of \vec{I}_{sd} depends on the firing angle of the DC/AC converter that connects the SMES to the power system. In most cases, the currents are lagging the load bus voltage and

$$\vec{I}_{td} \leq \vec{I}_d \quad [4.9]$$

Since the transmission line loading is proportional to the line current, a reduction in line current results in decreased line loading. During the day when the load demand is high, the reduction in transmission line losses would be

$$\Delta P_{LLd} = (I_d^2 - I_{td}^2) \times R = P_{LLd} - I_{td}^2 \times R \quad [4.10]$$

For t_n hours at night, the current injected from the power system to charge up the SMES is

$$I_{sn} = \frac{P_n}{DF_n \times v} \quad [4.11]$$

with DF_n as the displacement factor of the SMES converter for charging. The total transmission line current is then

$$\vec{I}_{tn} = \vec{I}_n + \vec{I}_{sn} \quad [4.12]$$

Since the currents are usually lagging the load bus voltage, $\vec{I}_{tn} > \vec{I}_n$. Thus the line loading at night is increased. The presence of SMES allows electric power to be transmitted

through the lightly loaded line at night so that the line loading can be reduced during day. When the load demand is low at night, the transmission line loss is increased by

$$\Delta P_{LLn} = (I_m^2 - I_n^2) \times R = I_n^2 \times R - P_{LLn} \quad [4.13]$$

Compared to the system without SMES, the transmission losses are increased at night during the charging of SMES and decreased during the day when the SMES is discharged. The overall savings in transmission energy loss per day is given by

$$E = (\Delta P_{LLd} \times t_d) - (\Delta P_{LLn} \times t_n) \quad [4.14]$$

Since the increase in transmission losses at night is supplied by low cost base units and the decrease in transmission losses during the day reduces the power output from the high cost peak units or even the intermediate units, the savings in fuel cost per day is given by

$$S = (\Delta P_{LLd} \times t_d \times F_{IP}) - (\Delta P_{LLn} \times t_n \times F_B) \quad [4.15]$$

where

F_B = fuel cost for the power supplied by the base units.

F_{IP} = fuel cost for the power supplied by the peaking units

The impact of SMES on electric power transmission depends on the location and size of the SMES system.

4.2 Simulation Study.

This study involves running load flows for each hour of the day with/without the SMES of different sizes at different locations and studying the various impacts on transmission as outlined in the introduction of this chapter. The AEP 14 bus system shown in figure 39 was used as the test system, the test data is shown in tables 10&11. A typical summer day profile based on EPRI's data for SE region [16] was assumed, the load data available was considered as the peak load data (at 6 P.M) and based on this the load data for the remaining hours of the day was estimated. The Planner load flow program [22] using the Gauss-Seidal algorithm was used. The way the SMES is modelled is discussed in section 4.2.1 and the selection of size/rating is discussed in section 4.2.2.

4.2.1 Modelling the SMES for the load flows.

The SMES functions both as a load (during the charging time) and as a generator (during the discharging time) over a 24 hour period. The converters in a SMES always consume reactive power (as delayed firing schemes are used in all the designs). Since the reactive power consumption is a function of the converter dynamics estimating the same would therefore be arbitrary. There are AC/DC schemes (Using GTO's [23] and artificially commuted converters [24]) by independent real and reactive power control, the converters can be controlled so that it does not introduce any reactive power change for the operating levels, for this study the use of such schemes is assumed. The SMES bus is modelled as a load bus, connected to the required bus by a line of very small impedance. The charge/discharge power of the SMES is the difference between the de-

Table 10. Bus data for test system

BUS		TYPEV(p.u)	Deg	PG	QG	PD	QD	QMIN	QMAX
GLEN LYN	1	1.06	0.0	-	-	0.0	0.0	-40.0	50.0
CLAYTOR	3	1.045	0.0	40.0	-	21.7	12.7	-40.0	50.0
FIELDALE	4	1.01	0.0	0.0	-	94.2	19.0	0.0	40.0
ROANK138	2	1.0	0.0	-	0.0	47.8	-3.9	-	-
HANCK138	2	1.0	0.0	-	0.0	7.6	1.6	-	-
HANCOK34	4	1.07	0.0	0.0	-	11.2	7.5	-6.0	24.0
ROANKMID	2	1.0	0.0	-	0.0	0.0	0.0	-	-
ROANKSYN	4	1.09	0.0	0.0	-	0.0	0.0	-6.0	24.0
ROANKE34	2	1.0	0.0	-	0.0	29.5	16.6	-	-
NORWICH	2	1.0	0.0	-	0.0	9.0	5.8	-	-
MUDLICK	2	1.0	0.0	-	0.0	3.5	1.8	-	-
SALEM	2	1.0	0.0	-	0.0	6.1	1.6	-	-
MELROSE	2	1.0	0.0	-	0.0	14.9	5.0	-	-
MASON CK	2	1.0	0.0	-	0.0	13.5	5.8	-	-

Table 11. Line data for test system

ST-BUS	END-BUS	DIST.	R(Ohms/mi)	X(Ohms/mi)	LCH(mho/mi)	Vol(KV)
GLEN LYN	CLAYTOR	22	.16776	.5122	.0000126	138
GLEN LYN	HANCK138	45	.228655	.9439	.00000574	138
CLAYTOR	FIELDALE	42	.21307	.89765	.00000547	138
CLAYTOR	ROANK138	43	.25736	.7809	.000004567	138
CLAYTOR	HANCK138	35	.30987	.9461	.0000051	138
FIELDALE	ROANK138	35	.36461	.9306	.0000052	138
HANCK138	ROANK138	7	.363196	1.1456	.0000096	138
HANCOK34	MUDLICK	1	1.1305	2.3674	0	34.5
HANCOK34	SALEM	12.5	1.1703	2.4358	0	34.5
HANCOK34	MASON CK	1	.78735	1.55	0	34.5
ROANKE34	NORWICH	0.5	.7572	2.011	0	34.5
ROANKE34	MELROSE	1.5	1.0086	2.1454	0	34.5
MELROSE	MASON CK	1.5	1.3563	2.7615	0.0	34.5
MASON CK	SALEM	1.5	1.5025	1.586	0.0	34.5
NORWICH	MUDLICK	0.9	1.0851	2.541	0	34.5

TRANSFORMER DATA

ST-BUS	END BUS	R	X	URNS RATIO
ROANK138	ROANKMID	0.0	.20912	.978
ROANK138	ROANKE34	0.0	.55618	.969
HANCK138	HANCOK34	0.0	.25202	.932
ROANKMID	ROANKSYN	0.0	.17615	1.0
ROANKMID	ROANKE34	0.0	.11001	1.0

STATIC CAPACITOR DATA

ST BUS	CAPACITANCE	VOL(KV)
ROANKE34	42.342	34.5

sired power level and the original for every hour of the day. Therefore during charging the load bus (SMES bus) has + P, 0Q, during standby 0P and 0Q and during discharging -P 0Q.

4.2.2 Sizing the SMES.

There are two important parameters that establish the capacity of the SMES one is the size which is the energy that can be stored usually in Mwh. The second is the rating of the converter this defines the maximum charge/discharge of the SMES at a given instant. The specific cost of both come down with increased size.[25] The size recommended is 10% of system capacity. Let the SMES charge from t_0 to t_c hours. Let it discharge from t_{d1} to t_{d2} . Let the load value with SMES in system be SPC and SPD during the charging and discharging times.

$$A_1 = \int_{t_0}^{t_c} (L - SPC) dt \quad [4.15]$$

$$A_2 = \int_{t_{d1}}^{t_{d2}} (L - SPD) dt \quad [4.16]$$

$$A_2 = A_1 \times \eta \quad [4.17]$$

The rating of the converter should be \geq the maximum charge/discharge. For a typical load curve it is the maximum charge that decides the limit (Because the charging is over

a shorter time, therefore maximum charge > maximum discharge). If PC_r is the converter rating, P_{\min} and P_{\max} are the minimum and the peak of the load then the limits are

$$SPC - P_{\min} \leq PC_r \quad [4.18]$$

$$P_{\max} - SPD \leq PC_r \quad [4.19]$$

For this study SMES of 100 Mwh 20 MW and 200 Mwh 40 MW were chosen.

4.3 Case Studies.

4.3.1 Case 1(system without SMES) Base case .

Based on the load curve shown in figure 40, transmission loss of the system was obtained from the load flow on an hourly basis and is plotted in figure 41. The shape of the transmission load curve has a close resemblance to the original load curve. To study the impact on line loadings only the peak load hours is considered (6 P.M) Ten transmission lines are loaded beyond 85%. Six 138 Kv lines are loaded beyond 85%, with four of them beyond 90%. The line loading is shown in table 12.

4.3.2 Case 2 with SMES

SMES is introduced in the system there are 4 sub cases with SMES of two different sizes in two locations each. The SMES is charged from base unit power for 8 hours from 12 A.M to 8 A.M. It is discharged from 11 A.M to 11 P.M with SMES the system peak is reduced to 228 MW. The methodology used to compute the savings in transmission loss energy is explained in section 4.3.3. For all the sub cases the transmission loss curves for different locations/sizes is shown in figure 41.

Case 2a 200 Mwh location A This location has local generation, is close to other generators and is far away from the major loads. The transmission loss curve, shows the transmission losses are increased during the charging period and is decreased during the discharging period (compared to the base case). The daily reduction loss in transmission loss energy is 1.95% and the daily reduction in fuel cost for transmission loss compared to the base case is 10.16%. The transmission line loading (at peak load) has only slightly improved over the base case. Out of the seven 138 Kv lines, the loading of four lines are reduced but the loading of the other three lines are increased. Five 138 Kv lines are loaded beyond 85%, with three of them beyond 90%. Totally there are nine lines loaded beyond 85%.

Case 2b 200 Mwh location B This location has a relatively heavy load, close to other major loads, but is far away from the generators. During the charging period when the load demand is low the increase is higher than the base case and case 2a. The daily reduction in transmission energy losses relative to the total daily transmission energy loss of the original system is 4.0% and the daily reduction in fuel cost compared to the base case is 21.44%.

Case 2c 100 Mwh location A The transmission loss pattern is similar to case 2a except that it is closer to the base case, the reduction in transmission energy loss is 1.35% and the reduction in fuel cost is 6.49%. The improvement in transmission line loading is only marginally better than the base case, total 9 lines are loaded beyond 85%. 5 of the 138 Kv lines are loaded beyond 85% with two of them over 90%.

Case 2d 100 Mwh location B The transmission loss pattern is similar to case 2b. The reduction in transmission energy loss is 3.14% and the reduction in fuel cost is 12.83%. 5 lines are loaded beyond 85% and only 1 138 Kv line is loaded beyond 85%.

The above results indicate from the viewpoint of transmission line loading it is better to put the SMES system (for diurnal load levelling applications) in the proximity of major loads. The smaller the SMES the less effective in transmission loss/loading benefits this is because less peak/intermediate units are being replaced during peak load hours and the base load units operate at lower power levels to charge up the SMES at light load hours. In cases where SMES is designed solely for the purpose of system stabilization, stabilization control will be more effective if the SMES is located close to the generator [23,26].

4.3.3 Methodology of estimating total savings in transmission loss energy.

Compared to the base case, the transmission losses are increased during the SMES charging hours when the load demand is low, and are reduced during the SMES discharging hours when the load demand is high. Since transmission losses are much higher when the system load is high, the latter is larger than the former. With the SMES in the system consider the reduction in transmission energy losses compared to the original system (without the SMES) be $x\%$. Due to the difference in the cost of fuel being used to supply the transmission losses for systems with and without SMES, the savings for

the fuel cost for transmission losses is more than x%. The savings is from two sources. Firstly, during the SMES discharging hours, its power output replaces those of the expensive peak units and some of the intermediate units. Since these units would provide their share of the losses if they are connected to the system, their replacement by the SMES causes a reduction in the fuel cost of the transmission losses. Secondly the transmission losses supplied by the SMES when it is discharged and the increase in transmission losses when it is charged come from low cost base units operating at higher output levels (than those in the original system without SMES) at light-load hours. Since the generator heat rate decreases with higher level of output power, the same amount of electrical energy can be generated at a lower \$/Mwh.

Mathematical representation

The following variables are defined thus

P_m = Peak load

P_b = load upto which the base load units operate = $k_b \times P_m$ ($k_b = 0.8$)

P_i = load upto which the base and all the intermediate load units operate = $k_i \times P_m$ ($k_b = 0.95$)

T_{t_b} = Transmission loss corresponding a load of P_b occurring at time t_b hours.

T_{t_i} = Transmission loss corresponding a load of P_i occurring at time t_i hours.

T_t = Transmission loss at any time t

F_p = Specific fuel consumption in Mbtu/Mwh for peak load units

F_i = Specific fuel consumption in Mbtu/Mwh for intermediate load units.

F_b = Specific fuel consumption in Mbtu/Mwh for base load units

C_p = Specific fuel cost in \$/Mbtu for peak load units

C_i = Specific fuel cost in \$/Mbtu for intermediate load units.

C_b = Specific fuel cost in \$/Mbtu for base load units

When

$$T_l \leq T_{lbs}$$

$$Cost = F_b \times C_b \times T_l \quad [4.21]$$

$$T_{li} \leq T_l \leq T_{lbs}$$

$$Cost = F_i \times C_i \times (T_l - T_{lbs}) + F_b \times C_b \times T_{lbs} \quad [4.22]$$

$$T_l \geq T_{li}$$

$$Cost = F_p \times C_p \times (T_l - T_{li}) + F_i \times C_i \times (T_{li} - T_{lbs}) + F_b \times C_b \times T_{lbs} \quad [4.23]$$

The cost of the transmission loss is computed using the above method as follows.

From [16] the base load capacity, intermediate load capacity and peak load capacity was fixed as 80%, 15% and 5% of peak load. For the 14 Bus system with a peak load of 259 MW the base load units would be on until the load is 207.2 MW (0.8×259), then base and intermediate load units supply the system load upto 246 MW (0.95×259), beyond 246 MW all units together would supply the system load upto 259 MW. The corresponding transmission losses is 8.2 MW (i.e when the base load capacity of 207.2 MW is reached), the corresponding transmission loss when intermediate load capacity is reached is 11.98 MW (when the load is 246 MW), Peaking units are on when transmission losses are greater than 11.98 MW.

The transmission loss value is available on an hourly basis for the different cases (base case, SMES at location A, SMES at location B). The energy for supplying the transmission losses comes from either base units, intermediate units or the peak units. The

\$/MWH for the three sources is computed from [16] from the specific fuel costs and the specific fuel consumptions and is as follows

$$\text{Base load units } \$/\text{MWH} = 23.59(10.04 * 2.35)$$

$$\text{Intermediate load units } \$/\text{MWH} = 72.57(11.8 * 6.15)$$

$$\text{Peak load units } \$/\text{MWH} = 114.1 (14 * 8.15)$$

The value of the transmission loss (available each hour for the different cases) can therefore indicate the sources supplying the energy and the cost of supplying that energy can be computed accordingly. For the 14 bus problem

$$T.L < 8.2 \text{ MW}$$

$$\$/H = 23.59 * T.L$$

$$11.98 \leq T.L \leq 8.2$$

$$\$/H = 72.57 * (T.L - 8.2) + 8.2 * 23.59$$

$$T.L \geq 11.98$$

$$\$/H = 114.1 * (T.L - 11.98) + 72.57 * (11.98 - 8.2) + 23.59 * 8.2$$

Based on the above logic the transmission loss energy cost are computed on an hourly basis for a 24 hour period for the different cases.

4.4 Savings due to producing cheaper energy.

For the test system almost all the power comes from the swing generator. The swing generator output for all the 3 case is shown in table 14. In an actual power system there would be base units, intermediate units and peak units and though in this test system it comes only from one generator the computer model is built to take into account all the three types of units. From EPRI [16] regional data the heat rates for 100%, 75%, 50%

Table 12. A comparison of the transmission line loadings between the original system and system equipped with SMES of different ratin

Line Number	Original System 40MW,200Mwh (without SMES)	20MW,100Mwh			
		at location A	at location B		
1	96.93	78.39	79.00	84.36	84.68
2	92.41	85.42	80.90	87.68	84.53
3	89.95	91.07	66.11	90.71	73.56
4	92.08	95.30	84.13	94.27	86.65
5	85.27	90.65	80.66	88.92	82.15
6	79.73	76.60	27.53	77.60	42.93
7	90.73	86.87	74.97	87.99	79.94
8	76.55	75.82	73.45	76.00	74.36
9	15.55	15.55	15.45	15.54	15.45
10	87.50	87.46	87.50	87.35	86.96
11	43.13	43.47	44.86	43.40	44.33
12	73.00	73.33	74.47	73.20	74.00
13	40.92	40.50	39.08	40.58	39.67
14	51.78	51.67	51.88	51.11	51.88
15	49.11	48.11	45.22	48.44	46.44
16	90.70	90.97	92.12	90.90	91.72
17	77.10	77.38	78.43	77.29	78.09
18	87.94	87.59	86.84	87.70	87.23
19	75.52	75.43	74.83	75.47	75.00
20	85.03	85.29	86.26	85.21	85.88

Table 13. A comparison of the reduction in transmission losses and the reduction in fuel cost

	40MW, 200 Mwh		20MW, 100Mwh	
	location a	location b	location a	location b
Daily reduction in transmission energy losses relative to the total daily transmission losses of the original system	1.95%	4.00%	1.35%	3.14
Daily reduction in fuel cost for transmission losses relative to daily fuel cost for total transmission losses of original system	10.16%	21.44%	6.49%	12.83

and 25% output for a typical base load, intermediate load and peak load plants, and the fuel cost are available. As the heat rates and the fuel cost data is available at four output values assuming a linear relationship between them the \$/Mwh vs P curve was generated in the computer model. The cost of producing energy for the 24 hour period is shown below. The savings in energy is due to 2 reasons. (a) Operating the base load generators in the night at a higher rating from the efficiency curve the specific cost of energy is cheaper (b) Highest specific cost in the base case is during peak load hours when the peaking units have to come on, now they are replaced by the quick responding SMES discharging the cheap base power.

Size/Rating	Base	SMES-A	SMES-B
20MW/100Mwh	172,241	145,738	145,212

4.5 Impact of SMES on planning.

When a transmission system is heavily loaded and there are indications that the load would be increased some more, the SMES system could provide a short term solution by enhancing the utilization of the existing transmission facility.

A study has been conducted to investigate this aspect. The load at location C (shown in figure 39) is projected to be increased by 25MW with a power factor of 0.7. This constitutes a 9.7% increase in the overall system peak load. The transmission line loading of

Table 14. The swing generator output for 24 hour period.

hour	base	SMES-A	SMES-B
0	146.48	146.48	146.48
1	127.09	126.02	125.48
2	116.10	125.93	125.71
3	110.57	127.82	127.96
4	105.04	126.34	126.76
5	105.04	126.37	126.8
6	113.28	127.92	127.98
7	129.84	128.90	128.18
8	152.02	152.02	152.02
9	171.63	171.63	171.63
10	185.79	185.79	185.79
11	194.27	194.27	194.27
12	199.94	199.94	199.94
13	205.74	205.74	205.74
14	211.45	207.55	206.74
15	217.17	206.01	204.79
16	222.90	206.43	204.77
17	228.77	206.71	204.73
18	231.65	207.61	205.68
19	222.90	210.59	209.63
20	211.45	205.74	205.74
21	211.45	207.66	209.94
22	199.94	199.94	199.94
23	177.24	177.24	177.24
24	157.57	157.74	157.74

the original system (without SMES) with this change is shown in Table 17. Four 138-Kv lines are loaded beyond their capacities with two more loaded beyond 95%.

With SMES system(40 MW, 200 Mwh, 97% roundtrip efficiency) installed at location B and performing diurnal load levelling,some of the electric power that needs to be transferred could be transferred at lightly loaded hours to the SMES at location B, which is close to the major loads.During the peak hours, the energy stored in the SMES is discharged to supply part of the load and the transmission lines have room to transfer more power.The line loading of the system with the 40 MW SMES system is shown in table 15.

4.6 Power Flow Control

Control of AC power flow is a major problem in the existing transmissiom networks. The paths for ac power flows are determined by the electrical characterstics of the network such as voltage magnitudes and phase angles and line impedances. Consequently, the actual path, of power flow for a simple power transaction between two utilities could be more extreme than the contractual path.Coordination and planning by intervening utilities may be required.This phenomenon is known as loop flow.This section shows that SMES when connected in an asynchronous configuration as discussed in Chapter 3 can provide power flow control.

Consider figure 42, L1 and L2 are the 2 parrelel ac lines.Line L1 has the SMES/dc link.Bus 1 and Bus 3 can be considered as the generator and load bus (100 MW, 50

Table 15. A comparison of the maximum transmission line loading for system with/without SMES

Line Number	System Equipped with 40MW, 200Mwh SMES at location B	Original System (without SMES)
1	90.86	108.46
2	91.70	103.25
3	71.35	95.55
4	97.45	105.07
5	91.73	96.04
6	15.93	71.87
7	90.91	106.19
8	82.27	85.82
9	15.73	15.82
10	88.93	89.92
11	38.07	35.73
12	70.60	68.87
13	43.83	45.92
14	51.67	51.44
15	55.78	60.00
16	93.85	92.82
17	77.05	75.71
18	87.51	88.57
19	88.57	90.52
20	84.38	83.06

MVAR), the impedances have been chosen to represent a length of 50 miles. C2 and C3 are the converters at the two ends of the link, each of which is capable of performing independent real and reactive power control. SMES/dc link in this configuration is capable of performing simultaneous charging/discharging and power transfer. This study discusses the various modes of power transfer (real and reactive), between bus 1 and bus 3 to bring out the range of control possibilities. As independent real and reactive control was considered the SMES/dc link operation in the system could be simulated using AC load flow program. The 2 ends of the link are seen by the ac system as load buses with corresponding real and reactive power injections. The system data for the test system is shown in table 16 .

4.6.1 Case studies.

The base case is without the link. L1 and L2 are 2 ac lines. 6 other cases are studied. C2 in all the 6 cases is operated at unity power factor. C3 is operated either under unity power factor (cases 1, 3, 5) or supplying 30 MVAR to the system (cases 2, 4, 6). P-C2 (power into C2) is made equal to P-C3 (power out of C3) for cases 1, 2, 5 & 6 (This is similar to a hvdc link). For cases 3 & 4 the simultaneous charge/ discharge property and power transfer of the link is utilized, therefore some stored energy is discharged through C3 to supplement the ongoing power transfer.

Tables 17, 18, 19 show the line flows, line losses and the voltages for this system for the various cases outlined above. Results in table 17 show that direct power flow control in L1 can be exercised through the control of C2. The line flows shown in table 17 are

Table 16. Test Data

Bus Data						
Bus No	V	ANG	PG(MW)	QG(MVR)	PD(MW)	QD(MVR) Type
	1.04	0.0				Swing
1	1.02	0.0	75		0.0	0.0 Gen
2	-	-	-	-	100.0	50.0 Load

Line Data						
Line No	Distance	F-Bus	T-Bus	R	X	Charging MVR
1	50	1	2	10	40	5
2	48	1	2	9.5	38	5

measured at bus 1 and thus include line losses. There is also an indirect control on the power flow in L2, for eg in case 5, the real power flow in L2 can be reduced by increasing the real power flow in L1. If L2 represents a group of parallel lines a group control would be achieved. For eg any one of the parallel lines is experiencing a heavy loading L1 flow can be increased temporarily, which would therefore reduce the flows in all the lines comprising of L2.

The overall loading of a line is determined by its real and reactive power loading. In conventional converter technologies (without independent P and Q control) both ends of the link would absorb reactive power thus burdening the system with additional load and if the consumption is large could effect the voltage profile of the system. As in all cases considered C2 is operated at unity power factor, the reactive power flow in L1 is mainly due to line losses, therefore for the same amount of real power transfer, this reduction in reactive power flow results in decrease in overall line loading for L1. As shown in table 18 real and reactive power losses in L1 are also reduced.

Since the SMES/dc link does not transmit reactive power, the reactive power needs to be transmitted by L2. For case 1 therefore the line loading of L2 is increased substantially over the base case. However when C3 is operated to supply 30 MVAR (cases 2, 4 & 6) only 20 MVAR has to be supplied by L2 the line loading in L2 is considerably reduced. (i.e the loading of L2 and the overall line losses for cases 2, 4 & 6 is much less than for the corresponding cases 1, 3, & 5 without reactive power support).

Table 17. Line Loadings.

Case	P-C2	P-C3	Q-C3	P-L1	Q-L1	S-L1	P-L2	Q-L2	S-L2
	MW	MW	MVAR	MW	MVAR	MVA	MW	MVAR	MVA
Base				52.93	29.17	60.44	50.64	27.58	57.67
1	50	50	0	51.27	1.22	51.28	53.42	59.96	80.30
2	50	50	30	51.27	1.22	51.28	51.68	22.78	56.47
3	50	60	0	51.27	1.22	51.28	42.72	57.17	71.37
4	50	60	30	51.27	1.22	51.28	41.13	20.57	45.99
5	60	60	0	61.85	3.59	61.95	42.72	57.17	71.37
6	60	60	30	61.85	3.59	61.95	41.13	20.57	45.99

Table 18. Line Losses.

Case	P-C2 MW	P-C3 MW	Q-C3 MVAR	PL-L1 MW	QL-L1 MVAR	PL-L2 MW	QL-L2 MVAR	PL (L1+L2) MW	QL (L1+L2) MVAR
Base				1.81	3.6	1.76	3.116	3.57	6.7
1	50	50	0	1.27	1.22	3.41	9.939	4.68	11.16
2	50	50	30	1.27	1.22	1.68	2.765	2.95	3.99
3	50	60	0	1.27	1.22	2.71	7.148	3.98	8.37
4	50	60	30	1.27	1.22	1.123	.545	2.39	1.765
5	60	60	0	1.85	3.59	2.71	7.148	4.56	10.74
6	60	60	30	1.85	3.59	1.123	.545	2.97	4.14

Table 19. Voltages.

Case	PD-2 MW	PD-3 MW	Q-3 MVR	V-1 pu	ANGLE deg	V-2 pu	ANGLE deg	V-3 pu	ANGLE deg
0				1.02	-.066			0.936	-5.509
1	50	50	0	1.02	-.08	0.9935	-5.79	0.868	-5.2183
2	50	50	30	1.02	-.059	0.9935	-5.77	0.947	-5.72
3	50	60	0	1.02	0.049	0.993	-5.667	0.877	-3.68
4	50	60	30	1.02	0.068	0.993	-5.648	.954	-4.31
5	60	60	0	1.02	-.078	0.985	-6.985	0.877	-3.813
6	60	60	30	1.02	-.059	0.985	-6.965	0.954	-4.438

4.6.2 Multiterminal link

The basic principle of a two-terminal SMES/dc link can be extended to develop a n-terminal SMES/dc link. Figure 43 shows the schematic diagram of a n-terminal SMES/dc link interconnecting n ac transmission lines. Each line is connected to the link through an ac/dc converter which can be operated in the rectifier, inverter, or standby mode. The ac/dc converters are connected in series on the dc side to form a multiterminal dc link which allows power interchange between any two or more of the n lines. The SMES system is connected in series with the converters so that the SMES unit can be charged from or discharged to any of the n lines.

When applied at strategic location, a multiterminal SMES/dc link can play an important role in electric power transmission. Firstly, the real power flow in each line as well as real power transfers between lines at the SMES/dc link are under direct control. Consequently, the loop flow problem discussed in introduction of this section can be minimized.

Secondly, with the SMES/dc link, power transfer does not need to take place immediately when the power is needed. Power can be transmitted to the link from one ac line when this line is not heavily loaded, stored in the SMES unit, and later transmitted to where it is needed through another ac line. Making use of relevant load forecasting information, the loadings of ac lines can be "scheduled" so that power can be arranged to be transmitted during light load hours in order to reduce the line loadings during heavy load hours. As discussed earlier in this chapter transmitting the same amount of

power at low current levels rather than high current levels would also reduce transmission losses and costs.

Thirdly, using advanced converter technology, the SMES/link can also provide reactive power so that the need to transmit reactive power over long distances can be minimized. This would result in further reduction of line loadings as well as line losses. Coordinating reactive power control with the scheduling of real power transmission, an existing transmission facility can transfer more power over a 24-hour period. Through the use of SMES/dc links, utilization of existing transmission networks can be enhanced.

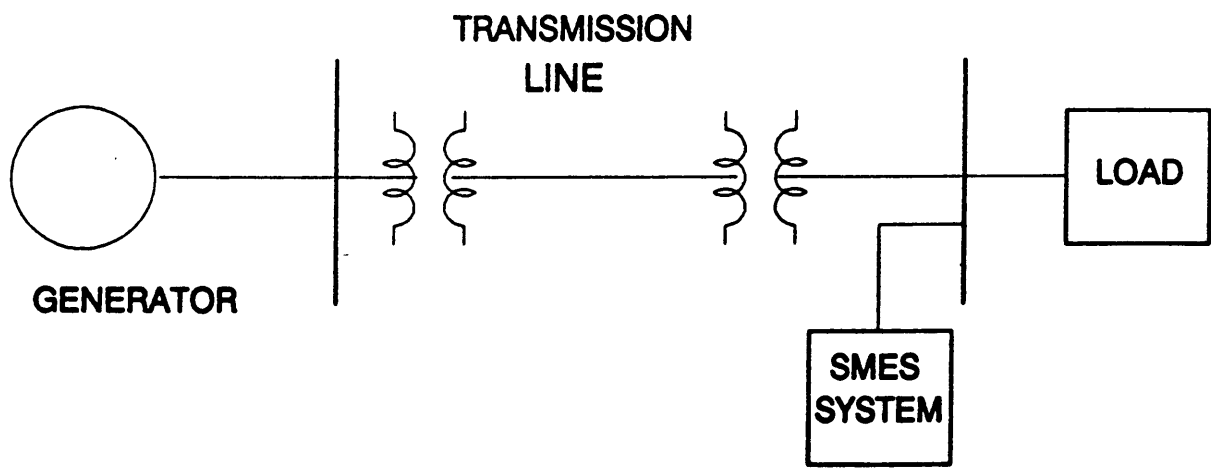


Figure 38. A simple Power system

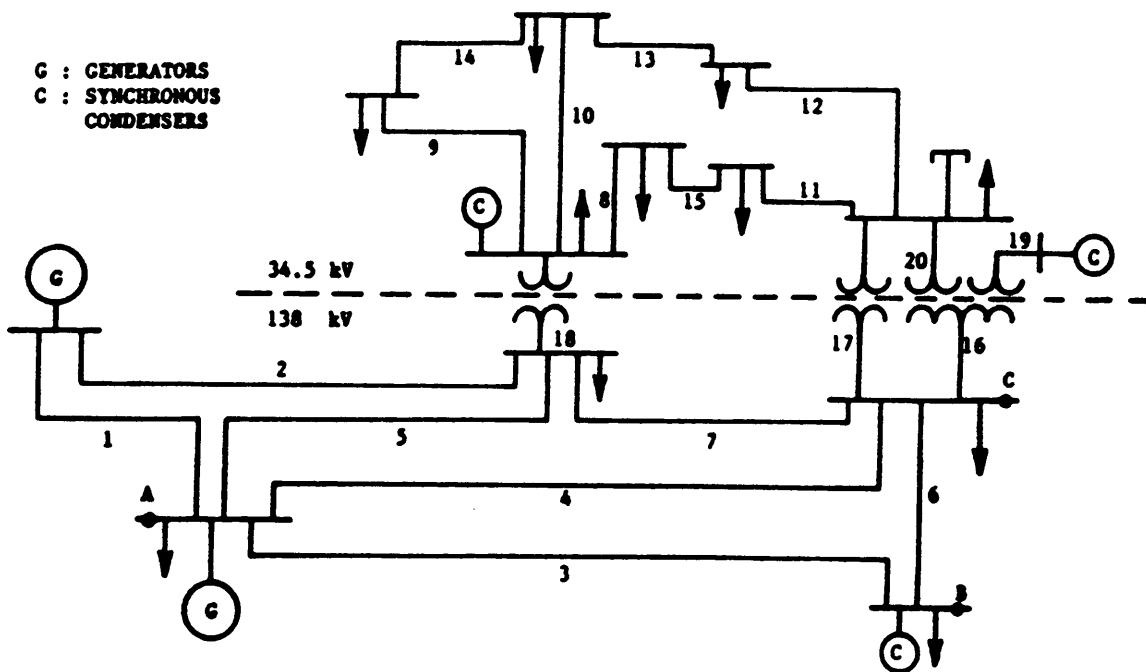


Figure 39. AEP 14 BUS system with SMES locations.

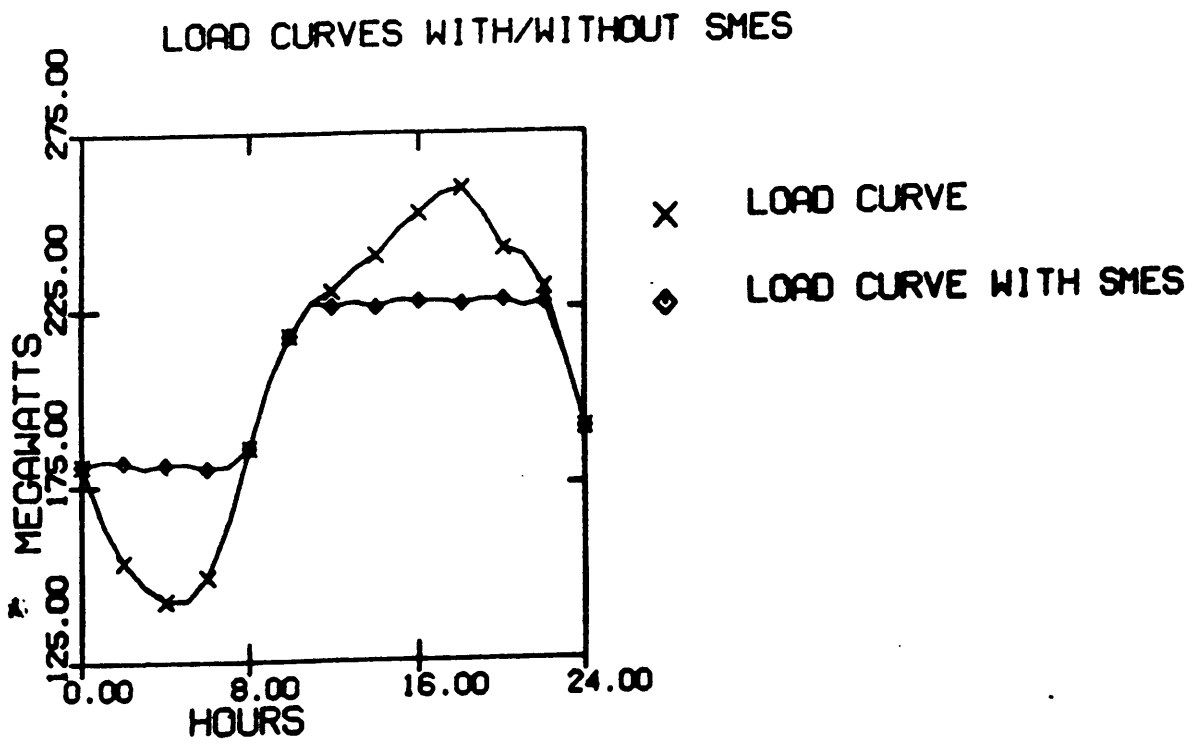


Figure 40. Load curve with/without SMES

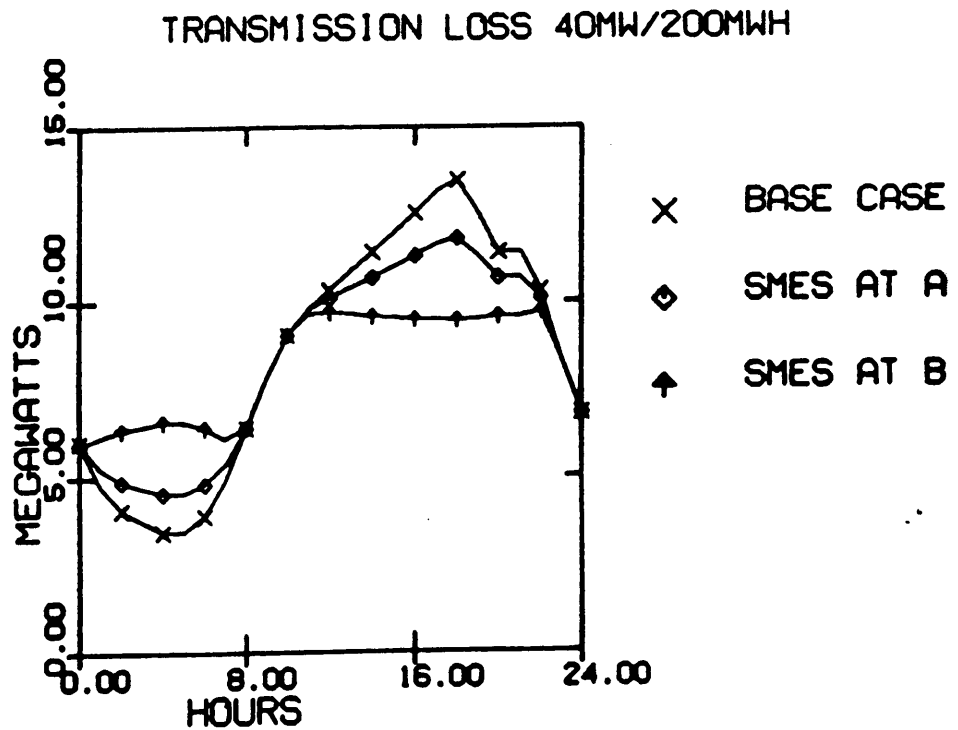
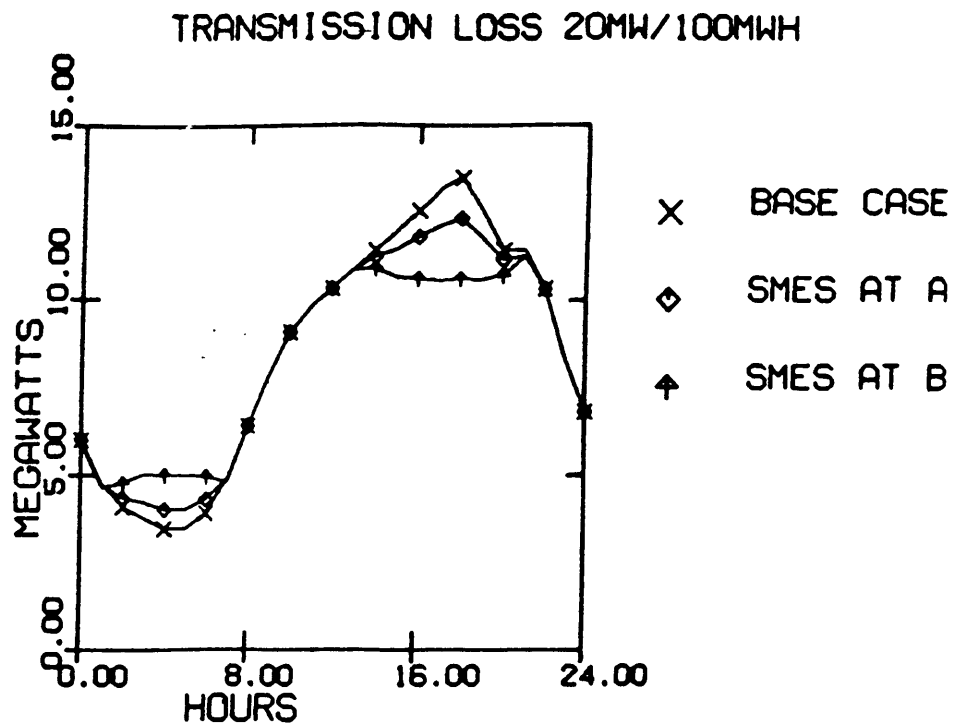


Figure 41. Transmission losses curve

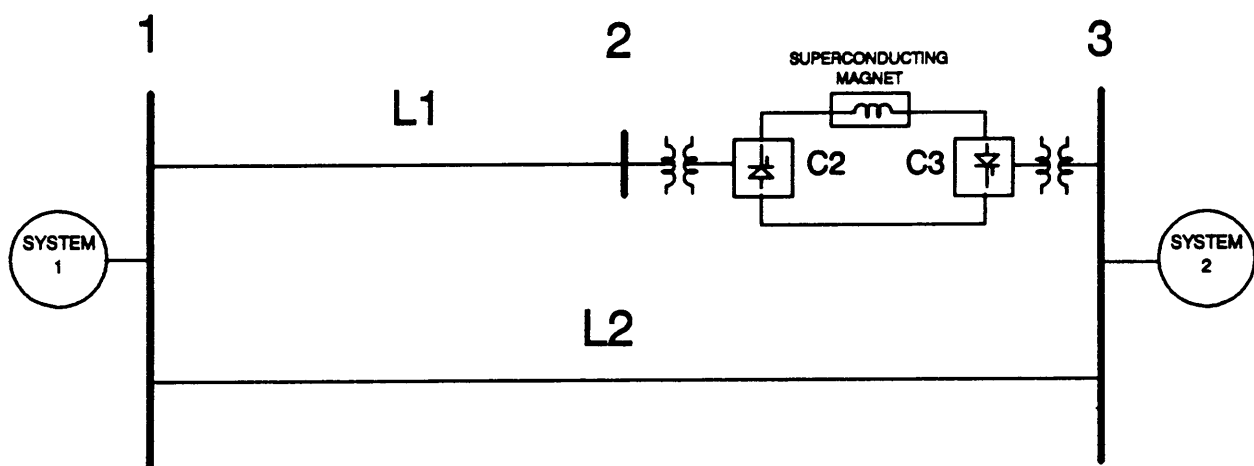


Figure 42. Test system

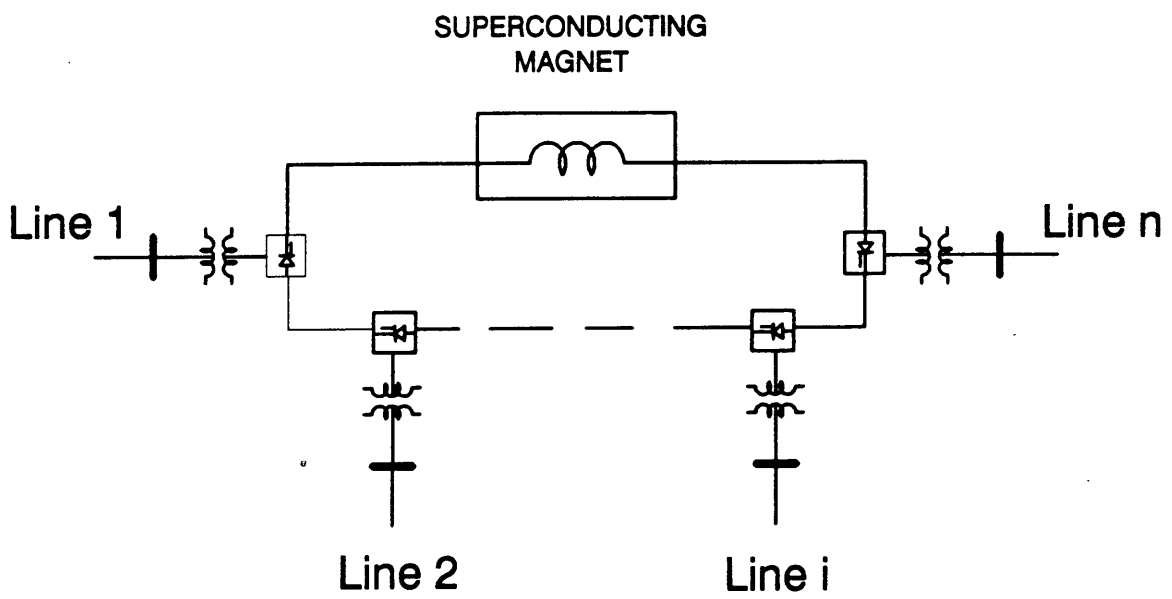


Figure 43. Multi-terminal link

5.0 Conclusions

The applications of SMES in Power Systems were explored. Three areas were identified, SMES in conjunction with PV, SMES used as an asynchronous link and the improvement of power transmission through the use of SMES.

Chapter 2 showed that a SMES system can enhance large scale utilization of PV generation. A hybrid SMES/PV scheme was developed and modelled accordingly and the results show that power output from a SMES system can be used to smooth out PV power fluctuations, so that the combined PV/SMES output is smooth and dispatchable under different weather conditions. Furthermore, the land occupied by an underground SMES system is more effectively used if PV arrays is installed on the surface.

Chapter 3 introduced the concept that SMES can be incorporated into a back-to-back DC link. This is shown to combine the benefits of energy storage, asynchronous connection and interconnection. The different modes of operation for interconnecting 2 power systems was shown. The extension of this concept for interconnecting n power systems was illustrated. A computer model was developed to demonstrate different modes

of operation for a two system operation and the results demonstrated limitations like high reactive power consumptions at low power levels and standby modes and also a limit to the maximum power that can be transferred when there is a requirement of simultaneous power transfer and charging/ discharging. The control of such a scheme was developed and the EMTP was used to demonstrate the control for various modes of operation for a two system operation. A Battery/DC link was also discussed. The economic benefits of a SMES/DC link over pure power interchange, pure SMES operation and Battery/DC link was shown.

Chapter 4 demonstrated that a SMES intended for diurnal load levelling can also provide improvement in the transmission of electric power. With SMES operation, the transmission line loading during peak-load hours is shown to decrease, the transmission losses are reduced and the cost of fuel for transmission losses reduces even further. The results also demonstrated the better utilization of existing transmission facility. The results showed that from the viewpoint of reducing transmission losses and transmission line loading, considerable benefits are derived when the SMES is located near major loads. SMES when used as an asynchronous link was shown to provide power flow control

5.1 Further Work

If large scale SMES are envisaged in the the future, work can be done in incorporating the SMES into the AGC algorithm. There are three factors to be considered (a) Estimating the cost of SMES power for the economic dispatch section (which was discussed

in section 3.4.2) (b) Response rates of the SMES (which are very high) to be considered when committing the units (c) As there is considerable reactive power consumption especially at low power requirements this would have to be effectively cost penalized.

Another area of possible work would be the modification of the ac/dc load flow program to provide capability of having an SMES link in the system. The dc equations giving the power relation between the two converters would have to be modified, as energy can be stored in the SMES/Link instead of merely being dissipated in the resistance of a DC link.

Bibliography

1. H.J.Boenig and J.F.Hauer, "Commisioning tests of the Bonneville Power Administration 30 MJ Superconducting Magnetic Energy Storage Unit ", IEEE Transactions on Power Appartus and Systems, Vol.PAS-104, No.2, Feb 1985, pp.302-312.
2. "Conceptual Design and Cost of a Superconducting Magnetic Energy Storage Plant"-EPRI Report EM-3457, April 1984.
3. M.Masuda and T.Shintomi, "The Conceptual Design of Utility Scale SMES ", IEEE Transactions on Magnetics, Vol.Mag-23, No.2, March 1987, pp.549-552.
4. J.D.Rogers, W.V.Hassenzahl and R.I.Schermer, "1 Gwh Diurnal Load Levelling Superconducting Magnetic Energy Storage System Reference Design ", Los Alomas Nat Lab Report LA 7885MS, Vols 1-8 1980.
5. R.W.Boom "SMES for diurnal use by electric utilities ", Vol.Mag-17, No.1, January 1981.

6. R.W.Boom et al, " The Design of Large low Aspect Ratio Energy Storage Solenoids for Electric Utilities", IEEE Transactions on Magnetics, Vol.Mag-17, No.5, Sept 1981, pp.2178-2181.
7. O.K.Mawardi et al, " A Force Balanced Magnetic Energy Storage System", Proceedings of the 1979 Mechanical and Magnetic Energy Storage meeting Department of Energy Conference.
8. Bi.Yanfang and Yan Luguang, " A Superconducting Toroidal Magnet with Quasi Force Free configuration ", IEEE Transactions on Magnetics, Vol.Mag-19, No.3, May 1983, pp.324-329.
9. K.S.Tam, P.Kumar and M.Foreman, "Enhancing the Utilization of PhotoVoltaic Power Generation by Superconductive Magnetic Energy Storage", 1989 IEEE/PES, Winter meeting, Paper 89 WM 022-5 EC.
10. K.S.Tam, P.Kumar and M.Foreman, "Using SMES to Support Large Scale PV Power Generation ", accepted for publication in the journal of Solar Energy.
11. K.S.Tam and P.Kumar, "Applications of Superconductive Magnetic Energy Storage in an Asynchronous Link between Power Systems", 1989 IEEE/PES Summer meeting, Paper 89SM 627-1-EC.
12. K Wollard and G.Zorpette, "Power/Energy", IEEE Spectrum Vol 26, No.1 56-58 1989.

13. M.G.Thomas, J.W.Stevens, G.J.Jones and P.M.Anderson , " The effect of Photovoltaic Systems on Utility Operations ", Proceedings of the 17th IEEE PV Specialists Conference, 1984, pp.1229-1233.
14. Arizona State University, "The effect of PhotoVoltaic Power Generation in Utility Operation ", Report SAND84-7000, Department of Electrical and Computer Engineering, Tempe, Arizona, 1984.
15. S.T.Lee and Z.A.Yamayee, "Load Following and Spinning Reserve Penalties for Intermittent Generation", IEEE Transactions in Energy Conversions, Vol.3, No.1, March 1988, pp.1203-1211.
16. "The EPRI Regional Systems", Report P-1950-SR, Electric Power Research Institute, Palo Alto, 1981.
17. A.J.Wood and B.F.Wollenberg, POWER GENERATION OPERATION AND CONTROL, John Wiley and Sons, New York, 1984.
18. A Pivec, B.M.Radimer, E.A.Hyman, "Utility Operation of Battery Energy Storage at the BEST facility ", IEEE Transactions on Energy Conversion, Vol.EC-1, No.3, September 1986, pp.47-54.
19. G.Rodriguez, R.V.Schainker and D.S.Carr, "Lead Acid Battery Energy Storage Demonstration Plant(10 MW - 4 Hrs)-Design and Expected Performance Characteristics ", Proceedings of the American Power Conference, 1987, pp.200-203.
20. D.Morris, " The Chino Battery Facility ", EPRI Journal, March 1988, pp.46-50.

21. P.Wood, SWITCHING POWER CONVERTERS, Van Nostrand Reinhold Company, New York 1981.
22. M.Oates, " A Digital Computer Program for the Comprehensive Analysis of Power Systems. ", M.S Thesis, Virginia Polytechnic Institute & State University, Blacksburg, 1980.
23. T.Ise, Y.Murakami and K.Tsuji, "Simultaneous Active and Reactive Power Control of SMES using GTO converters ", IEEE Transactions on Power Delivery , Vol.PWRD-1, No.1, January 1986, pp.143-150.
24. K.S.Tam and R.Lasseter, "A Hybrid Converter for HVDC Applications", IEEE Transactions on Power Electronics, Vol.PE-2, No.4, October 1987, pp.313-319.
25. W.V.Hassenzahl, "Superconducting Magnetic Energy Storage", Proceedings of the IEEE Vol.71, No.9, Sept 1983.
26. Y.Mitani, K.Tsuji and Y.Murakami, "Applications of Superconducting Magnet Energy storage to Improve Power System Dynamic Performance", Paper 88 WM 191-9 presented at the IEEE/PES 1988 Winter meeting, New York.
27. J.Arriliga, C.P.Arnold and B.J.Harker, COMPUTER MODELLING OF POWER SYSTEMS, John Wiley & Sons, New York, 1983.

Appendix A. Model Results on BPA SMES system

The BPA SMES test system data is found in [1] the parameters used by the program are listed below, these were used to validate the computer model developed in section 3.2.2.

Size	30 MJ
Current Rating	5KA
Voltage across magnet each)	2.5KV(two six pulse bridges of 1.25 Kv
Inductor	2.6H
Tap Range	+/- 5%

The variation of I_d , V_d , P_{smes} , Q_{smes} from the model are plotted for 15 seconds. There is close agreement between the model and the actual system. The model results are on the left coloum of the figure.

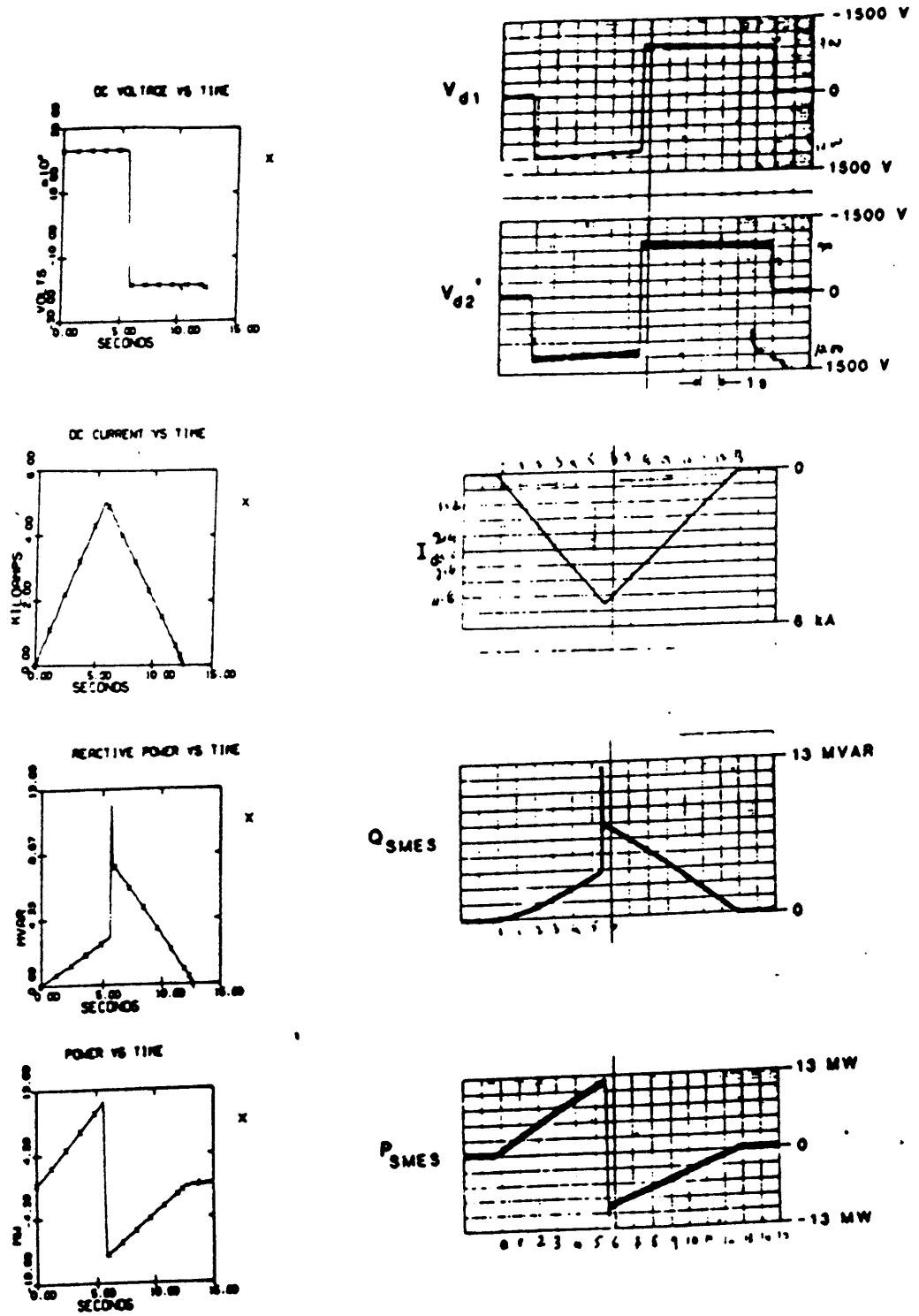


Figure 44. Model Results for BPA system

**The vita has been removed from
the scanned document**